Assessment of Potentially Toxic Elements and their Species in Selected Water Systems in Limpopo Province

Report to the

WATER RESEARCH COMMISSION

by

Abayneh Ataro Ambushe[1], Mokgehle Refiloe Letsoalo[1], Dithobolong Lovia Matabane[2], Conny Putsane Mokgohloa[2], Lizzy Shibe Molele[2], Taddese Wondimu Godeto[1,3] and Takalani Magadzu[2]

[1]Department of Chemical Sciences, University of Johannesburg, [2]Department of Chemistry, University of Limpopo & [3]Laboratory Services Branch, Ministry of the Environment, Conservation and Parks, Ontario

WRC Report No. 2515/1/19
ISBN 978-0-6392-0105-4

February 2020

Obtainable from
Water Research Commission
Private Bag X03
GEZINA, 0031

EXECUTIVE SUMMARY

Water is an important resource and fundamental to all forms of life as humans, animals and plants regularly need water for their well-being and survival. In South Africa, the quality of this precious resource has been threatened by pollution from different sources. These sources include mining and smelting activities, agricultural activities and wastes from residential areas and industrial and commercial establishments. Water pollution is a major global problem which requires ongoing monitoring of pollutants including potentially toxic elements. If not properly controlled, heavy metals pollution could pose serious challenges to the community particularly in the mining areas. Frequent monitoring of the levels of heavy metals and their sources will help in policy making and easy management of water bodies. This will also assist in preventing disaster and in saving lives.

The aim of this project was to assess and quantify the levels of potentially toxic elements and their species in water and sediment samples collected from selected rivers in Limpopo province, South Africa. The Limpopo province of South Africa has a number of rivers subjected to pollution by potentially toxic elements from mining activities and other sources. The Mokolo, Blood and Great Letaba Rivers are to mention few, among others. This study focused on these rivers. The study assessed the levels of V, Mn, Pb, Cd, Ni, Cu, Fe, Zn, Cr, As and Se in water and sediments. In particular, chemical speciation of As and Cr in water and sediment samples were conducted to accurately determine the chemical form of an element responsible for toxic effect. This will assist us to evaluate the potential health risks that rise from the consumption of contaminated water. Moreover, the sequential extraction procedure proposed by the European Standard, Measurements and Testing (SM & T) program, formerly the Community Bureau of Reference (BCR), was applied for partitioning of potentially toxic elements in river sediments. The microwave-assisted sequential extraction procedure was employed to obtain extraction efficiencies similar to the conventional BCR procedure, in less time, while using smaller volume of reagents. The flame-atomic absorption spectrometry (F-AAS), inductively coupled plasma-mass spectrometry (ICP-MS) and inductively coupled plasma-optical emission spectrometry (ICP-OES) were used for quantification of potentially toxic elements in water and sediment samples. The high performance liquid chromatography (HPLC) coupled to ICP-MS was employed for speciation of As in water and sediment samples. This report focuses on methods employed for quantification of potentially toxic elements in water and sediments, sequential extraction of potentially toxic elements in sediments, and speciation of As and Cr in water and sediments.

The validation of methods employed for total concentration determination of potentially toxic elements in water and sediments were conducted by analysing the standard reference materials of water and sediments using the F-AAS and the ICP-MS. The obtained recoveries are quantitative. The results showed that the concentrations of most of the selected potentially toxic elements, particularly in Blood River, exceeded the permissible limits of drinking water by WHO. Furthermore, method was developed for sequential extraction of selected potentially toxic elements in sediments by employing microwave extraction system. The developed method for sequential extraction of potentially toxic elements were validated by analysing certified reference material of sediment using ICP-OES.

The chromatographic separation and determination of As(III), dimethylarsinic acid (DMA), monomethylarsonic acid (MMA) and As(V) in water and sediment samples were achieved by on-line coupling of HPLC to ICP-MS. A new method was developed for extraction of As species in sediments using microwave-assisted extraction system. This method was based on 0.3 M $(NH_4)_2HPO_4$ and 50 mM EDTA and showed no species interconversion during extraction. Baseline separation of four As species was achieved in 12 minutes using gradient elution with 10 mM and 60 mM of NH_4NO_3 at pH 8.7 as mobile phases.

The solid phase extraction (SPE) method was also employed to separate As(V) in water samples. The separation was achieved using multi-walled carbon nanotubes (MWCNTs) impregnated branched polyethyleneimine (BPEI) adsorbent material. The characterisation of multi-walled carbon nanotubes-branched polyethyleneimine (MWCNTs-BPEI) by X-ray diffraction (XRD), thermogravimetric analysis (TGA), Fourier transform infrared (FTIR) spectroscopy and Raman spectroscopy showed successful modification of the nanomaterial. The MWCNTs-BPEI exhibited selective retention of As(V) in the presence of As(III) in water samples. The percentage recovery

of 81.0% for spiked water samples validated the accuracy of the method. The separated and pre-concentrated As(V) was quantified using inductively coupled plasma-mass spectrometry (ICP-MS).

For speciation of Cr in water samples, solid phase extraction method was employed to separate and pre-concentrate Cr(VI) in the presence of Cr(III). A Chromabond NH_2/ 3mL/500mg columns (i.e. aminopropyle phase with a 3 mL volume and 500 mg of sorbent were used to separate and pre-concentrate Cr(VI) selectively both in mixed standard solution and water samples prior to quantification by graphite furnace-atomic absorption spectrometry (GF-AAS). The validation of the procedure was performed by spiking method and the obtained recovery was 90.0% and acceptable.

A microwave-assisted extraction method was employed to separate Cr(VI) in sediment samples using 10.0 mL of 0.1 M Na_2CO_3 as extractant. The separated Cr(VI) was quantified by GF-AAS. The method was validated by spiking the sediment samples. A microwave-assisted extraction method using 10.0 mL of 0.01 M Na_3PO_4 as extractant solution was also applied for separation of Cr(VI) in sediment samples based on previous reported method. The separated Cr(V) was determined using GF-AAS. The method for determination of Cr(VI) using 0.1 M Na_2CO_3 extractant was compared to the method that employed 0.01 M Na_3PO_4 as extractant solution. More quantitative percent recovery of Cr(VI) was obtained by employing 0.1 M Na_2CO_3 extractant solution. Therefore, the extraction method using 0.1 M Na_2CO_3 extractant solution and quantification by GF-AAS is recommended for determination of Cr(VI) in sediments.

In this project, the effect of modified multi-walled carbon nanotubes (MWCNTs) for removal of Pb(II), Cr(VI), and Cu(II) from contaminated water were also assessed. Multi-walled carbon nanotubes modified with polyvinyl alcohol (PVA), ethylenediamine (EDA) and polyamido-amine (PAMAM) were prepared and compared with pristine MWCNTs to check their adsorption impact on selected metal ions mentioned above. Fourier transform infrared (FTIR) spectroscopy, thermal gravimetric analysis (TGA), scanning electron microscope (SEM), transmission electron microscope (TEM) and X-ray diffraction (XRD) were employed for characterisation of MWCNTs and modified MWCNTs. Removal of metal ions from synthetic solutions was carried out varying parameters such as solution pH, initial metal concentration, contact time and

adsorbent dosage. The adsorbent was separated from solution by filtration using 0.45 μm membrane filters. The concentration of metal ions in the filtrate was determined by F-AAS.

In general, efficient methods have been developed for quantification of potentially toxic elements and their species in water and sediment samples. The developed method are cost effective and easy to operate, and can be employed for determination of ultra-trace levels of potentially toxic elements and their species in water and sediments. High levels of potentially toxic elements were detected in water and sediment samples particularly from Blood River demonstrating the impact of anthropogenic activities in the river. To assess the retention of potentially toxic elements in sediments collected from Blood River, the contamination factor of each element was calculated. The calculated contamination factor showed high mobility potential for Cr, Cu, and Pb in sediments. Therefore, there is the increased possible risk of these potentially toxic elements to the biota. Finally, the investigation of MWCNTs/EDA, MWCNTs/PVA and MWCNTs/PAMAM nano composites for adsorption yielded higher removal of metal ions from synthetic solutions than the raw MWCNTs. Therefore, adsorption of metal ions was found to be improved by incorporation of MWCNTs with EDA, PVA and PAMAM.

OBJECTIVES AND AIMS

This project aims to assess the levels of potentially toxic elements (V, Mn, Pb, Cd, Ni, Cu, Fe, Zn, Cr, As and Se) and their species in wastewater, water and sediment samples collected from selected rivers in Limpopo province, South Africa.

AIM 1

To collect water and sediment samples from selected sites.

AIM 2

To develop sample mineralisation method for digestion of wastewater and sediment samples using microwave assisted digestion system for the determination of total concentrations of potentially toxic elements.

AIM 3

To develop sample preparation procedures solid phase extraction (SPE) and supported liquid membrane (SLM) using chemical and biological adsorbents for sample pre-concentration and speciation of potentially toxic elements.

AIM 4

To apply the sequential extraction procedure proposed by the European Standard, Measurements and Testing (SM & T) program, formerly the Community Bureau of Reference (BCR) for fractionation of potentially toxic elements in river sediments.

AIM 5

To develop microwave-assisted sequential extraction procedure for fractionation of the elements in sediments in less time, while using smaller volume of reagents.

AIM 6

To validate the developed/improved analytical methods by using standard reference materials (SRMs).

AIM 7

To determine the levels of potentially toxic elements and their species in water and sediment samples using F-AAS, ICP-MS and HPLC-ICP-MS.

AIM 8

To evaluate the potential health risks that rise from the consumption of contaminated water.

ACKNOWLEDGEMENTS

We would like to thank the following Reference Group members of the WRC Project for the assistance and the constructive discussions during the duration of the project:

Dr E Ubomba-Jaswa	Water Research Commission (Chairperson)
Dr JB Molwantwa	Water Research Commission (Former Chairperson)
Dr L Marjanovic	SGS South Africa
Prof NS Mokgalaka	Tshwane University of Technology
Ms H Pearson	ToxSolutions Kits & Services
Prof P Forbes	University of Pretoria
Dr D Odusanya	Department of Water & Sanitation

PUBLICATIONS

1. Mokgehle R. Letsoalo, Taddese W. Godeto, Takalani Magadzu and Abayneh A. Ambushe, Quantitative speciation of arsenic in water and sediment samples from Mokolo River in Limpopo Province, South Africa, Analytical Letters, 2018, 51(17), 2761-2775, DOI:10.1080/00032719.2018.1450879

2. Mokgehle R. Letsoalo, Taddese W. Godeto, Takalani Magadzu and Abayneh A. Ambushe, Selective speciation of inorganic arsenic in water using nanocomposite based solid phase extraction followed by inductively coupled plasma-mass spectrometry detection, Journal of Environmental Science and Health, Part A, 2019, https://doi.org/10.1080/10934529.2019.1609321

3. Tumelo M. Mogashane, Munyaradzi Mujuru, Robert I. McCrindle and Abayneh A. Ambushe, Quantification, source apportionment and risk assessment of polycyclic aromatic hydrocarbons in sediments from Mokolo and Blood Rivers in Limpopo Province, South Africa, Journal of Environmental Science and Health, Part A, 2019 (Under Review)

4. Dithobolong L. Matabane, Taddese W. Godeto, Richard M. Mampa and Abayneh A. Ambushe, Sequential extraction of potentially toxic elements in sediments of Blood River in Limpopo Province, South Africa (Manuscript to be submitted)

CONFERENCES AND WORKSHOPS ATTENDANCE

1. LS Molele, T Magadzu and **AA Ambushe**, Modified multi walled carbon nanotubes for adsorption of selected metals from contaminated water, 43rd SACI National Convention, CSIR, ICC, Pretoria, 2-7 December 2018.**(Oral)**

2. LS Molele, T Magadzu and **AA Ambushe**, Modified multi walled carbon nanotubes for adsorption of selected metals from contaminated water, University of Limpopo Faculty of Science and Agriculture Research Day, Fusion Boutique Hotel, Polokwane, 20-21 September 2018.**(Oral)**

3. **Abayneh Ambushe**, Potentially Toxic Elements in Sediment, The Sediment Conundrum Workshop, Water Research Commission, Pretoria, South Africa, 01 November 2017. (**Invited talk**)

4. Mokgehle Letsoalo, Takalani Magadzu, Taddese Godeto and **Abayneh Ambushe**, Speciation of arsenic in water and sediments using high performance liquid chromatography coupled to inductively coupled plasma-mass spectrometry, CHROM SA, University of Pretoria, 08 September 2017. **(Oral)**

5. **Abayneh Ataro Ambushe,** Mokgehle Refiloe Letsoalo and Taddese Wondimu Godeto, Speciation of arsenic in water and sediments using high performance liquid chromatography coupled to inductively coupled plasma-mass spectrometry, 100th Canadian Chemistry Conference, Toronto, Canada, 28 May to 1 June 2017. **(Poster)**

6. Miyelani Chauke and **Abayneh Ambushe**, Potentially toxic elements in water and sediment samples collected from Great Letaba River, SACI Young Chemists Symposium, University of Limpopo, 23 November 2016.(**Poster**)

7. Mokgehle Letsoalo, **Abayneh Ambushe**, Takalani Magadzu and Taddese Godeto, Speciation of arsenic in water and sediments using high performance liquid chromatography coupled to inductively coupled plasma-mass spectrometry,

SACI Young Chemists Symposium, University of Limpopo, 23 November 2016. (**Oral**)

8. **Abayneh Ataro Ambushe,** Mokgehle Refiloe Letsoalo, Dithobolong Lovia Matabane and Taddese Wondimu Godeto, Sequential extraction of potentially toxic elements in sediments and speciation of arsenic in sediments and water, Nordic Conference on Plasma Spectrochemistry, Loen, Norway, 5 to 8 June 2016**.** (**Oral**)

CONTRIBUTION ON CAPACITY BUILDING

Surname, Initials, Gender & Citizenship	**Dissertation/Thesis Title**	**Institution**	**Degree**
Letsoalo MR (Female) South Africa	Speciation of arsenic in water and sediments from Mokolo and Great Letaba Rivers, Limpopo province	UL	MSc (completed in 2017)
Mogashane TM (Male) South Africa	Assessment of the levels of polycyclic aromatic hydrocarbons (PAHs) in sediments and water from Mokolo and Blood Rivers of the Limpopo Province, South Africa	UL	MSc (completed in 2018)
Matabane DL (Female) South Africa	Identification and determination of potentially toxic elements in water and sediments from Blood and Mokolo Rivers in Limpopo province, South Africa	UL	MSc (completed in 2019)
Mokgohloa CP (Female) South Africa	Speciation of chromium in water and sediments from Mokolo and Blood Rivers, Limpopo Province	UL	MSc (completed in 2019)
Molele LS (Female) South Africa	Modified multi-walled carbon nanotubes for removal of selected metals from contaminated water	UL	MSc (writing and expected to complete Sept 2019)

CONTRIBUTION ON CAPACITY BUILDING (Continued)

Surname, Initials, Gender & Citizenship	**Dissertation/Thesis Title**	**Institution**	**Degree**
Matjena MM (Female) South Africa	Speciation of inorganic selenium in water and sediment samples collected from Capricon and Vhembe Districts in Limpopo Province	UL	MSc (expected to complete Dec 2020)
Chauke M (Female) South Africa	Potentially toxic elements in water and sediment samples collected from the Great Letaba River, Limpopo Province, South Africa	UL	BSc Honours (completed in 2016)
Letsoalo MR (Female) South Africa	Quantitative speciation of selected toxic elements in water and sediments and fabrication of ion-imprinted polymer sensors to detect toxic elements in water	UJ	PhD (expected to complete Dec 2020)

This page was intentionally left blank

TABLE OF CONTENTS

LIST OF FIGURES

LIST OF TABLES

LIST OF ABBREVIATIONS

APDC	Ammonium Pyrrolidinedithiocarbamate
BCR	Community Bureau of Reference of the Commission of the European Communities
BPEI	Branched Polyethyleneimine
CE	Capillary Electrophoresis
CNFs	Carbon Nanofibers
CNTs	Carbon Nanotubes
CPE	Cloud Point Extraction
CSIR	Council for Scientific and Industrial Research
DWA	Department of Water Affairs
DWS	Department of Water and Sanitation
EDA	Ethylenediamine
ET-AAS	Electrothemal-Atomic Absorption Spectrometry
F-AAS	Flame-Atomic Absorption Spectrometry
FTIR	Fourier Transform Infrared Spectroscopy
GF-AAS	Graphite Furnace-Atomic Absorption Spectrometry
HG-AAS	Hydride Generation-Atomic Absorption Spectrometry
HG-AFS	Hydride Generation-Atomic Fluorescence Spectrometry
HPLC	High Performance Liquid Chromatography
ICP-MS	Inductively Coupled Plasma-Mass Spectrometry
ICP-OES	Inductively Coupled Plasma-Optical Emission Spectrometry
ICP-SF-MS	Inductively Coupled Plasma-Sector Field-Mass Spectrometry
IDP	Integrated Development Planning
IL	Ionic Liquid
IUPAC	International Union of Pure and Applied Chemistry
MWCNTs	Multi-Walled Carbon Nanotubes
PAMAM	Polyamido-amine
PHEMA	Polyhydroxyethyl Methacrylate
PVA	Polyvinyl Alcohol
SEM	Scanning Electron Microscope
SPE	Solid Phase Extraction

SWCNTs	Single-Walled Carbon Nanotubes
TEM	Transmission Electron Microscope
TGA	Thermogravimetric Analyser
WHO	World Health Organisation
WRC	Water Research Commission
XRD	X-ray Diffraction

1. INTRODUCTION AND OBJECTIVES

Pollution of water is on the increase due to industrial, commercial, domestic and mining activities directly or indirectly emitting potentially toxic elements, which end up in ground and surface water. Even though mining has played an important role in the development of South African economy, it also emerged as a threat to the water resources, aquatic life, human health and the general environment (Durand, 2012; Hobbs *et al.*, 2008; McCarthy, 2011). In South Africa, the mining activities in some cases brought some serious environmental problems in a country with limited water resources (WRC, 2012). Mining and related activities require significant amounts of water and impact on the environment through associated potential pollution (Department of Water Affairs, 2013). Hazardous materials such as heavy metals from mining activities tend to leach through tailings into the surrounding areas causing the contamination of groundwater, sediment, fauna and flora (Sims *et al.*, 2013). Alarming environmental effects of an abandoned coalmine in the Witbank coalfield were reported (Bell *et al.*, 2001). The findings showed the deterioration of the quality of water, which led to the abolition of aquatic flora and fauna in a nearby stream (Bell *et al.*, 2001). The water quality of the river systems, wetlands and groundwater has continued to deteriorate due to mine effluent issuing from mines in Gauteng and North West Province (Durand, 2012). In some of these affected areas, certain rivers are devoid of macroscopic organisms and the riparian vegetation has suffered a loss of biodiversity (Durand, 2012). Thus, the environmental pollution caused by anthropogenic activities such as mining have a profound effect on the dynamics and functioning of ecosystem.

Waste generated from mining and industrial activities are a major concern. It may contain high levels of potentially toxic elements such as As, Cd, Cr, Cu, Fe, Mn, Ni, Pb, Se, V and Zn that may have an adverse effect on humans and animals living in the vicinity or downstream of the contaminated site. Monitoring heavy metals is crucial due to their potential toxicity, bioaccumulation and biomagnification capability, long persistence in the environment and organisms (Achary *et al.*, 2016). Fish species have been widely used as sentinel organisms in monitoring pollution in aquatic environments by toxic elements (Gerber *et al.*, 2016). Fish are susceptible to toxic elements present in water and the accumulation of toxic elements in fish muscle has a negative effect on humans through consumption of fish (Monferran *et al.*, 2016). When aquatic organisms such as fish are exposed to elevated levels of toxic metals in their environment, the bioavailable fraction they are exposed to is generally absorbed (Gerber *et al.*, 2016). Chronic exposure to toxic metals may disrupt fish's swimming ability, growth and ion regulation (du Preez & Wepener, 2016). The levels of toxic elements are biomagnified up the food chain where large predatory fish such as tuna, shark and swordfish contain the highest levels (Bosch *et al.*, 2016). The presence of toxic elements persists in the environment due to accumulation in sediments and fish (Bosch *et al.*, 2016). Potentially toxic elements such as Cd and Pb in water bodies has been a source of worry to environmentalists, government agencies and health practitioners (Awofolu *et al.*, 2005). Thus, there is need to quantify the levels of potentially toxic elements and their species in water.

1.1. Pollution of South African water bodies

South Africa is a water-stressed country and is facing a number of water challenges, which include security of supply, environmental degradation and resource pollution (Department of Water Affairs, 2013). The pollution of water may aggravate water scarcity since the contaminated water may pose a health risk, reduce water productivity in crop production and become unsuitable for other purposes (Pahlow *et al.*, 2015). The pollution caused by gold mining in South Africa has had substantial environmental consequences (Tutu *et al.*, 2008). One of the most consistent and pressing problems caused by gold mining has been its impact on the water bodies in and adjacent to the Witwatersrand (Durand, 2012). The acid mine drainage (AMD) is a common legacy in most gold and coal mines and results from the oxidation of pyrite (FeS_2) in the host rock (Masindi *et al.*, 2016). The acidity in AMD increases the leaching of heavy metals from the surrounding geology (Masindi *et al.*, 2015). Coal mining, coal-fired power stations, industrial activities and agricultural practices, combined with a general decline in the efficiency of wastewater treatment facilities, have all contributed to a steady deterioration of water quality of upper Olifants River system (Genthe *et al.*, 2013). The combustion of coal may lead to the release of volatile trace elements such as As, Cd, Hg, Pb and Se into the atmospheric environment (Wagner and Tlotleng, 2012). Heavy metals are naturally present in the environment but can be introduced into water bodies through waste from industrial activities (Bosch *et al.*, 2016). The recent study on sediments of Richards Bay beaches indicated that the measured metal concentrations were from natural origin attributed to leaching, weathering process and industrial sources (Vetrimurugan *et al.*, 2016). The heavy metals have been referred as common pollutants, which are widely distributed in the environment with sources mainly from the weathering of minerals and soils (Awofolu *et al.*, 2005). However, the levels of heavy metals in the environment have increased immensely in the past decades as a result of human inputs and activities. The study by Gerber *et al.* (2015) in Luvuvhu, Letaba and Olifants Rivers revealed anthropogenic inputs of metals into these rivers. Relatively few studies have been conducted in South Africa dealing with the levels of heavy metals particularly their speciation in surface waters (Okonkwo & Mothiba, 2005). In South Africa, most of the drinking water, which is supplied to communities is obtained from surface water sources (rivers and reservoirs), though the groundwater supplies are important in more arid areas (Oberholster & Ashton, 2008). Limited reports dealing with the chemical species of potentially toxic elements in South African rivers make it difficult to assess the potential health risks.

Potentially toxic elements such as arsenic, cadmium, chromium, lead, selenium and many others are usually determined after acid digestion of samples followed by atomic spectrometric analysis to yield total element concentrations. However, it has been known for many years that the chemical form of the element can greatly affect its bioavailability and hence toxicity. Thus, the identification and quantification of actual organic or inorganic form of the element in the environmental samples is necessary to assess the toxic effect of trace elements. Chemical speciation has become an important research area in elemental analysis, to accurately determine the chemical form of an element (inorganic, organic, organometallic, and/or oxidation state) responsible for toxic effect.

1.2. South African acts and legislation on waste and pollution

Like many aspects of its constitution, South Africa has progressive legislation to prevent and clean up environmental contamination (Papu-Zamxaka *et al.*, 2010). The Constitution of the Republic of South Africa stipulates that everyone has a right to an environment that is not harmful to their health or well-being. The National Water Act, 1998 (Act No 36 of 1998) seeks to ensure that the country's water resources are protected, used, developed, conserved, managed and controlled in a sustainable and equitable way for the benefit of all people (DWS, 2015). Although access to clean water is a right of every person, water pollution is ultimately making it difficult for people to enjoy this right (Nkosi and Odeku, 2014). It is more difficult and costly to clean contaminated water than to maintain clean and safe water. The best option would be pollution prevention rather than attempting to solve the problem after it had occurred.

In 2008, the National Environmental Management Waste Act, which particularly governs the local management of waste, was formed. Section 16 (1) of this Act states that 'waste resulting in environmental pollution should be avoided and where it cannot be avoided altogether, should be minimised and recycled where possible and otherwise disposed of in an environmentally sound manner'. In South Africa, there is a clear legislation framework for the prevention and clean-up of environmental pollution (Papu-Zamxaka *et al.*, 2010). However, there is a large gap between legislation and practice.

1.3. Health risk implications

South Africa has expanding economies with active mining and agricultural activities that pose health risks to the working population (Moyo *et al.*, 2015). Communities residing around the mining areas may be exposed to contaminants through multiple pathways including ingestion of contaminated water and foodstuffs and inhalation/ingestion of tailings dust (Schonfeld *et al.*, 2014). Currently, there is a knowledge gap in translating observed impacts on water quality and ecosystem health into possible human health risks as well as the implications of multiple threat exposure. Ma *et al.* (2016) in their findings suggested that the presence of multiple heavy metals could be detrimental to human health even though the presence of a single heavy metal does not pose a significant risk. They further recommended that the guidelines for stormwater should consider the combined risk from multiple heavy metals rather than the threshold concentration of an individual element. Health risks associated with contaminated water include infectious diseases, acute or chronic chemical toxicity and carcinogenicity, among others (Genthe *et al.*, 2013). Toxic metals can damage the nervous, skeletal, circulatory, enzymatic, endocrine, and immune systems, as well as can harm liver, kidney and/or lung (Cherfi *et al.*, 2015).

1.4. Potential pathways of exposure

Living around polluted areas is one of the most common sources of exposure to toxicants from the environment. Among various toxicants, heavy metals are widely used in foundries, mining, and manufacturing industries (Al Bakheet *et al.*, 2013). Health hazards from heavy metals are both dose and exposure dependent (Davies & Mundalamo, 2010). Long-term exposure and accumulation of toxic metals in the body may disturb oxidative stress genes and thus increase the vulnerability to various diseases (Al Bakheet *et al.*, 2013). Furthermore, risk is also affected by ingestion through various pathways, and by interaction between constituents (Figure 1.1). Heavy metals derived from natural processes of mineralisation, as well as from mining and ore processing operations and associated activities, can enter the human body by three main pathways (Davies & Mundalamo, 2010). These main pathways are:

1. Ingestion: through consumption of food crops or/and water having anomalous concentrations of heavy metals. The absorption and retention capacity of ingested heavy metal for example Mn by infants greatly increased compared to adults (Rollin and Nogueira, 2011).
2. Inhalation of particulate matter and dust in the mining environment or from other industrial sources. For example inhalation uptake of Mn by large number of occupationally exposed workers were reported (Rollin and Nogueira, 2011).
3. Direct dermal contact with ores and associated materials. However, the dermal route of exposure does not appear to be of significant concern (Rollin and Nogueira, 2011).

Both inhaled and ingested heavy metals such as manganese have a substantial effect on intellectual function in children (Hess *et al.*, 2015). Manganese levels commonly found in tap water, about 34 µg/L are enough to cause a reduction in IQ (Hess *et al.*, 2015). Clinical and imaging evidence of neurotoxicity in chronically Mn exposed workers was reported (Nelson *et al.*, 2012).

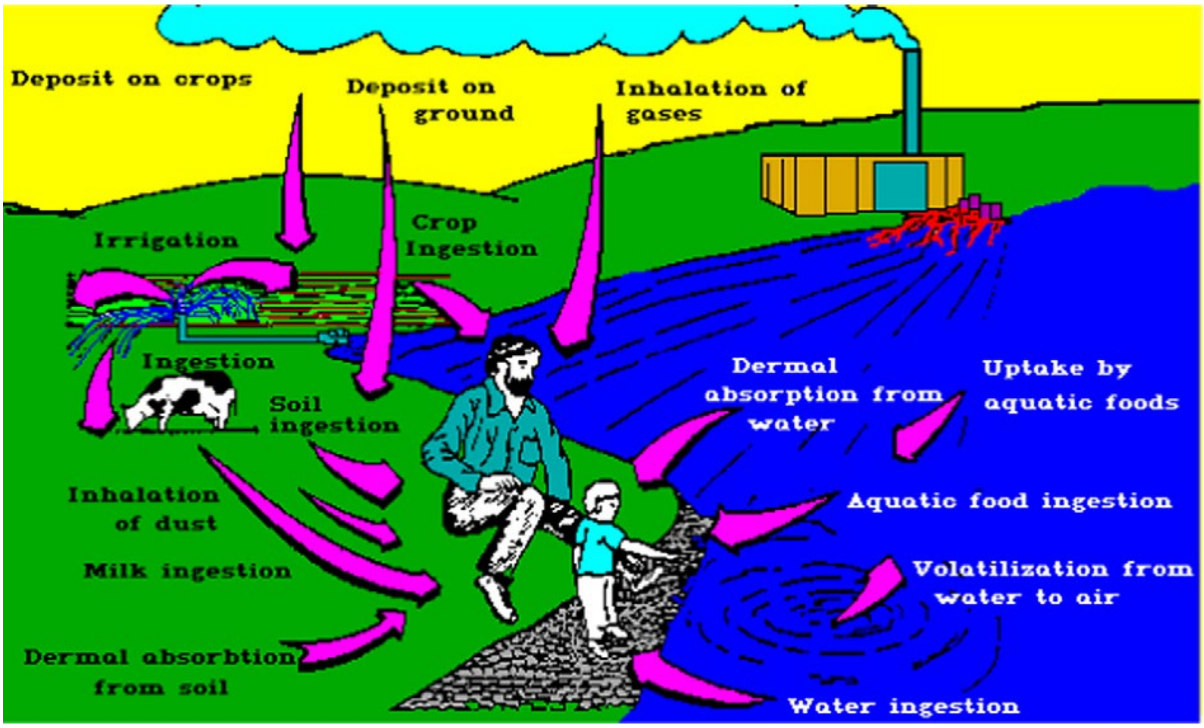

Figure 1.1: Health risk exposure pathways (Davies & Mundalamo, 2010).

Frequent consumption of fish from polluted water system may lead to an increased exposure to potentially toxic elements which can pose a risk to human health (Bosch *et al.*, 2016). In Japan, outbreak of acute poisoning with Hg was reported in Niigata and Minamata due to ingestion of fish heavily contaminated with industrial discharge of Hg (Al Bakheet *et al.*, 2013).

1.5. Speciation of potentially toxic elements

Speciation is defined by the International Union of Pure and Applied Chemistry (IUPAC) as “Analytical activities of identifying and/or measuring the quantities of one or more individual chemical species in a sample”. A chemical species is defined as a “specific form of an element defined as isotopic composition, electronic or oxidation state and/or complex or molecular structure” (Forsgard, 2007).

In the environmental studies, the significant information is not obtained by the quantification of total concentrations of elements, but by determination of the chemical forms in which these elements occur in the environment. The chemical forms of an element can affect many of its characteristics, e.g. toxicity, which makes speciation analysis important. The toxicity of an element strongly depends on its physical-chemical form present in the sample and in its capacity to move through the intestinal barrier. Speciation includes the elucidation of the oxidation state, total charge, molecular weight of the species and binding strength of the elements. In all the cases, the information provided leads to the ultimate identification of the particular species of interest and, as necessary, its quantification (Meija *et al.*, 2004). Elemental speciation studies have been reviewed and discussed in detail (Cubadda, 2004; Meija *et al.*, 2004; Krishna *et al.*, 2005; Sun *et al.*, 2006; Chen *et al.*, 2007; Forsgard, 2007; Hill, 2007; Hu *et al.*, 2008; Ma & Tanner, 2008; Zhang *et al.*, 2008; Latorre *et al.*, 2013; Chen *et al.*, 2014). The current study focuses on speciation of arsenic, chromium and selenium in water and sediment samples.

1.5.1. Speciation of arsenic in water and sediments

Arsenic is widely known as a deadly toxic element for human beings. Arsenic exists widely in air, soil, water, and a wide variety of minerals (Ozcan, 2010). The processes such as natural weathering reactions, geochemical reactions and other anthropogenic activities mobilise arsenic. Aquatic ecosystems are contaminated as the high volumes of industrial and urban waste are discharged into such environments leading to significantly increased arsenic concentrations in water, which may diminish quality of the freshwater (Rezende *et al.*, 2014). Arsenic can also be derived from mine wastes and mine tailings. Exposure to drinking water with levels of arsenic greater than 10 µg/L has been associated with adverse effects (WHO Guidelines for Drinking water Quality, 2011). Ingestion of arsenic, even at very low levels can cause a variety of health problems including carcinogenic effect.

The health effects of arsenic are not only dependent on the total concentration but also on quantities of chemical species. Furthermore, total concentration of arsenic does not provide useful information to evaluate the processes in which arsenic is involved in a given ecosystem (Pizarro *et al.*, 2003; Akinsoji *et al.*, 2013). The chemical speciation serves as a vital tool in the environmental protection, toxicological and analytical research because of actual toxicity, availability or accumulation, migration and reactivity of arsenic depend on the availability of chemical forms (Pizarro *et al.*, 2003; Akinsoji *et al.*, 2013). The identification of the chemical species in the natural environment either as specific chemical compounds, which refers to individual speciation or groups of compounds known as operational speciation allows drawing conclusions on the element's essential relations and effects (Pizarro *et al.*, 2003). The alteration of conditions, especially factors such as pH, redox potential, salinity and temperature strongly affects the existing chemical species since the physical and chemical state of species of the compound plays a prominent role in the biochemical, medical and toxicological effects of the element on the environment (Terlecka, 2005). Arsenic occurs in environmental samples mainly as inorganic species, including arsenite (As(III) and arsenate (As(V)) and as methylated species, including monomethylarsonic acid (MMA) and dimethylarsinic acid (DMA) (Pizarro *et al.*, 2003; Terlecka, 2005).

The inorganic arsenic species (As(III) and As(V)) are considered the most toxic forms of arsenic and the degree of toxicity is roughly 100 times more toxic than organic arsenic monomethylarsonic acid (MMA), dimethylarsinic acid (DMA) and trimethylarsenic oxide (TMAO) (Jablonska-Czapla, 2015). Trivalent arsenic species As(III) is about 60 times more toxic than the oxidised pentavalent state As(V). Arsenite and arsenate are of comparable bioavailability but differ in terms of their biochemistry, in part due to the increased preference of the arsenite for binding thiols (Plant *et al.*, 2003). Arsenate can replace phosphate in several biochemical reactions, whereas arsenite may react with critical thiols in proteins and inhibit their activity (Pizarro *et al.*, 2003; Plant *et al.*, 2003). The methylated forms of arsenic (MMA and DMA) are less toxic followed by arsenocholine (AsC), arsenobetaine (AsB) and arsenosugars, which are regarded as non-toxic (Jablonska-Czapla, 2014). DMA(III) and MMA(III) are of considerable interest since they found to be more cytotoxic, genotoxic and potent enzyme inhibitors than As(III) (Plant *et al.*, 2003). The toxicity of arsenic species summarised as arsine gas (AsH_3) > (As(III) > (As(V) >MMA > DMA > AsB, AsC, TMAO (Ozcan, 2010). The most common species of arsenic likely to be found in soils, water and sediments are As(III) and As(V) and traces of MMA and DMA (Hudson-Edwards *et al.*, 2004). Inorganic arsenic is the dominant form in water (Doker *et al.*, 2013).

Contamination of drinking water by arsenic has been widely reported in different places including Bangladesh, Argentina and Chile (Plant *et al.*, 2003). In South Africa, the same was reported in an area called Gravellote, Limpopo Province (Akinsoji *et al.*, 2013). Recent studies on epidemiology have revealed that long term exposure to arsenic can cause adverse health effects to human beings such as dermal changes, neurological development, pulmonary cardiovascular, mutagenic and carcinogenic effects (Pizarro *et al.*, 2003). The emanating health conditions were reported to be linked with intake of drinking water having arsenic concentration of ≥ 50 µg/L (Pizarro *et al.*, 2003). Speciation of arsenic in water and sediments is crucial since the toxicity depends on specific species. Suspended sediments consisting of silt-sized and clay-sized particles trap heavy metals to protect water quality but they also present the potential for further water contamination (Terlecka, 2005).

Ali (2010) reported arsenic levels in the range of 14-18 µg/L in water from Gravellote. Gilber and Avenant-Oldewage (2014) determined the levels of trace elements such as arsenic, chromium, iron, manganese, lead, selenium and zinc in the water, sediment and tissues of *Labeobarbus kimberleyensis* from the Vaal Dam, South Africa. The total elemental concentrations were determined using ICP-MS. Total arsenic concentration in water samples were below detection limit of 0.045 µg/L, whereas arsenic levels as high as 29 µg/g were reported in sediments.

The oxidation states of arsenic in water differ in accordance to their origination but are likely to occur dominantly as As(III) when sourced from smelters, coal burning or volcanic sources (Plant *et al.*, 2003). For instance, organic arsenic species (DMA and MMA) are likely to be sourced by volatilization from soils, and arsine (As(-III)) may be derived from landfills and reducing soils such as paddy soils and peats. The presence of As(V) on the environment may be due to marine aerosols (Cullen & Reimer, 1989). The mobility of a relatively small amount of arsenic extricated into stream water during weathering processes is facilitated by the low pH and redox potential (Eh) to favour its persistence in trivalent form. The pH of water ranging from 6.5-8.5 mobilise arsenic under both oxidising and reducing conditions (Cullen & Reimer, 1989). The chemical reactions such as reduction, oxidation and methylation control species of arsenic in water subsequently, affecting its solubility, transport, bioavailability, and toxicity (Hering & Kneebone, 2002).

The speciation of arsenic species is a vital requisite in water quality analysis as the total arsenic concentration could not explain the actual environmental impacts (Plant *et al.*, 2003). Therefore, to obtain an accurate arsenic species information, the integrity of species should be maintained throughout the entire analytical procedures (Le *et al.*, 1998). Several countries have recommended different maximum permissible levels (MPLs) of arsenic in water (Kumar & Riyazuddin, 2010). The significant toxicity effects of diverse arsenic species led to the reduction in the regulatory limit from 50 µg/L to 10 µg/L of arsenic in drinking water (Garcia-manyes *et al.*, 2002).

1.5.1.1. Detection techniques for arsenic speciation

Numerous studies have been published on the investigation of arsenic species in water, employing a variety of methods hyphenated to inductively coupled plasma-mass spectrometry (ICP-MS) detection system. The techniques such as high performance liquid chromatography (HPLC) and hydride generation-atomic fluorescence spectrometry (HG-AFS) were also explored (Hudson-Edwards *et al.*, 2004). The hydride generation technique is limited to execute ultra-trace amount of arsenic as it requires large injection of sample into detection system. Therefore, species determination is unattainable and the effects of matrix interferences are observed (Jablonska-Czapla, 2015).

1.5.1.2. Sample pre-concentration techniques for arsenic speciation

In the determination of trace elements such as As, Cr and Se in complex matrices, enrichment and separation of analytes is of great importance. The establishment of simple, ecologically safe, sensitive and selective methods for the determination of trace components is trending in the modern analytical chemistry. A wide variety of methods have been advanced for pre-concentration because of low concentration of trace elements in order to increase sensitivity of the analytical method used and to eliminate possible matrix interferences (Türker, 2012). Commonly, pre-concentration refers to a process in which the ratio of the concentration or the amount of trace components (trace constituents) to the concentration of macro-components (matrix) is increased (Türker, 2012). Separation and pre-concentration procedures is crucial in sample preparation processes. It affects directly the accuracy, precision and detection limits. Additionally, they are considered to be the rate determining step of the analytical methods (Türker, 2012). In pre-concentration and speciation techniques, elution or desorption procedure are accompanied by separation procedure and detection and quantification of the analytes by a suitable detection technique perhaps ICP-MS, ICP-OES, GF-AAS, HG-AAS, and F-AAS (Türker, 2012).

Pre-concentration and separation technique such solid phase extraction (SPE) which is based on sorption appears to be convenient, rapid and with the ability to attain sufficient pre-concentration factor (Terada, 1991). In solid phase extraction, compounds, elements or species of elements of interest which have been selectively retained by sorption on different solid-phases are eluted with acids or other reagents (Türker, 2012). Therefore, in order to achieve the higher pre-concentration factor the eluent volume should be as small as possible and the volume of sample solution should be as high as possible (Türker, 2012). The mechanism of retention of analytes on solid phases depends on the nature of the solid phase and the nature of the species to be retained (Terada, 1991; Türker, 2012). The retention process mostly involves adsorption of the metal ions at the surface of the sorbent through interactions with various functional groups, and ion exchange, chelation and ion-pair formation processes. Moreover, it also depends on the experimental conditions, such as pH, temperature and metal ion concentrations (Terada, 1991; Türker, 2012). However, throughout the sorption process, the equilibrium is established between the species adsorbed on the surface of sorbent and the species remaining in the solution (Türker, 2012).

Most recently reported studies on speciation analysis of arsenic deal with HPLC or capillary electrophoresis (CE) coupled to ICP-MS or other detection techniques. However, often when handling ultra-trace level of arsenic in complex matrices the direct determination of arsenic species is difficult. The preliminary sample pre-treatment with separation and pre-concentration is highly recommended to enhance favourable enrichment factor and recoveries of analytes of interest while eliminating matrix interferences (Chen *et al.*, 2013). A SPE is an effective sample pre-treatment technique for the extraction and pre-concentration of analytes from complex matrices, with the merits of satisfactory recovery and preconcentration efficiency, low cost and reduced reagent consumption as well as environmental friendliness (Chen *et al.*, 2013).

The conventional sorbents such as ion exchange resin, glass and modified mesoporous silica have been proposed for arsenic speciation (Chen *et al.*, 2014). The effective arsenic separation was achieved by SPE cartridges packed with anion exchange resin in which As(V) is retained on the column, meanwhile As(III) passes through it. The detection limit of arsenic using inductively coupled plasma sector field mass spectrometric (ICP-SF-MS) was reported to be 0.06 µg/L (Chen *et al.*, 2014). Chen *et al.* (2014) reviewed a highly efficient separation and pre-concentration technique for arsenic speciation based on ionic liquid (IL) dispersive micro-extraction technique implemented in a flow analysis system. The dispersed IL phase was retained by a microbore glass column filled with resin and followed by eluting with acidified methanol. As(III) was determined in eluent solution by electro thermal atomic absorption spectrometry (ET-AAS) with a detection limit of 0.05 µg/L (Chen *et al.*, 2014).

Chen *et al.* (2014) reported that with the great progress in material sciences, functional nanomaterial emerged providing excellent sorbent materials in the field of sample pre-treatment such as carbon nanofibers and carbon nanotubes. The carbon nanotubes (CNTs) have been used widely and effectively as solid phase extraction sorbent materials to separate and pre-concentrate the target element species for speciation analysis (Su-Tae *et al.*, 2015). The discovery of crystalline carbon nanotubes by Iijima (1991) have attracted the worldwide interest due to their exceptional properties such as high mechanical strength, high electrical conductivity, high surface area, competency of forming π-π interaction and high thermal conductivity. Carbon nanofibers have similar chemical properties as carbon nanotubes. They play a significant role in a tremendously diverse range of research and application. Carbon nanotubes exist as a pack of bundles largely hampered by their poor dispensability due to strong van der Waals forces within the tubules. However, to improve the chemical reactivity and interaction of CNTs with foreign molecules, it is necessary to modify the surface for efficiently to execute their analytical capabilities (Su-Tae *et al.*, 2015). Furthermore, CNTs can be seen hollow nanometer size tubes of graphitic carbon, resembling a graphene sheet rolled in the form of seamless cylinder. Two forms of carbon nanotubes are mainly singled-walled carbon nanotubes (SWMCTs) and multi-walled carbon nanotubes (MWCNTs). MWCNTs are described as a number of concentric SWMCTs having different diameters (Iijima, 1991).

Modified nanomaterial exhibit highly specific binding affinities to effectively separate and pre-concentrate the species of interest. MWCNTs functionalised with branched polyethyleneimine (BPEI) were reported excellent sorbent material for the selective retention of As(V) in the presence As(III) when applied for solid phase extraction of water samples. Moreover, the amino rich BPEI is known to be effectively attached on the side walls of the modified MWCNTS through physisorption (Su-Tae *et al.*, 2015). The retained As(V) species is stripped off using diluted NH_4HCO_3 as an eluent (Chen *et al.*, 2013). Carbon nanofibers (CNFs) modified with ammonium pyrroine-dithiocarbamate (APDC) have acquired analytical capabilities to selectively retain As(III). The use of solid phase procedure for arsenic speciation in groundwater samples using micro column packed surface modified CNFs was reported (Karimi *et al.*, 2014). Chen *et al.* (2014) demonstrated that the hydrophobic poly hydroxyethyl methacrylate (PHEMA) is an effective adsorbent for the retention of As-APDC complex. The retained arsenic could be quantitatively eluted by NH_3 solution.

Nanomaterials such as modified magnetite nanoparticles have shown the ability to separate and pre-concentrate arsenic species based on molybdenum blue using spectrophotometric technique (Karimi *et al.*, 2014). The application of the method was based on adsorption of As(V) on cetylmethylammonium bromide immobilised on alumina-coated magnetite nanoparticles (CTAB@ACMNPs) after the oxidation of As(III) using $KMNO_4$ (Karimi *et al.*, 2014).

Various procedures have been reported to modify the surface of nanomaterials. Surface modifications is usually carried out by acid treatment to introduce surface oxides, carboxylic (-COOH), alcohol (-C-OH) and ketone (-C=O) (Malikov *et al.*, 2014; Karimi *et al.*, 2014). The surface oxides act as anchoring sites for the active surface species (polymers, chelating resins, peptides and proteins) to meet the demand for retaining a target analytes of interest attributed to its orientation and specificity (Chen *et al.*, 2013; Malikov *et al.*, 2014; Karimi *et al.*, 2014). The aqueous solutions oxidising agents such as H_2SO_4, HNO_3, $H_2SO_4 + H_2O_2$, $H_2SO_4 + HNO_3$, HCl, HF, $KMNO_4 + H_2SO_4$ are generally used to oxidise carbon nanotubes (Malikov *et al.*, 2014).

This study will focus on speciation of arsenic species in water using SPE technique by employing multi walled carbon nanotubes with branched polyethyleneimine

(MWCNTs-BPEI) sorbent material and detection by ICP-MS (Niedzielski *et al.*, 2002). Multi-walled carbon nanotubes branched polyethyleneimine (MWCNTs-BPEI) composites offer distinct binding affinity with regard to selective retention of arsenic species due to high surface area, the competency of forming π-π interaction as well as chemical and thermal stability (Jablonska-Czapla, 2015). HPLC coupled to ICP-MS will also be used to separate and quantify inorganic and organic arsenic species (George & Gqaza, 2015).

1.5.2. Speciation of chromium in water and sediments

About 90% of chrome ore produced is used in the metallurgical industry for manufacturing of steel and production of ferrous and nonferrous alloys, 5% of it is used in chemical industry, production of Cr pigments, electroplating, leather tanning and wood treatment and 5% in other industrial applications like automotive industry, machinery, glass and ceramics (Gomez & Callao, 2006). The widespread use of Cr in industrial processes has resulted in the release of large amounts Cr emissions into the air, water and terrestrial environments.

In natural environments, chromium mainly exists in two stable oxidation states: chromium(III) and chromium(VI). The two species are very different in charge and physico-chemical properties as well as chemical and biochemical activities. Chromium(III) is an essential trace element for both humans and animals, playing an important role in the normal glucose tolerance factor in insulin action and influencing carbohydrate, lipid and protein metabolism (Underwood, 1977; Anderson & Kozlosvky, 1985). In contrast, chromium(VI) is carcinogenic and mutagenic, and has the capability of crossing cell membranes by way of non-specific anion carriers, causing skin ulcerations, nasal perforations and lung cancer (Underwood, 1977; O'brien & Wang, 1989).

The toxic nature of chromium(VI) is attributed to its action as an oxidising agent, as well as the formation of free radicals during the reduction of chromium(VI) to chromium(III) occurring within the cell. Chromium(III) formed intracellularly, in significant concentration, can cause further adverse effects due to its capacity to inhibit certain metallo-enzyme systems (Kotas & Stasicka, 2000). Accurate and precise speciation of chromium species in environmental and biological samples has become essential, due to these significant differences in toxicity of chromium(VI).

Total chromium measurements alone cannot determine the actual environmental impact/potential hazards on toxicity. Therefore, there is a need to perform a speciation analysis which will determine how much of each chromium species is present in the sample (Beaublen *et al.*, 1994). However, speciation of chromium is a challenging task, conditions during sample collection and treatment can easily affect the stability of different chromium species (DeJong & Brinkman, 1978). Another challenge encountered with chromium speciation is that the concentration of these species in natural waters is usually very low, in the order of a few µg/L, as such, these low concentrations necessitates the use of very sensitive analytical techniques or the application of suitable pre-concentration methods prior to instrumental determination (Nriagu & Nieboer, 1988).

The speciation of chromium is carried out by separation and determination of the different chromium species and then followed by the determination of total chromium (Lund, 1990). The quantification of trace levels of chromium species requires separation and/or pre-concentration stages, followed by detection by an instrumental technique. Main selective techniques known for speciation and determination of chromium are: co-precipitation, separation with ion exchanger and/or chelating resin, solid phase extraction and solvent extraction (Kotas & Stasicka, 2000).

Solid phase extraction procedures have been widely used in chromium speciation studies in water and sediments due to their simplicity, selectivity, flexibility, high enrichment factors, safety, absence of emulsion formation, sampling in the field, economic and environment friendliness and ease of automation (Rao & Sastri, 1980). In these procedures, various solid phases such as artificial adsorbents, activated carbon, sephiolite, etc. have been used. Ambushe *et al.* (2009) used the chromabond NH_2 column for the speciation of chromium in milk samples prior to ICP-MS detection. Chromabond NH_2 column are preferred because they provide rapid, economical and effective systems for sample preparation. Chromabond NH_2 column will be used for pre-concentration and separation of hexavalent chromium in water.

1.5.3. Speciation of selenium in water and sediments

Naturally occurring selenium is trace element of concern in the South African geological environment. However, little is known about its occurrence and distribution in South African water bodies. Selenium is abundant in sulphide minerals, such as galena, arsenopyrite, pyrrhotite, marcasite and chalcopyrite (Sami & Druzynski, 2003). Natural sources of selenium include cretaceous marine sedimentary rocks, coal and other fossil fuels. Anthropogenic sources of selenium in surface water include coal ash from coal-fired power plants, irrigation waters from seleniferous soils and wastewaters from some industrial processes. The fact that trace constituents of selenium are relatively common in aforementioned sources suggests the distribution and mobilisation of selenium species should be of concern to human beings, animals and aquatic ecosystem.

Selenium is an essential element, which is required in trace amounts for good health due to its antioxidant activity, but it is toxic at three to five times higher concentrations than the bio-essential level (Latorre *et al.*, 2013). This narrow difference between the essential and toxic levels of selenium compels the quantification and speciation of selenium in water. Selenium toxicity depends on the chemical form of the element. The inorganic forms of selenium; selenite (Se(IV)) and selenate (Se(VI)) showed toxicity up to 40 times higher than the organic forms selenomethionine and selenocysteine (Vinceti *et al.*, 2013). Recent studies revealed that the tolerable upper daily intake limit for selenium is 40 µg/l. When this tolerable daily intake limit is exceeded, selenosis can occur. Taking these facts into consideration, it is very important to determine the levels of selenium species in water and sediment samples (Herrero *et al.*, 2013).

Selenium toxicity related diseases were reported in China. The incident was associated with selenium derived from nearby mines. Between 1923 and 1988, 477 cases of human selenosis were reported. Among the 477 cases, 338 resulted in hair and nail loss, and disorders of the nervous system (Fordyce, 2012). In South Africa, there are potential sources of selenium that water may contain unacceptable levels of selenium and where the problem remains unknown for many years until detrimental effects are recognised by health practitioners.

Selenium species concentrations in an environmental samples are very low. In order to determine selenium species in water, some rapid, simple, inexpensive, more sensitive and reproducible separation and pre-concentration methods are always required (Zhang *et al.*, 2013).

For a simple elemental speciation, especially for different oxidation states of a given element, non-chromatographic methods are more popular than chromatographic techniques. However, these techniques are time consuming and hazardous to the environment and human health, especially in the case of liquid-liquid extraction in which large volumes of solvents are used (Li, 2008; Najafi *et al.*, 2010). Because of the disadvantages of conventional extraction techniques, solvent-free sample preparation methods or those employing fewer organic solvents are becoming increasingly important (Najafi *et al.*, 2010).

A SPE has widely been used as a pre-concentration procedure for trace elements due to its high enrichment factor, good recovery, fast phase separation, low consumption of organic solvents and time saving. Appropriate enhancements in sensitivity and adequate elimination of interferences and sample matrix have been achieved with this procedure (Herrero *et al.*, 2013).

Cloud Point Extraction (CPE) using non-ionic surfactants have also attracted attention as an alternative to the traditional methods. A CPE is simple, inexpensive, using less organic solvents with capacity to pre-concentrate a wide variety of analytes with high recoveries and high pre-concentration factors (Tadayon *et al.*, 2014).

In recent years, many modern instrumental techniques have been used for the determination of Se(IV) and Se(VI). Among these techniques, ICP-MS has been frequently applied for the determination of selenium due to its high sensitivity with a wide linear dynamic range and the capability of isotopic determination (Zhang *et al.*, 2013).

1.6. Sequential extraction of potentially toxic elements in sediments

South Africa’s freshwater resources, including rivers, man-made lakes and groundwater, are under increasing stress due to increased pollution caused by industrialisation, urbanisation, mining, agricultural activities and power generation (Oberholster & Ashton, 2008). Mining is a significant contributor to water pollution due to pyrite oxidation that generates potentially high levels of acidity, metal ions (mainly Fe) and sulphate (Bologo *et al.*, 2012). Different sources of pollution of Umtata River by potentially toxic elements were reported (Fatoki *et al.*, 2002). The sources include rural, urban and agricultural runoff in the catchment, although there may be contributions from natural and point sources. Sand mining within Mokolo River is another factor of potential concern reported by de Klerk *et al.* (2016). The Council for Scientific and Industrial Research (CSIR) reported that raw sewage disposal, irresponsible mining and agricultural fertilisers seeping into Olifants River have polluted the river and resulted in death of crocodiles (de Villiers & Mkwelo, 2009). High levels of Cd and Pb were detected in water and sediments from Tyume River, Eastern Cape Province, South Africa (Awofolu *et al.*, 2005). The high levels of toxic metals such as Cd and Pb are detrimental to the health of the aquatic ecosystem and the rural communities that utilise river water for domestic purposes without any treatment.

Sediments are important sources of information about the current and long-term trends in geochemical and ecological conditions of aquatic systems and their catchment areas. Potentially toxic elements may be adsorbed directly by the sediments of the water course. However, these elements are not permanently fixed by sediment. Changes in environmental conditions, such as acidification, redox potential or organic ligand concentrations, can cause mobilisation of potentially toxic elements from sediment to overlying waters, and in turn adversely affects aquatic environment (Yuan *et al.*, 2004). Several factors such as nature of the sediments, grain size, properties of adsorbed particles and metal characteristics control the mobility and accumulation of heavy metals in sediments (Vetrimurugan *et al.*, 2016). Therefore, sediments characterise the degree of environmental contamination by metals and therefore are suitable target for pollution studies.

The risk of contaminated sediment by potentially toxic elements strongly related with their specific chemical fraction and binding state. Thus, analysing the total concentration alone is insufficient. Furthermore, speciation analysis of potentially toxic elements in sediment is helpful to understand their source, mode of occurrence, mobility, and bioavailability related with the realistic risk assessment (Yang *et al.*, 2014). Determination of total metal content cannot provide information about mobility, bioavailability and toxicity of the metals. These properties depend on the chemical speciation of the different components of the sample (Qjao *et al.*, 2013). Thus, fractionation of potentially toxic elements in sediment by sequential extraction is helpful to understand their source, mode of occurrence, mobility, and bioavailability related with the realistic risk assessment (Yang *et al.*, 2014).

The growth in interest in sequential extraction of potentially toxic elements may be traced back to the classic work of Tessier, Campbell and Bison in 1979 (Tessier *et al.*, 1979). They used sequential extraction method that includes five stages to fractionate Cd, Co, Cu, Fe, Pb, Mn, Ni and Zn in river sediments. The reagents for extraction were selected on the basis of their ability to remove analytes from specific and major sediment phases either by exchange processes or by dissolution of the target phase. Extraction stages also corresponded with, or at least represented extremes of important changes in environmental conditions that could affect metal binding in sediments. These include acidification (for example in response to an input of acidified rainwater or industrial discharge), reduction (for example as may occur following post-depositional burial in a sediment column) and oxidation (for example as might occur following dredging and land-deposition of anoxic sediments) (Bacon & Davidson, 2008). Sequential extraction method was originally developed to provide information on potential impacts of potentially toxic elements on water quality. However, the procedure has been applied to other environmental matrices (Pagnanelli *et al.*, 2004; Anju & Banerjee, 2010; Arenas-Lago *et al.*, 2014; Zhu *et al.*, 2014).

The Community Bureau of Reference of the Commission of the European Communities (BCR) commissioned a research that led to the development of a harmonised three step sequential extraction protocol. The BCR protocol consists of three successive steps for selective extractions of the following: acid soluble (step 1), for example carbonates, reducible (step 2), for example oxides of ferric and manganese, and oxidisable metals (step 3), for example organic matter and sulphides (Castillo *et al.*, 2011). The sequential extraction procedure has been widely accepted and applied to fractionation of potentially toxic elements in different environmental samples (Yuan *et al.,* 2004; Arain *et al.*, 2008; Anju & Banerjee, 2010; Arenas-Lago *et al.*, 2014; Zhu *et al.*, 2014).

Metal ions in sediments are portioned in different phases such as organic matter, oxyhydroxides of iron, aluminum and manganese, phyllosilicate minerals, carbonates and sulphides. Moreover, metal ions in these solid phases are retained by different mechanisms. These mechanisms include ion exchange, outer- and inner-sphere surface complexation (adsorption) and precipitation or co-precipitation (Nemati *et al.*, 2011). Although the separation of various chemical forms of potentially toxic elements is very difficult, the use of sequential extraction method proves to be an effective approach. Sequential extraction provide information that helps in identifying the main binding sites, the strength of metal binding to the particulates and the phase associations of trace elements in sediment. This could help us to understand the geochemical processes governing potentially toxic elements mobilisation and potential risks associated with their mobilisation.

There is inadequate data on potentially toxic elements levels in South African water bodies. This could be attributed to relatively few studies that have been conducted in South Africa dealing with the levels of potentially toxic elements particularly the speciation in surface waters.

Supply of potable water is particularly problematic in the rural areas of South Africa where poverty levels are higher than those in urban areas (Oberholster & Ashton, 2008). Lack of adequate potable water supplies often results in poor households having no option but to use unsafe sources of water. In rural areas, poor households have limited access to treated tap water and need to fetch water from a well, stream or river each day (Oberholster & Ashton, 2008; Genthe *et al.*, 2013). Therefore, assessment of the levels of potentially toxic elements and their species in water samples collected from rivers is necessary.

2. EXPERIMENTAL

2.1. Description of Study Areas

The Limpopo province of South Africa has a number of rivers subjected to pollution by heavy metals from mining activities and other sources. The Blood, Mokolo and Great Letaba Rivers are to mention few among others. Collection of water and sediment samples were conducted from the selected sites in these rivers.

2.1.1. Blood River

The Blood River is located at Seshego area about 14.5 km away from Polokwane and it originates in the west of the Polokwane municipal area. According to the Polokwane municipality report in 2012, it was stated that municipal and domestic wastes are the factors that contribute to environmental pollution. Lack of waste removal services, illegal dumping sites close to the river banks, lack of storm water drainage among others contribute to Blood River contamination (Polokwane Municipality Report, 2012). The river is heavily polluted by municipal and domestic wastes. Furthermore, run off from urban areas and wastewater arising from human activities such as domestic residences, institution and commercial establishments could be the potential source of pollution.

There are dumping sites near different parts of Blood River, sand mining activities and direct discharge of effluents into the river. Increased organic matter from sewage effluents reduces the amount of dissolved oxygen in the water body which is essential for fish and other aquatic life to survive in the water (Munawar *et al.*, 1993). Sewage effluents can also introduce other chemicals and heavy metals into the water system. Local farmers utilise water from Blood River for irrigation purposes and fishing activities. However, residents do not collect water for drinking purposes. Sampling sites in Blood River are shown in Figure 2.1.

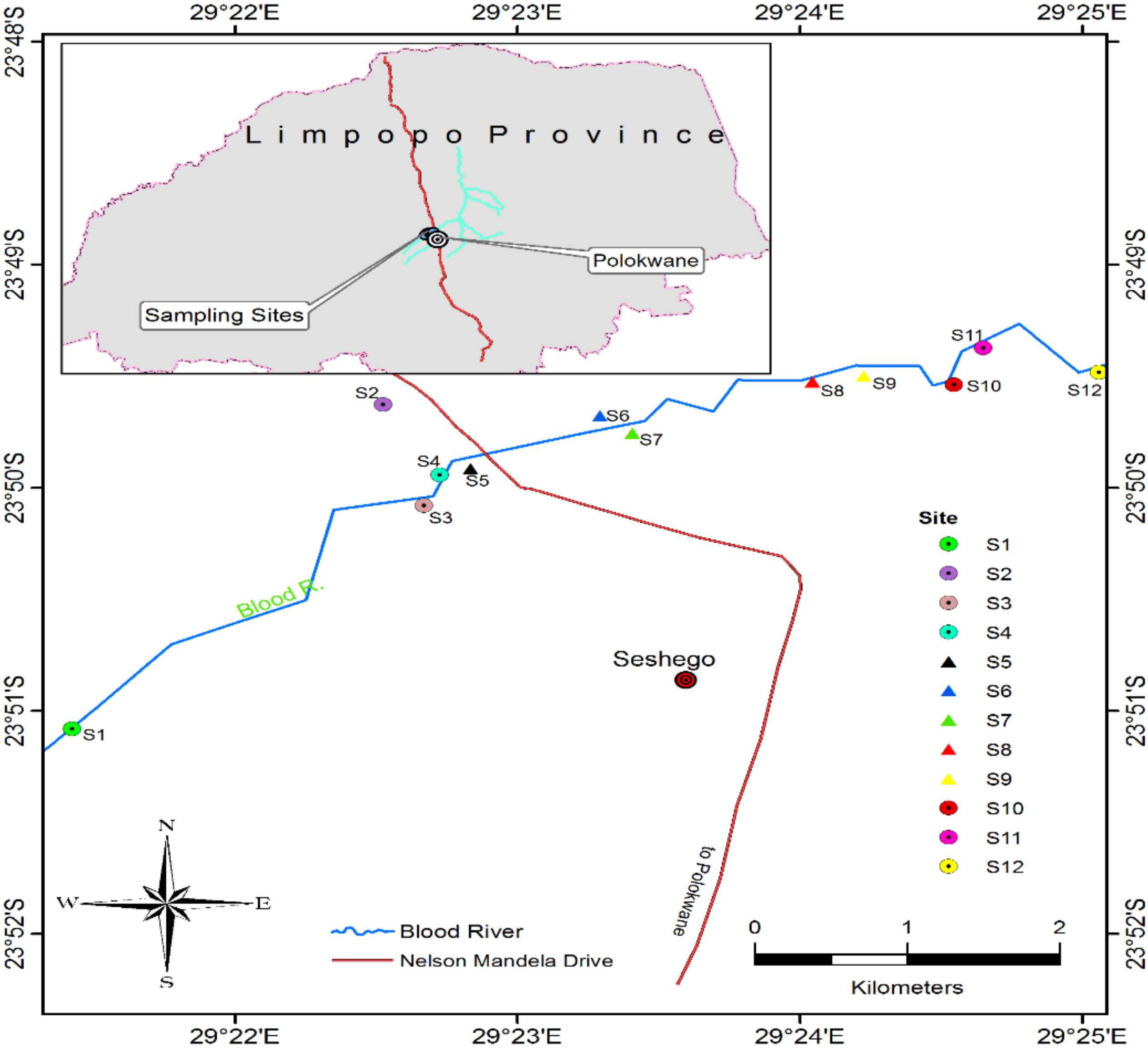

Figure 2.1: Sampling sites in Blood River.

Figure 2.2: Photos showing the conditions of Blood River.

2.1.2. Mokolo River

Lephalale local municipality falls within a water-scarce region in which the demand for water is increasingly high and cannot be met by the already available water resources in the area (Schachtschneider *et al.*, 2010). Water source for Lephalale area is Mokolo River. The Mokolo River is located in the Waterberg region of the Limpopo province. The Mokolo River flows in a north-western direction and reaches the Limpopo River at the border of South Africa and Botswana, which highlights the international importance of Mokolo River (de Klerk *et al.*, 2016). Mokolo dam was constructed to supply water to Lephalale municipality, power stations, coal mine as well as for irrigation of downstream farmlands (DWA, 2008). The majority of people in Lephalale live in scattered rural settlements, which puts a strain on the supply of potable water

(Lephalale Municipality Report, 2009). The main industrial sources of pollution in the Lephalale are the Matimba coal-fired power station and the Grootegeluk coal mine (Lephalale Municipality Report, 2012; Oosthuizen, 2013). Potentially toxic elements such as, Cd, Cr, Cu, Hg, Mn, Mo, Ni, Pb, Sb, Se, V, and Zn are associated with coal (Wagner & Hlatshwayo, 2005). Mokolo River in Lephalale, which is situated close to Grootegeluk coal mine as well as Medupi and Matimba power stations has been selected.

The Mokolo River currently faces risks that exert adverse impacts on water quality. These risks include the possible contamination of water of the river through treated and untreated sewage effluent discharges, agricultural runoff and return flows, as well as contamination from mining activities. The developments in the area (i.e. mining, power generation and associated activities), particularly around Lephalale town, have the potential to cause widespread adverse impacts on the water and sediment quality of the river (de Klerk *et al.*, 2016). Monitoring the impact of the Grootegeluk coal mine and Medupi and Matimba power stations on Mokolo River is necessary to control and improve the quality of water. Mokolo River is mostly utilised for agricultural, recreational (swimming) and mining activities. Furthermore, local residents collect the water for household use.

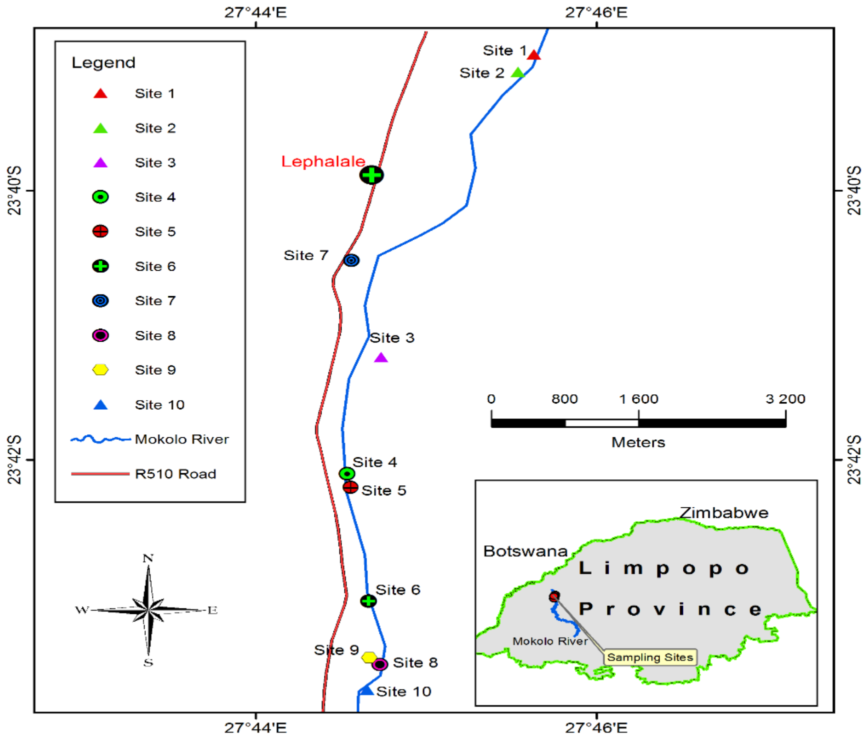

Figure 2.3: Sampling sites in Mokolo River.

Figure 2.4: Photos depicting sand mining and water abstraction for irrigation of agricultural crops in Mokolo River.

2.1.3. Great Letaba River

The headwater streams of the Great Letaba River originate in the Drakensberg Escarpment, descending in long runs with an occasional riffle or pool. The river banks are of gentle slope (WRC Report, 2001). The Tzaneen Dam on the Great Letaba River and the Middle Letaba Dam are the two largest dams in Limpopo Province. Other large dams in the catchment include the Ebenezer, Magoebaskloof, Nsami and Modjadji Dams (WRC Report, 2001). The Great Letaba River is mainly used for irrigation of agricultural crops. The Tzaneen and Letsitele regions of this river support the farming of citrus, mango, and banana crops (Iwuoha and le Roux, 2012). The agricultural activities alongside of the river banks could contribute to the contamination of the river since potentially toxic elements in chemical fertilisers and pesticides will end up in the river.

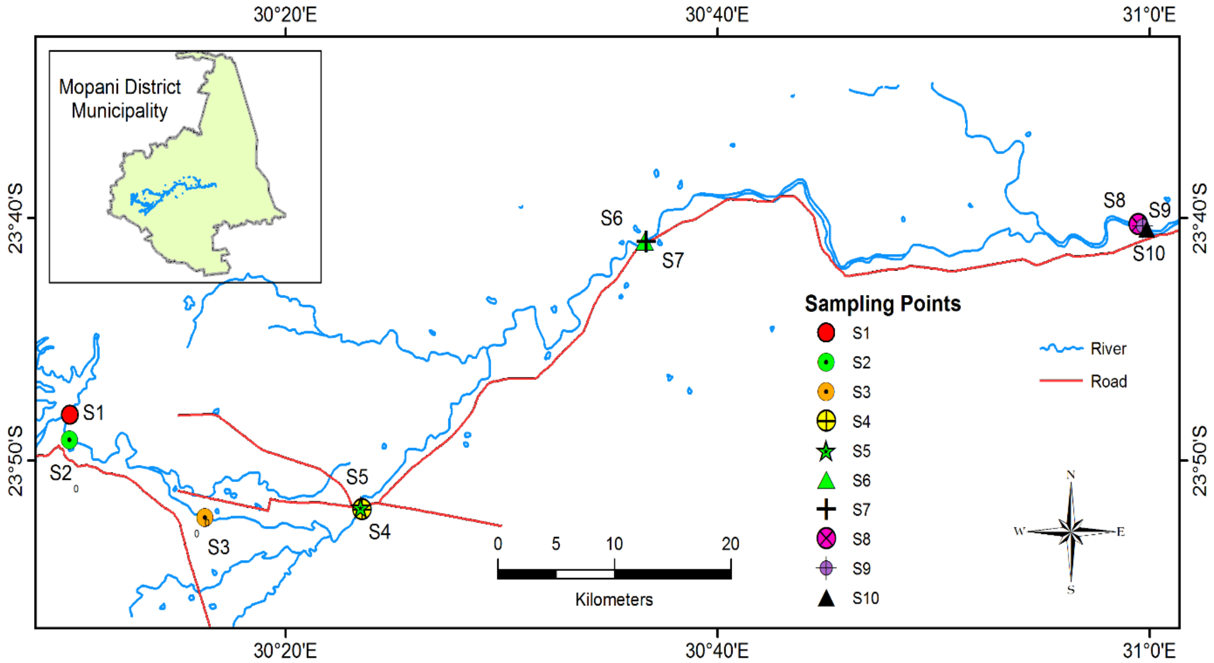

Figure 2.5: Sampling sites in Great Letaba River.

Figure 2.6: Photo showing livestock, swimming and fishing activities in Great Letaba River.

2.2. Sample collection and field measurements

Water quality parameters, namely temperature, pH and electrical conductivity were measured at each sampling site using 900P Bate Instruments Limited a portable multi-parameter meter. Water samples were collected at each site in clean, pre-rinsed 1-L polyethylene bottles and kept in cooler box and transported to the laboratory. Water samples were filtered using 0.45 µm membrane filter. Water samples for total concentration determination of potentially toxic elements were acidified using 1% ultrapure HNO_3 and kept at 4°C in refrigerator until taken out for analysis. Water samples for speciation analysis were kept at 4°C in refrigerator until taken out for analysis after filtration without acidification. Sediment samples were collected at a depth of 20 cm using a plastic scoop. Both water and sediment samples were collected from 10 different sampling sites in each river. Ten water and ten sediment samples were collected from each river. Samples were collected on 14 April 2016, 20 April 2016 and 26 April 2016 from Great Letaba River, Mokolo River and Blood River, respectively.

2.3. Sample preparation for determination of total concentrations

Water samples were filtered using a 0.45 µm syringe filter and acidified with 1% (v/v) ultra-pure HNO_3 before determination of total concentrations of trace elements. The sediment samples were dried, grinded, homogenized and sieved using a sieve size of 63 µm before mineralization using microwave-assisted acid digestion. The procedure presented in table 2.1 was developed for complete digestion of sediment samples. The complete digestion of sediment samples were confirmed by obtaining clear solutions.

Table 2.1: Microwave-assisted acid digestion conditions.

Parameters	Stage 1 conditions	Stage 2 conditions
Temperature	150°C	200°C
Ramp time	20 min	20 min
Hold time	20 min	15 min
Cooling time	10 min	10 min
Pressure	800 psi	800 psi
Power	1600 W	1600 W
Volume of reagent	4 mL, 2 mL and 2 mL	2 mL
Reagents	HCl, HNO_3 and HF	H_3BO_3

2.4. Reagents, Standard Reference Materials and Standards

High-purity reagents were employed in all experiments. Doubly deionised water with a resistivity of 18.2 MΩ cm, produced by milli-Q water system was used throughout. Standards of 1000 mg/L (Fluka, Buchs, Switzerland) were used for preparation of calibration standards for each analyte.

2.5. Apparatus and instrumentation

A portable multi-parameter meter 900P was used to measure pH readings of the water samples during sample collection. A Microwave acid assisted digestion system (CEM Corporation, MARS 5, USA) was used for mineralisation of the potentially toxic elements in sediments samples. Quantification of levels of potentially toxic elements in both water and sediment samples was performed by ICP-MS (Perkin Elmer, Elan 6100, USA) and F-AAS (Perkin Elmer, Syngistix, USA). The instrument parameters are presented in table 2.2. The extraction of As species was carried out using microwave extraction system (Anton Paar Multiwave Pro, Canada). The HPLC (Flexar, Perkin Elmer, Singapore) coupled to ICP-MS (Elan 6100, Perkin Elmer, Germany) was used for separation and detection of As species. The concentrations of potentially toxic elements in sediments were measured using ICP-OES (Table 2.3).

Table 2.2: Instrumental conditions for ICP-MS analysis.

Parameters	**Instrumental settings**
Model	Perkin Elmer Elan 6100
Lens voltage	10 V
RF power	1150 W
Main water temperature	18°C
Interface water temperature	32.6°C
Analog stage voltage	-2250 V
Pulse stage voltage	1050 V
Torch box temperature	31.6°C
Argon flow rate: nebuliser	1.0 L/min
: plasma	14 L/min
: auxiliary	1.2 L/min

Table 2.3: Instrumental conditions of ICP-OES.

Parameters	**Operating conditions**
Instrument	ICP-OES-9000 Shimadzu
RF power	1.20 kW
Plasma gas flow rate	10 L/min
Nebuliser gas flow rate	0.7 L/min
Auxiliary gas flow rate	0.60 L/min
Sample flow rate	1.0 L/min
Nebuliser type	Cross flow
Plasma torch	Mini torch
View direction	Axial
View position	Low
Gas type	Argon

The GF-AAS with Zeeman background correction was employed for determination of Cr species in water and sediment samples. The heating program is presented in Table 2.4.

Table 2.4: The furnace program employed for the measurement of Cr species

Step	Temperature °C	Ramp time s	Hold time s	Gas flow mL/min
1	110	1	20	250
2	150	5	30	250
3	1000	5	10	250
4	2300	0	5	0
5	2450	1	3	250

2.6. Determination of arsenic species in water and sediment samples using HPLC/ICP-MS

Filtered water samples were transferred into plastic vials and loaded to HPLC (Flexar, Perkin Elmer) coupled to ICP-MS (Elan 6100, Perkin Elmer) for As species separation and quantification. Mobile phases were prepared in a sterilised glassware by dissolving appropriate amount NH_4NO_3 in de-ionised water. Mobile phases were adjusted to a pH of 8.7 using NH_3 solution. The powdered sediment samples of 500 mg were transferred into pre-cleaned Teflon vessels for extraction of As species using microwave extraction system (Anton Paar Multiwave Pro, Canada). A 10 mL of extractant solutions was then added into Teflon vessels. The extractant solution was prepared from 0.3 M $(NH_4)_2HPO_4$ and 50 mM EDTA. The EDTA was dissolved in 5% NH_4OH before preparation of extractant solution. The vessels were mounted in the rotor and placed in the microwave extraction system. Extracts were allowed to cool and filtered using 0.45 µm Acrodisc syringe filters. Later, 5 mL of extracts were diluted to 10 mL and kept in the refrigerator at 4°C for maximum of 3 days before analysis using HPLC-ICP-MS. The optimised microwave heating conditions for extraction and HPLC-ICP-MS parameters are presented in tables 2.5 and 2.6, respectively.

Table 2.5: Heating conditions for microwave extraction system.

Parameters	settings
Power	100 W
Pressure	30 bar
Maximum pressure rate	0.5 bar/s
Internal temperature limit	150°C
Ramping time	20 min
Holding time	15 min

Table 2.6: The HPLC-ICP-MS operating conditions for separation and detection of arsenic species.

Parameters	Settings
HPLC parameter and setting instrument	Perkin Elmer Flexar solvent manager
Analytical column	Hamilton PRP-X100
Column dimension	4.6 x 250 mm, 5 µm
Guard column dimension	4.6 x 150 mm, PEEK
Pump flow rate	1 mL/min
Pump pressure	2320 psi
Injection volume	100 µL
Mobile phase A	10 mM NH_4NO_3 at pH 8.7
Mobile phase B	60 mM NH_4NO_3 at pH 8.7
ICP-MS parameter and setting instrument	PerkinElmer Elan 6100
Nebulizer gas flow	1.0 L/min
Auxiliary gas flow	1.2 L/min
Plasma gas flow	14 L/min
ICP RF power	1350 W
Lens voltage	14 V

2.7. Modification of adsorbent material for solid phase extraction inorganic arsenic in water samples

The oxidisation of MWCNTs was achieved by exploring the performance of combinations of various acids under the optimised conditions to successfully introduce the functional groups of interest. A 300 mg of MWCNTs were sonicated with a mixture of H_2SO_4/HNO_3 (3:1, v/v) at 30°C for 30 minutes. The oxidised MWCNTs were collected by filtration and repeatedly washed with de-ionised water until the pH of 7 is reached. Oxidised MWCNTs were dried in an oven at 50°C for overnight before the modification with BPEI polymer.

The incorporation of BPEI polymer to oxidised MWCNTs (3:1; w/v) was achieved by stirring a mixture of 500 mg oxidised MWCNTs and BPEI polymer, which was prepared by dissolving 1500 mg of BPEI into 30 mL of 1.0 M NaCl for 12 hours using magnetic stirrer plates at room temperature. The MWCNTs-BPEI nanocomposite was collected by vacuum filtration and washed thoroughly with de-ionised water to remove the impurities. The complete removal of NaCl impurities were tested using 0.1 M $AgNO_3$ solution.

2.8. Column preparation for solid phase extraction and sample analysis

A syringe was blocked at the end with small amount of glass wool to avoid the leakage of nanocomposites during the adsorption process. A 40 mg of the MWCNTs-BPEI was used to pack the column. Prior to adsorption process, column was conditioned with de-ionised water and let it to dry. Water samples with volume of 350 mL were passed through a packed column. The SPE columns were dried completely before the elution step. The retained As(V) in all the columns were stripped off from the walls of the nanocomposites by passing 2 mL of 0.6% (m/v) NH_4HCO_3 through the columns. The eluents from all the columns were diluted to 15 mL and analysed using ICP-MS.

2.9. Pre-concentration and determination of Cr(VI)

A standard solution of Cr(III) and Cr(VI) containing 0.5 µg/L of each in 100 mL was mixed with 5 mL of 0.001% alizarin sulphonic acid solution. The pH of the sample solution was adjusted to 5.5 using acetic acid and sodium acetate.

Column conditioning was achieved with two column volumes of 1 M HNO_3 followed by two column volumes of de-ionised water. Selective retention of Cr(VI) in the column was quantitatively achieved by passing the sample through the column at a flow rate of 3 mL/min. After retention of Cr(VI), the content was dried under vacuum. The retained Cr(VI) was eluted with two column volumes of 2 M HNO_3.

A 100 mL of water sample was mixed with 5 mL of 0.001% alizarin sulphonic acid solution. The pH of the sample was adjusted to 5.5 using acetic acid and sodium acetate buffer.

The stability of separated Cr(VI) solution was evaluated. The separated Cr(VI) solution was kept in the refrigerator at 4°C. The stability of Cr(VI) was assessed by analysing the solution every seven days for three weeks.

2.10. Determination of Cr(VI) in sediment samples

A 0.25 g of sediment sample was transferred into a vessel. A 10 mL of 0.1 M Na_2CO_3 was added to the content and Cr(VI) in sediment sample was extracted using microwave extraction system following the extraction conditions presented in Table 2.7. After cooling, the sample was filtered through Whatman No: 540 filter paper and diluted to a final volume of 50 mL using de-ionised water. The sample solution was further filtered through Hydrophilic Millipore PVDF 0.45 µm filter prior to determination of Cr(VI) by GF-AAS. The method was validated by spiking Cr(VI) into sediment sample and applying the extraction procedure before analysis of the sample using GF-AAS.

Table 2.7: Extraction conditions employed for extraction of Cr(VI) in sediment samples.

Parameter	Conditions
Temperature	120°C
Ramp time	15 min
Hold time	15 min
Cooling	15 min
Pressure	700 psi
Power	100 W

Similarly, the extraction of Cr(VI) in sediment samples using 0.01 M Na_3PO_4 was done applying the extraction conditions in table 2.7. A 0.25 g sediment sample was transferred into a microwave vessel. A 10 mL of 0.01 M Na_3PO_4 was added to the content and Cr(VI) in sediment sample was extracted using a microwave extraction system. After cooling, the sample was filtered through Whatman No: 540 filter paper and diluted to a final volume of 50 mL with de-ionised water. The diluted solution was filtered through Hydrophilic Millipore PVDF 0.45 µm filter prior to determination of Cr(VI) by GF-AAS.

2.11. Sequential extraction procedure

Potentially toxic elements in sediments were sequentially extracted employing the BCR protocol applied by Castillo *et al.* (2011). The procedure is summarised in table 2.8.

Table 2.8*:* Summarised sequential extraction procedure.

Fractionation	**Fraction**	**Reagent**	**Time**
F1	Exchangeable	0.11 M acetic acid	16 h
F2	Reducible	0.50 M hydroxyl ammonium chloride	16 h
F3	oxidisable	8.8 M hydrogen peroxide & 1.0 M ammonium acetate	1 h/16 h
F4	Residual	Nitric acid, hydrochloric acid & hydrofluoric acid	Ramp: 15 min Hold: 15 min

During stage 1 of the BCR protocol, 1.0 g of powdered and sieved sediment sample was weighed into a pre-cleaned 15 mL centrifuge tube and 4 mL of 0.11 M acetic acid was transferred into the centrifuge tube then shaken for 16 h on the mechanical shaker. The extraction solution was separated from the solid residue by centrifugation at 3000 rpm for 15 min and decantation of the supernatant liquid was done. The latter was then removed with a pipette, the extracted fraction was transferred into a centrifuge tube and stored at 4°C in a refrigerator. The residue was washed by adding 2 mL of 0.11 M acetic acid and shaking for 15 min at 3000 rpm in the centrifuge. Further washing with 2 mL of de-ionised water, centrifuging for 15 min at 3000 rpm was done and the residue was used to proceed with stage 2 of the procedure.

In stage 2, 4 mL of 0.50 M hydroxyl ammonium chloride solution was added to the residue from stage 1 and shaken for 16 h at room temperature. The extractant was stored and the residue was continually used in stage 3 of the extraction procedure. In stage 3, 1 mL of 8.8 M hydrogen peroxide was added to the residue from stage 2 and the centrifuge tube was covered and left to react at room temperature for 1 h. The extraction was continued for a further 1h at 80°C in an ultra-sonic bath, the volume was reduced by further heating the content. Another 1 mL aliquot of 8.8 M hydrogen peroxide was added and heated again at 80°C for 1 h. The cover was removed and the volume reduced. A 5 mL of 1.0 M ammonium acetate was added to the cool the residue and the extraction performed as in stage 1.

An additional procedure to mineralise the residue from stage 3 was added to BCR sequential extraction procedure. A mixture of HNO_3, H_2O_2 and HF was employed to digest the residue. The solution was diluted to 50 mL with de-ionised water and potentially toxic elements were determined using ICP-MS.

2.12. Microwave-assisted sequential extraction procedure

Microwave-assisted sequential extraction procedure was employed by modifying the method reported by Castillo *et al.* (2011) and summarised in table 2.9.

A 0.25 g of the powdered and sieved sediment sample was weighed directly into each pre-cleaned Teflon vessel and the reagents from the BCR sequential extraction protocol were added as described with respect to the different stages. The vessels were placed inside a rotor of the microwave extraction system, sealed, tightened using a torque wrench and finally submitted to the microwave extraction program. After cooling, the supernatant liquid was separated from the solid phase by centrifugation at 3000 rpm for 30 min. The solution was evaporated near to dryness to eliminate unreacted reagents. The residue from the extraction stages was subjected to the mixture of HCl, HNO_3 and HF for complete mineralisation of silicate materials. The solution were diluted to 25 mL using de-ionised water. The different fractions were analysed by ICP-OES.

Table 2.9: Instrumental conditions and microwave-assisted sequential extraction procedure.

Stages	**Stage 1**	**Stage 2**	**Stage 3**	**Residual stage**
Reagents	Acetic acid (0.11 M)	Hydroxylamine hydrochloride (0.50 M)	Hydrogen peroxide (32%) and ammonium acetate (1.0 M)	Hydrochloric acid, Nitric acid and Hydrofluoric acid.
Volume of reagent	4 mL	4 mL	2 mL:4 mL	3 mL:1 mL: 2 mL
Temperature	200°C	150°C	200°C	200°C
Ramp time	20 min	15 min	20 min	15 min
Hold time	20 min	15 min	20 min	15 min
Cooling time	10 min	10 min	10 min	10 min
Pressure	800 psi	800 psi	800 psi	800 psi
Power	1600 W	1600 W	1600 W	1300 W

2.13. Preparation of functionalised MWCNTs

Functionalisation of the MWCNTs was achieved by sonicating 2 g of MWCNTs at 25°C in 1300 mL mixture of H_2O_2 and HNO_3 in a ratio of 3:1 (v/v). After 3 h of sonication, the acid treated MWCNTs were diluted with de-ionised water and filtered through 0.45 μm pore sized nylon membrane. The acid-treated MWCNTs were washed thoroughly with de-ionised water until neutral pH was reached and dried overnight.

2.14. Preparation of the functionalised MWCNTs/ polyvinyl alcohol (PVA) composites

A 0.2 g of functionalised MWCNTs was poured in the mixture of 2 g of polyvinyl alcohol (PVA) and 20 mL dimethyl sulfoxide (DMSO) in a three-necked flask equipped with a magnetic stirrer. The mixture in the flask was slowly heated from room temperature to 90°C. When the PVA was completely dissolved, 1 g aluminum chloride ($AlCl_3$), which serves as a catalyst was added. The mixture was continually stirred at 70°C for 24 h under a nitrogen atmosphere. The reaction was terminated by pouring the mixture into methanol/hydrochloric acid (volume ratio 1:1), then centrifuged at 3000 rpm for 15 min and the precipitate was washed with de-ionised water several times until no $AlCl_3$ could be detected. Finally, the functionalised MWCNTs were obtained after drying at 70°C for 3 h. Since PVA exists in many different molecular weights, the small molecular weight ranging between 13.00 g/mol to 23.00 g/mol (PVA1) and high molecular weight ranging between 146.00 g/mol to 186.00 g/mol (PVA2) were chosen.

2.15. Synthesis of MWCNTs-ethylenediamine (EDA)

For the synthesis of MWCNTs-ethylenediamine (EDA), 2 g of MWCNTs-COOH was suspended in 75 mL of EDA under stirring and heating. The solution was refluxed under nitrogen gas for 48 h and the product was filtered, washed off and dried in an oven overnight.

2.16. Preparation of polyamido-amine (PAMAM) dendrimer on the MWCNTs surface initiated by MWCNTs-NH_2

Michael addition of methyl acrylate (MA) to peripheral amino groups was carried out as follows. A 0.1 g of MWCNTs-NH_2 was dispersed in methanol (20 mL) while stirring and then added to 40 mL of methanol/MA solution (1:1) to react at 30°C for 48 h. The product was filtered, washed, and dried, yielding functionalised MWCNTs containing the “first generation” ester group (MWCNTs-$G_{0.5}$-$COOCH_3$).

The MWCNTs-$G_{0.5}$-$COOCH_3$ was dispersed in methanol (20 mL) while stirring and then added to 40 mL of methanol/EDA solution (1:1) to react at 30°C for 48 h. The resultant was washed with methanol, filtered, and dried, yielding functionalised MWCNTs containing the "first generation" amino groups (MWNTs-G_1-NH_2). The resulting nanocomposites were characterised using FTIR, TGA, scanning electron microscope (SEM), transmission electron microscope (TEM) and X-ray diffraction (XRD).

2.17. Batch experiments for simulated metal ion solutions

Batch experiments were carried out using a series of 80 mL beakers with 10 mL of metal ion solution. The effect of pH was investigated in range 2.5 to 12.5 and was adjusted with 0.1M HCl and 0.P NaOH. The mixture of 0.05 g nanocomposite and 20 mg/L of metal ion was stirred vigorously for 60 min to facilitate adsorption of the metal ion onto the adsorbents. The adsorbent was filtered and the filtrate concentration was determined by FAAS.

To study the effect of initial metal ion concentration, a series of 80 mL beakers containing different concentration solutions ranging from 20 mg/L to 100 mg/L were investigated in a 10 mL of metal ion solution. The mixture of 0.05 g nanocomposite at optimum pH was stirred vigorously for 60 min. At the end of the predetermined time the adsorbent was filtered and the final concentration of the filtrate was determined using FAAS.

Similar procedure was also performed to assess the effect of time on adsorption of metal ion. However, the optimum pH and metal ion concentration that provided high percentage removal were fixed. Five solutions with 30min time interval were stirred until investigated time was reached. The solutions were filtered and the filtrate was analysed.

Similarly, the effect of adsorbent dose was assessed applying the optimized parameters. The adsorbent dosage was 0.03, 0.05, 0.07, 0.09, 0.11 and 0.13 g, all the experiments were performed at room temperature. After the established time the solution was filtered then filtrate was analysed using F-AAS.

2.18. Sample analysis

Analysis of water and sediment samples were conducted using F-AAS and ICP-MS. Blanks, standards and water samples were analysed. Concentrations of potentially toxic elements in water and sediment samples were determined using an external calibration curve method.

2.19. Limit of detection and limit of quantification

To determine the limit of detection (LOD), reagent blanks were prepared following the same experimental procedure for the quantification of trace elements in water samples. The LODs were calculated as three times the standard deviation (3σ) of six prepared blank solutions. The limit of quantification (LOQ) of each element was determined by multiplying standard deviation of six blank solutions by ten.

2.20. Quality assurance/Quality control

Standard reference materials of sediments (SRM 8704 and BCR 280R) were used for validation of the method employed for determination of total concentrations of trace elements in the river sediments. A standard reference material of trace elements in water (NIST SRM 1643f) was used to check the accuracy of the method used for quantification of potentially toxic elements. A BCR-701 certified reference material was used to validate the sequential extraction procedures.

To validate procedures for speciation analysis spiking and recovery experiments were conducted. The speciation analysis using HPLC/ICP-MS was validated by spiking samples with each As species standards at low level (1x LOQ) and high level (10x LOQ) to investigate percentage recoveries. The evaluation of percentage recovery for SPE method was based on the assessment of the adsorbed As(V) which was eluted and quantified using ICP-MS. Briefly, a mixture of 2.0 µg/L As(V) and 1.0 µg/L As(III) was prepared using de-ionised water and passed through SPE column packed with MWCNTs-BPEI nanocomposites. The obtained eluent was analysed using ICP-MS.

3. RESULTS AND DISCUSSION

The concentration of potentially toxic elements in the water and sediment samples were monitored using ICP-MS. When ICP-MS is employed for quantification of elements, careful selection of the isotopes of the given element is critical. For element of interest with more than one isotope, at least two masses were monitored and the isotope with less interference and higher abundance was selected for subsequent analysis. The following isotopes were used for the final analysis: ^{51}V, ^{53}Cr, ^{55}Mn, ^{60}Ni, ^{63}Cu, ^{66}Zn, ^{75}As, ^{82}Se, ^{112}Cd, and ^{208}Pb. Quantification of all elements were conducted using linear calibration curves established from the analysis of a blank and a series of standard solutions with typical correlation coefficients greater than 0.999 for all elements.

3.1. Limit of detection and limit of quantification

The LODs and LOQs of potentially toxic elements in the water samples were determined by analysing blanks and based on three times the standard deviation and ten times the standard deviation of six individual prepared blank solutions (Table 3.1). For determination of potentially toxic elements in water samples by ICP-MS, the LOD ranged from 0.010 to 0.99 and the LOQ ranged from 0.033 to 3.30. Similar trends were observed for sediments. The calculated LODs and LOQs indicated that all the quantified analytes had good or acceptable LODs and LOQs.

Table 3.1: Limit of detection and limit of quantification of trace elements in water and sediments determination procedure.

Analyte	**Water analysis**		**Sediment analysis**	
	LOD (µg/L)	**LOQ (µg/L)**	**LOD (ng/g)**	**LOQ (ng/g)**
Mn	0.049	0.163	0.069	0.23
Zn	0.99	3.30	1.18	3.93
Ni	0.05	0.17	0.55	1.83
Cu	0.012	0.04	0.110	0.366
Cr	0.11	0.38	1.13	3.76
Pb	0.009	0.029	0.029	0.097
V	0.19	0.64	0.69	2.30
Cd	0.01	0.033	0.030	0.10
As	0.14	0.46	0.54	1.80
Se	0.12	0.40	2.48	8.27
Fe	0.049	0.16	0.017*	0.057*

*LOD and LOQ values obtained by F-AAS in mg/kg

3.2. Accuracy and precision

The concentrations of potentially toxic elements in standard reference material of water (SRM 1643f, NIST, USA) were determined to test accuracy of the method. Repeatability of the results has been estimated by calculating the relative standard deviations (RSDs). Relative differences between the measured concentrations and the certified concentrations for each analyte are reported as percent error (% Relative error = 100 x (C_M-C_C)/C_C, where C_M and C_C are measured and certified concentrations, respectively). Results depicting the analytical quality are reported in table 3.2. The precision of the entire analytical procedure for each element was estimated by calculating the percent RSD. The percent RSD is in an acceptable range, which varied from 0.044-9.3%.

Table 3.2: Comparison of the measured and certified concentrations in SRM 1643f.

Analyte	**Measured value (mean ± SD) in µg/L**	**Certified value (mean ± SD) in µg/L**	**Percent Recovery**	**Relative error (%)**
Mn	37.6 ± 0.75	37.1 ± 0.60	101	+1.35
Zn	82.4 ± 7.7	74.4 ± 1.7	111	+10.6
Ni	62.1 ± 0.16	59.8 ± 1.4	104	+3.85
Cu	24.8 ± 0.011	21.66 ± 0.71	114	+14.5
Cr	27.4 ± 0.42	18.50 ± 0.10	148	+48.1
Pb	22.8 ± 0.15	18.488 ± 0.084	123	+23.3
V	38.4 ± 1.2	36.07 ± 0.28	106	+6.45
Cd	6.44 ± 0.010	5.89 ± 0.13	109	+9.34
As	57.8 ± 1.2	57.42 ± 0.38	101	+0.662
Se	13.1 ± 0.0085	12.64 ± 0.13	104	+3.64

The levels of potentially toxic elements in standard reference material of sediments (SRM 8704 and BCR 280R) were determined to validate the method employed for determination of the selected elements in sediment samples. The measured results together with certified values, percent recovery and relative error are presented in table 3.3.

Table 3.3: The concentrations of potentially toxic elements in BCR 280R obtained using ICP-MS.

Analyte	**Measured value (mean ± SD) in mg/kg**	**Certified value (mean ± SD) in (mg/kg)**	**Percent Recovery**	**Relative error (%)**
Zn	208±0.91	224±25	92.9	-7.14
Ni	63.3±2.6	69.0±5.0	91.7	-8.26
Cu	61.4±0.63	53.0±6.0	116	+15.8
Cr	190±14	126±7.0	151	+50.8
As	38.1±0.65	33.4±2.9	114	+14.1
Se	0.251±0.044	0.46±0.09	54.6	-45.4
Cd	0.912±0.002	0.85±0.10	107	+7.29

The method validation results are within acceptable range for Zn, Ni, Cu, As and Cd as presented in table 3.3. The percent recovery for Se and Cr in BCR 280R is high when ICP-MS is used for quantification. The elevated values for these elements could be attributed to polyatomic ion interferences. The Cr determination method was validated using F-AAS. The obtained percent recovery of 84.9% (Table 3.4) is quantitative. Thus, further quantification of Cr in sediment samples conducted using F-AAS. A F-AAS showed better percentage recovery for Cr compared to ICP-MS result of 151%. The elevated concentration of Cr by ICP-MS could be due to polyatomic ions interferences. The method for quantification of Se need to be optimised to achieve acceptable percent recovery.

Table 3.4: The concentration of Cr in BCR 280R obtained using F-AAS.

Analyte	**Measured value (mean ± SD) in mg/kg**	**Certified value (mean ± SD) in (mg/kg)**	**Percent Recovery**	**Relative error (%)**
Cr	107±0.40	126±7.0	84.9	-15.1%

The SRM 8704 was analysed to validate the method for the selected elements. The results are presented in table 3.5. The achieved percent recoveries for Mn, Zn, Ni, V and Cd were quantitative, which confirms the validity of the method. However, the measured value for Pb was found to be much higher than the certified value. Therefore, the SRM 8704 was analysed using F-AAS to determine Pb content. Quantitative percent recovery of 99.3% (table 3.6) was achieved confirming the accuracy of the method. The concentration of Fe in SRM 8704 was also measured using F-AAS. Percent recovery of 93.0% (table 3.6) was achieved for Fe, which depicts the validity of the method.

Table 3.5: The concentrations of potentially toxic elements in SRM 8704 obtained using ICP-MS.

Analyte	Measured value (mean ± SD) in mg/kg	Certified value (mean ± SD) in (mg/kg)	Percent Recovery	Relative error (%)
Mn	577±1.9	544±21	106	+6.06
Zn	402±2.0	408±15	98.5	-1.47
Ni	38.6±10	42.9±3.7	90.0	-10.0
V	97.6±0.059	94.6±4.0	103	+3.17
Cd	3.33±0.023	2.94±0.29	113	+13.3
Pb	210±3.8	150±17	140	+40.0

Table 3.6: The concentrations of potentially toxic elements in SRM 8704 obtained using F-AAS.

Analyte	Measured value (mean ± SD)	Certified value (mean ± SD)	Percent Recovery	Relative error (%)
Pb (mg/kg)	149±0.026	150±17	99.3	-0.667
Fe (%w/w)	3.69 ± 0.15	3.97±0.10	93.0	-7.05

3.3. Concentrations of potentially toxic elements in water

Total elemental concentrations of Mn, Zn, Ni, Cu, Cr, Pb, V, Cd, As and Se in water samples were determined simultaneously using ICP-MS. Table 3.7 shows the analytical results (mean ± standard deviation) for the water samples collected from Blood River. The concentrations of trace elements in water samples collected from Mokolo River are presented in Table 3.8. The concentrations of Mn, Zn, Ni, Cu, Cr, Pb, V, Cd, As and Se in Blood River varied from 40.7 to 672, 37.1 to 162, 11.6 to 34.4, 8.00 to 34.9, 21.4 to 72.1, 1.64 to 14.4, 27.3 to 48.5, 0.76 to 1.88, 6.30 to 19.3, and 44.6 to 93.6 µg/L, respectively. The levels of Mn, Zn, Ni, Cu, Cr, Pb, V, Cd, As and Se in Mokolo River varied from 35.1 to 1160, <0.99 to 141, 1.98 to 6.18, 2.87 to 17.5, <0.11 to 15.4, 1.79 to 5.41, <0.19 to 6.80, <0.01 to 0.990, <0.14 to 6.19, and 2.65 to 33.0 µg/L, respectively. It has been noted that except Mn level, the highest concentrations of all the elements were observed in Blood River. We observed dumping of domestic wastes around the river, sand mining from the river and direct discharge of effluents into the river during our sampling campaign, which could raise the levels of pollutants in Blood River. Dumping of domestic wastes from Seshego town in different parts of the river, sand mining activities and direct discharge of effluents into the river presumably contributed to the elevated levels of potentially toxic elements. For all elements except Pb, the lowest concentrations were observed in Mokolo River.

Table 3.7: Total concentrations (μg/L) of potentially toxic elements in water samples obtained from Blood River.

Analyte	**Site**									
	B1	B2	B3	B4	B5	B6	B7	B8	B9	B10
Mn	**49.5^{c}** ± 0.19	**50.3^{c}** ± 6.0	**40.7^{c}** ± 0.24	**129^{b,c}** ± 2.3	**452^{a,b,c,d}** ± 4.6	**303^{b,c,d}** ± 3.9	**231^{b,c,d}** ± 0.67	**81.7^{c}** ± 0.30	**209^{b,c,d}** ± 5.7	**672^{a,b,c,d}** ± 2.4
Zn	87.2± 0.20	**162^{a}** ± 11	50.4± 2.8	56.4± 0.41	37.1± 9.2	41.0± 0.83	53.5± 0.03	64.5± 0.50	57.8± 4.9	60.7± 0.42
Ni	14.3± 1.7	34.4± 2.5	15.9± 1.8	15.0± 028	16.9± 0.17	14.5± 0.06	14.2± 2.7	11.6± 0.46	14.5± 0.73	18.3± 0.26
Cu	21.1± 0.47	34.9± 6.4	11.6± 0.20	10.9± 1.4	12.9± 3.9	8.00± 0.061	13.4± 0.44	17.0± 0.24	14.5± 0.47	17.0± 2.1
Cr	21.8± 3.6	**47.3^{a}** ± 10	**42.9^{a}** ± 1.32	**45.1^{a}** ± 1.9	**72.1^{a}** ± 1.7	**62.5^{a}** ± 2.4	**59.6^{a}** ± 0.42	**62.0^{a}** ± 0.43	21.4± 2.9	**39.5^{a}** ± 1.3
Pb	5.20± 0.81	**13.4^{a}** ± 2.1	**14.4^{a}** ± 0.27	2.60± 0.010	2.37± 0.14	1.64± 0.021	3.51± 0.13	2.47± 0.15	6.38± 0.45	**11.5^{a}** ± 0.20
V	27.3± 4.2	43.6± 7.0	48.3± 0.41	43.5± 1.4	45.8± 1.6	39.0± 0.54	36.0± 0.84	35.7± 0.14	29.7± 1.1	48.5± 2.7
Cd	0.990 ± 0.23	1.84± 0.31	1.46± 0.016	1.88± 0.035	1.23± 0.22	0.844 ±0.040	0.767 ±0.013	0.961 ±0.055	0.819 ±0.13	1.05± 0.16

Analyte	Site									
	B1	B2	B3	B4	B5	B6	B7	B8	B9	B10
As	6.30± 0.43	**12.5**[a,b] ± 2.2	9.63± 1.2	**10.2**[a,b] ± 0.43	**14.6**[a,b] ±0.40	**17.0**[a,b] ± 0.87	**18.5**[a,b] ± 0.042	**19.3**[a,b] ± 0.26	**11.4**[a,b] ± 0.29	**11.4**[a,b] ± 0.0
Se	**44.6**[a,b,c] ± 19	**70.7**[a,b,c] ± 0.77	**60.2**[a,b,c] ± 1.8	**57.0**[a,b,c] ± 5.8	**61.3**[a,b,c] ± 6.3	**85.3**[a,b,c] ± 1.3	**85.3**[a,b,c] ± 1.3	**93.6**[a,b,c] ± 5.8	**83.9**[a,b,c] ± 1.8	**90.8**[a,b,c] ± 4.4

[a] Concentrations above guideline value set by World Health organisation (WHO)
[b] Concentrations above South African National Standards (SANS)
[c] Concentrations above Department of Water Affairs and Forestry (DWAF)
[d] Concentrations above Canadian Council of Ministers of the Environment (CCME)

Manganese level as high as 1160 µg/L has been detected in Mokolo River. Manganese is one of the most abundant elements in the earth's crust, usually occurring with Fe. The desirable limit is specified as 400 µg/L for drinking water by WHO (2011), 100 µg/L for drinking water by South African National Standards (SANS) (2005), 20 µg/L for irrigation water by Department of Water Affairs and Forestry (DWAF) (1996) and 200 µg/L for irrigation water by the Canadian Council of Ministers of the Environment (CCME) (1999), whereas the analysed samples in both rivers showed higher concentrations than the guideline values. The levels of Mn in water exceeded the stipulated limit for drinking water set by WHO (2011) in sites 5 and 10 in Blood River and sites 1, 3 and 10 Mokolo River. The levels of Mn in sites 4, 5, 6, 7, 9 and 10 in Blood River, and in sites 1, 2, 3, 4, 7 and 10 in Mokolo River exceeded the MPL set by SANS (2005) for drinking water. The concentrations of Mn exceeded MPL of 20 µg/L set by DWAF (1996) for irrigation water in all samples analysed from both rivers. The levels of Mn measured in water samples from sites 5, 6, 7, 9 and 10 of Blood River and from sites 1, 3 and 10 of Mokolo River exceeded the MPL value of 200 µg/L set by CCME (1999).

The levels of Zn exceeded the guideline value of 123 µg/L set for drinking water (WHO, 2011) in site 2 of Blood River and site 10 of Mokolo River. But the levels of Zn measured in all the samples from both rivers were below the stipulated limits of 5000 µg/L (SANS, 2005), 1000 µg/L (DWAF, 1996) and 200 µg/L (CCME, 1999). Zinc is an essential trace element found in virtually all potable water in the form of salts or organic complexes. Zinc is an essential trace element and plays an important role in the physiological and metabolic processes of many organisms, however, in high concentrations it can be toxic (Abdul *et al.*, 2012).

The maximum recommended value of Ni in drinking water is 70 µg/L (WHO, 2011). The levels detected in this analysis were less than recommended value. The levels of Ni in water samples from both rivers were below the MPLs of 150 µg/L (SANS, 2005), 200 µg/L (DWAF, 1996) and 200 µg/L (CCME, 1999). The compounds of Ni induce nasal, laryngeal and lung cancer (Abdul *et al.*, 2012).

The stipulated limit of Cu in drinking water is 2000 µg/L, above the desirable limit Cu imparts color and an undesirable bitter taste to water (WHO, 2011). The concentrations of Cu in water samples were far below the desirable limits of 1000 µg/L (SANS, 2005) and 200 µg/L (DWAF, 1996). No guideline value has been proposed by CCME for Cu.

Total Cr concentrations in the Mokolo River water samples were within the desirable limit of 25 µg/L for drinking water (WHO, 2011). Whereas, total Cr levels in Blood River exceeded the desirable limit for water samples collected from sites 2, 3, 4, 5, 6, 7, 8 and 10. The levels of Cr in water samples were far below the desirable limits of 100 µg/L (SANS, 2005) and 100 µg/L (DWAF, 1996). No guideline value has been set by CCME for Cr.

The concentrations of Pb in water samples collected from Mokolo River were within the permissible limit of 10 µg/L (WHO, 2011). However, Pb concentrations for samples collected from Blood River in sampling sites 2, 3 and 10 were above the permissible limit. The element Pb is highly toxic and even at small amounts; taken over a longer period it accumulates and may cause serious illness. The levels of Pb in water samples were below the desirable limits of 20 µg/L (SANS, 2005), 200 µg/L (DWAF, 1996) and 200 µg/L (CCME, 1999).

For V, no guideline value for drinking water has been reported by WHO (2011). The levels of V in water samples from both rivers are below the MPLs of 200 µg/L (SANS, 2005), 100 µg/L (DWAF, 1996) and 100 µg/L (CCME, 1999).

The levels of Cd in all water samples collected from both rivers were found to be below the stipulated limit of 3 μg/L (WHO, 2011). The concentrations of Cd in water samples from both rivers were below the MPLs of 5 μg/L (SANS, 2005), 10 μg/L (DWAF, 1996) and 5.1 μg/L (CCME, 1999).

The concentrations of As in water samples collected from Mokolo River were found to be below the permissible limit of 10 μg/L (WHO, 2011). However, the levels of As in water samples collected from Blood River exceeded the permissible limit in all the sites except sites 1 and 3. The levels of As in water samples from both rivers were below the MPLs of 10 μg/L (SANS, 2005), 100 μg/L (DWAF, 1996) and 100 μg/L (CCME, 1999).

Table 3.8: Total concentrations (μg/L) of potentially toxic elements in water samples obtained from Mokolo River.

Analyte	**Site**									
	M1	M2	M3	M4	M5	M6	M7	M8	M9	M10
Mn	**783**^{a,b,c,d} ± 66	**105**^{b,c} ± 7.5	**1160**^{a,b,c,d} ± 110	**164**^{b,c} ± 1.0	**41.3**^{c} ± 2.2	**35.1**^{c} ± 1.2	**185**^{b,c} ± 1.9	**36.0**^{c} ± 4.86	**91.1**^{c} ± 2.8	**830**^{a,b,c,d} ± 19
Zn	25.6± 0.030	23.6± 2.0	11.0± 1.1	7.87± 0.97	9.23± 0.09	6.46± 1.1	7.38± 0.83	4.28± 0.49	<0.99	**141**^{a} ± 2.7
Ni	2.75± 0.090	2.14± 0.11	3.36± 0.25	2.22± 0.06	2.14± 0.09	1.98± 0.09	2.18± 0.04	2.12± 0.08	2.08± 0.07	6.18± 0.21
Cu	3.45± 0.17	5.76± 0.17	4.85± 0.080	3.16± 0.0	3.22± 0.060	3.11± 0.020	4.05± 0.64	2.87± 0.040	2.97± 0.020	17.5± 0.48
Cr	5.62± 0.080	6.24± 0.13	15.3± 0.58	7.47± 0.33	12.2± 0.13	7.49± 0.37	15.4± 2.5	5.90± 0.45	5.25± 0.30	<0.11
Pb	4.24± 0.10	4.68± 0.070	4.13± 0.090	5.41± 0.020	3.93± 0.010	3.99± 0.030	4.53± 0.69	3.97± 0.050	3.94± 0.030	1.79± 0.045
V	4.61± 0.18	4.57± 0.020	6.16± 0.090	4.72± 0.10	5.83± 0.14	4.61± 0.21	6.80± 0.020	4.35± 0.11	3.74± 0.00	<0.19

Analyte	Site									
	M1	M2	M3	M4	M5	M6	M7	M8	M9	M10
Cd	0.970± 0.030	0.960± 0.020	0.930± 0.01	0.950± 0.01	0.96± 0.030	0.95± 0.020	0.990± 0.030	0.95± 0.020	0.91± 0.010	<0.01
As	4.31± 0.10	4.28± 0.070	5.95± 0.21	4.42± 0.050	5.43± 0.13	4.29± 0.20	6.19± 0.26	3.98± 0.25	3.67± 0.16	<0.14
Se	**33.0**^{b,c} ± 1.5	**29.3**^{b,c} ± 3.6	**27.0**^{b,c} ± 0.42	**31.8**^{b,c} ± 1.1	**30.7**^{b,c} ± 1.0	**28.6**^{b,c} ± 2.00	**30.6**^{b,c} ± 1.6	**28.9**^{b,c} ± 2.1	**22.6**^{b,c} ± 1.24	2.65± 0.079

[a] Concentrations above guideline value set by World Health organisation (WHO)

[b] Concentrations above South African National Standards (SANS)

[c] Concentrations above Department of Water Affairs and Forestry (DWAF)

[d] Concentrations above Canadian Council of Ministers of the Environment (CCME)

Guideline value for Se in drinking water is 40 µg/L (WHO, 2011). The concentrations of Se in water samples collected from Mokolo River were found to be below the guideline value. Whereas, the levels of Se in water samples collected from Blood River surpassed the stipulated limit in all the sites except site 1. The levels of Se in all water samples from Blood River were below the MPL values of 20 µg/L (SANS, 2005) and 20 µg/L (DWAF, 1996). The concentrations of Se in all the analysed water samples from Mokolo River exceeded the MPLs of 20 µg/L (SANS, 2005) and 20 µg/L (DWAF, 1996) in all the sites except site 10. No guideline value has been set by CCME for Se.

3.4. Concentrations of potentially toxic elements in sediments

Total elemental concentrations of potentially toxic elements in sediment samples were determined simultaneously using ICP-MS. Table 3.9 shows the analytical results (mean ± standard deviation) for the sediment samples collected from Blood River. Furthermore, the total concentrations of Cr, Fe and Pb in sediment samples were measured using F-AAS and presented in table 3.10. Similarly, the concentrations of trace elements in sediment samples collected from Mokolo River are presented in tables 3.11 and 3.12.

Table 3.9: Total concentrations (mg/kg) of potentially toxic elements in sediment samples collected from Blood River and measured by ICP-MS.

	Site									
Analyte	B1	B2	B3	B4	B5	B6	B7	B8	B9	B10
Mn	262±5.9	379±12	376±3.3	509±5.2	361±3.0	487±15	295±10	99.3±1.2	134±3.0	236±1.6
Zn	15.4±0.087	19.0±0.18	17.5±0.88	119±0.10	53.7±0.42	54.2±0.81	34.6±1.2	19.2±1.5	18.8±1.1	40.3±1.0
Ni	33.7±0.43	37.2±1.5	39.4±0.53	51.6±0.093	49.8±0.65	45.7±0.68	29.4±0.12	14.4±0.61	20.0±1.0	32.9±1.2
Cu	15.1±0.50	17.9±1.0	18.3±0.080	33.7±0.10	28.5±0.12	28.1±1.1	15.7±0.88	11.5±0.52	10.0±0.43	17.7±0.64
Cr	86.2±2.4	89.7±1.6	110±1.0	146±2.10	124±4.4	116±4.3	69.5±2.9	38.6±0.76	53.4±3.6	79.7±0.84
V	29.3±0.44	40.1±1.7	41.7±0.21	51.9±0.54	49.8±2.3	47.8±0.58	30.4±1.1	17.6±0.0054	21.5±0.15	31.8±0.14
As	2.24±0.013	3.1±0.15	3.49±0.12	5.52±0.002	5.47±0.61	4.640±0.16	2.23±0.041	2.20±0.072	1.20±0.55	2.06±0.69
Se	<0.12	<0.12	<0.12	<0.12	<0.12	<0.12	<0.12	<0.12	<0.12	<0.12
Cd	0.0130±0.00028	0.0144±0.0	0.0172±0.0017	0.115±0.0071	0.0486±0.0020	0.0626±0.0085	0.0440±0.0023	0.0210±0.0085	0.0266±0.0037	0.0352±0.0023
Pb	6.56±0.15	7.71±0.11	5.66±0.027	23.2±0.048	12.4±0.14	14.9±0..77	18.5±3.3	3.26±0.12	4.49±0.14	7.86±0.15

Table 3.10: Total concentrations (mg/kg) of potentially toxic elements in sediment samples collected from Blood River and measured by F-AAS.

Analyte	Site									
	B1	B2	B3	B4	B5	B6	B7	B8	B9	B10
Fe	3330 ±23	3450 ±9.6	3350 ±97	3380 ±90	3370 ±77	3330 ±130	3740 ±15	3600 ±42	3630 ±25	3610 ±38
Cr	49.8±0.85	49.8±1.1	70.0±0.57	89.3±0.42	73.6±3.7	57.7±0.99	58.2±4.5	24.7±3.0	23.2±0.85	54.2±1.1
Pb	<0.00636	<0.00636	<0.00636	<0.00636	<0.00636	<0.00636	<0.00636	<0.00636	<0.00636	<0.00636

Table 3.11: Total concentrations (mg/kg) of potentially toxic elements in sediment samples collected from Mokolo River and measured by ICP-MS.

Ana-lyte	Site									
	M1	M2	M3	M4	M5	M6	M7	M8	M9	M10
Mn	443 ±9.0	136±1.9	<0.28	371±15	114±3.5	127±0.24	624±15	79.8±4.4	56.7±3.8	48.8±5.4
Zn	15.3 ±0.30	11.1 ±1.3	27.3±0.61	8.52 ±0.33	4.93 ±0.43	5.80 ±0.30	7.93 ±0.13	4.29±0.043	5.43±0.015	6.47±0.077
Ni	12.6 ±0.067	7.74 ±0.023	29.0±0.69	10.8 ±0.20	5.63 ±0.063	6.47 ±0.079	7.58 ±0.13	5.21±0.25	5.80±0.21	5.74±0.063
Cu	7.00 ±0.94	10.2 ±2.3	15.1±0.38	4.65 ±0.010	2.67 ±0.11	2.73 ±0.023	2.49 ±0.061	2.60±0.10	2.96±0.064	4.29±0.27
Cr	40.0 ±3.4	25.8 ±1.6	63.8±2.8	30.3 ±0.79	22.1 ±2.7	25.3 ±0.13	22.2 ±0.73	17.3±1.3	20.4±0.81	28.4±0.99
V	26.0 ±2.4	17.2 ±0.42	45.2±1.8	21.3 ±0.36	13.0 ±0.30	16.4 ±0.021	15.9 ±0.60	12.5±0.97	13.9±0.95	17.9±0.34

Analyte	Site									
	M1	M2	M3	M4	M5	M6	M7	M8	M9	M10
As	2.82±0.48	1.97±0.24	3.05±0.18	1.17±0.038	1.12±0.28	1.5±0.018	1.49±0.024	1.30±0.052	0.928±0.0011	1.47±0.086
Se	<0.12	<0.12	<0.12	<0.12	<0.12	<0.12	<0.12	<0.12	<0.12	<0.12
Cd	<0.030	<0.030	0.035±0.0051	<0.030	<0.030	<0.030	<0.030	<0.030	<0.030	0.477±0.013
Pb	8.34±0.15	8.12±0.28	13.5±0.31	9.46±0.45	4.97±0.47	4.37±0.025	5.31±0.13	5.27±0.62	4.01±0.019	5.61±0.15

Table 3.12: Total concentrations (mg/kg) of potentially toxic elements in sediment samples collected from Mokolo River and measured by F-AAS.

Analyte	Site									
	M1	M2	M3	M4	M5	M6	M7	M8	M9	M10
Fe	3620±43	3650±42	3790±10	3950±41	3700±14	3850±77	3830±250	3720±94	3660±43	3500±37
Cr	142±0.57	37.9±6.1	765±15	683±21	275±25	484±27	531±23	510±3.5	1190±25	973±29
Pb	<0.00636	<0.00636	<0.00636	<0.00636	<0.00636	<0.00636	<0.00636	<0.00636	<0.00636	13.5±2.7

The total concentrations of Mn, Zn, Ni, Cu, V, As, Cd, Pb, Fe and Cr in Blood River varied from 99.3 to 509, 15.4 to 119, 14.4 to 51.6, 10.0 to 33.7, 17.6 to 51.9, 1.20 to 5.52, 0.0130 to 0.115, 3.26 to 23.2, 3330 to 3740, and 23.2 to 89.3 mg/kg, respectively. The levels of Mn, Zn, Ni, Cu, V, As, Cd, Pb, Fe and Cr in Mokolo River varied from <0.28 to 624, 4.29 to 27.3, 5.21 to 29.0, 2.49 to 15.1, 12.5 to 45.2, 0.928 to 3.05, <0.030 to 0.477, 4.01 to 13.5, 3500 to 3950, and 37.9 to 1190, respectively. It has been observed that except Mn, Fe and Cr levels, the highest levels of all the elements were detected in sediment samples collected from Blood River. Similar trends were observed for measured trace elements in water. During our sampling campaign, we observed dumped domestic wastes near Blood River, sand mining activities and direct discharge of effluents into the river. The elevated levels of potentially toxic elements in Blood River could be attributed to the aforementioned activities. For all measured elements except Pb, Fe and Cr the lowest concentrations were detected in Mokolo River.

3.5. The LODs and LOQs for determination of As species

The LODs and LOQs for As speciation determination in water and sediments samples are indicated in table 3.13.

Table 3.13: The LODs and LOQs for analytical procedure for water and sediments analysis using HPLC-ICP-MS

Analyte	LOD		LOQ	
	Water (µg/L)	Sediment (ng/g)	Water (µg/L)	Sediment (ng/g)
As^{+3}	0.22	0.11	0.74	0.37
DMA	0.094	0.07	0.31	0.23
MMA	0.13	0.09	0.43	0.30
As^{+5}	0.078	0.03	0.26	0.10

The obtained LOD of As species in water samples are comparable with the LODs reported by Martinez-Bravo *et al.* (2001). The authors reported LODs as 0.19 µg/L for As^{+3}, 0.16 µg/L for DMA, 0.067 µg/L for MMA and 0.040 µg/L for As^{+5} in water samples using HPLC-ICP-MS. The obtained LODs suggest that the optimised method could efficiently quantify levels of As species in water samples.

The results show that the LOD of As^{+3}, DMA, MMA and As^{+5} are 0.11, 0.07, 0.09 and 0.03 ng/g, respectively. This study obtained lower LODs as compared to that reported by Lou *et al.* (2014). The authors reported 0.82 ng/g for As^{+3}, 2.3 ng/g for DMA, 1.45 ng/g for MMA and 2.31 ng/g for As^{+5} in guano and ornithogenic sediments using

HPLC-HG-AFS. The LODs obtained in this study shows the reliable quality of the analytical procedure.

The SPE procedure for determination of As^{+5} in water samples was also evaluated using quantitative terms. The LOD and LOQ of 0.0537and 0.179 µg/L, respectively were obtained by employing off-line mode procedure after detection using ICP-MS. A previous study conducted by Zhad *et al.* (2009) reported LOD of 0.24 µg/L using ICP-MS which is 4.5 times higher than that obtained in this study. The LOD in this study show adequate sensitivity of detection technique for quantification of As^{+5}.

3.6. Validation of analytical procedures for As speciation

The analytical procedures for As speciation analysis in water and sediment samples were validated based on by spiking-and-recovery procedures due to lack of SRMs, which have certified values of As species.

Method validations were conducted by spiking water and sediment samples with standards at 1x LOQs and 10x LOQs levels to investigate the percent recoveries. The same samples were spiked at 1x LOQ and 10x LOQ levels and quantified using the HPLC-ICP-MS. The concentrations of each species were obtained from the differences of spiked and unspiked samples to assess the percentage recoveries. Quantification was based on the integration of peak area to account for tailing peaks rather the use of peak heights intensities using technical graphics software Origin 6.1. The percentage recoveries were evaluated with references to the standard guidelines recommended by USEPA which are guidelines for method development and validation (USEPA, 2010). The USEPA recommended suitable percentage recoveries to be within 75-125% (EPA, 2010). The percentage recoveries obtained at 1x LOQs and 10x LOQs are presented in tables 3.14 and 3.15.

Table 3.14: Percentage recoveries at 1x LOQ levels for water samples.

Analyte	Unspiked sample (µg/L)	Spiking at 1x LOQ (µg/L)	Concentration after spiking (µg/L)	Percent recovery
As^{+3}	0.26 ± 0.001	0.74	0.865 ± 0.035	81.8
DMA	0.096 ± 0.003	0.31	0.241 ± 0.0023	46.8
MMA	0.22 ± 0.005	0.43	0.62 ± 0.007	93.0
As^{+5}	7.7 ± 0.24	0.26	8.0 ± 0.14	115

The HPLC-ICP-MS procedure was applied for analysis of water samples which were spiked at 1x LOQs of As species standards. The satisfactory percent recoveries were obtained for As^{+3}, MMA and As^{+5} in the range of 81.8-115.4%. These percent recoveries are within the acceptable range of USEPA guidelines (USEPA, 2010). The percent recovery of 46.8% for DMA is far below the acceptable range. The analytical results for DMA would not be reliable because of the low percentage recoveries obtained. The percent RSDs for concentrations after spiking were found to be 4% for As^{+3}, 9.5% for DMA, 0.076% for MMA and 0.37% for As^{+5}. The relative standard deviation (RSD) less than 15% demonstrate a high degree of repetitiveness for the analytical procedure (Lou *et al.*, 2014). The similar study published by Martinez-Bravo *et al.* (2001) reported percentage recoveries at 1x LOQ levels As species in the range 80-97% with an adequate precision.

Table 3.15: Percentage recoveries at 10x LOQ level for water samples.

Analyte	Unspiked sample (µg/L)	Spiking at 10x LOQ (µg/L)	Concentration after spiking (µg/L)	Percent recovery
As^{+3}	0.26 ± 0.001	7.4	6.32 ± 0.51	81.9
DMA	0.096 ± 0.003	3.1	1.64 ± 0.026	49.9
MMA	0.22 ± 0.51	4.3	4.62 ± 0.39	102
As^{+5}	7.7 ± 0.24	2.6	10.1 ± 0.055	92.3

The percent recoveries obtained in the range of 81.9-102% for As^{+3}, MMA and As^{+5} are consistent with USEPA guidelines (USEPA, 2010). The recovery of DMA has not significantly improved at 10x LOQ level. The RSDs after spiking were found to be 8.1% for As^{+3}, 1.6% for DMA, 1.5% for MMA and 0.5% for As^{+5}. Chen *at al.* (2006) reported percent recoveries of 89.2% for As^{+3}, 96.4% for DMA, 95.2% MMA and 103.1% for As^{+5} after spiking water sample with 50 µg/L of each species. The As species were separated and detected using ion chromatography (IC) coupled to ICP-MS (Chen *et al.*, 2006). The percentage recoveries at 1x LOQs and 10x LOQs levels shows the efficiency of the analytical procedure to quantify As^{+3}, MMA and As^{+5} in water samples using HPLC-ICP-MS.

The validation of analytical method for speciation analysis in sediment samples was also based on spiking-and-recovery procedures to evaluate percentage recoveries. The extraction efficiency of the analytical procedure was assessed at 1x LOQs and 10x LOQs levels and percentage recoveries are presented in tables 3.16 and 3.17.

Table 3.16: Percentage recoveries at 1x LOQ level for sediment samples.

Analyte	Unspiked sample (µg/g)	Spiking at 1x LOQ (µg/g)	Concentration after spiking (µg/g)	Percent recovery
As^{+3}	0.340 ± 0.0021	0.37	0.640 ± 0.035	73.0
DMA	0.09 ± 0.003	0.23	0.122 ± 0.0023	14.0
MMA	0.311 ± 0.004	0.30	0.570 ± 0.017	86.0
As^{+5}	0.189 ± 0.005	0.10	0.274 ± 0.014	85.0

The analytical results obtained show adequate percent recoveries at 1x LOQ level of 85.0% and 86.0% for As^{+5} and MMA, respectively. A fair recovery of 73.0% As^{+3} may be quantitative and poor recovery of 14.0% DMA would not produce reliable analytical results. The recoveries of As species were further investigated at 10x LOQs level.

Table 3.17: Percentage recoveries at 10x LOQ level for sediment samples.

Analytes	Unspiked sample (µg/g)	Spiking at 10x LOQ (µg/g)	Concentration after spiking (µg/g)	Percent recovery
As^{+3}	0.35 ± 0.0020	1.2	1.33 ± 0.028	82.0
DMA	0.09 ± 0.002	0.77	0.439 ± 0.04	45.0
MMA	0.312 ± 0.004	1.0	1.18 ± 0.09	87.0
As^{+5}	0.188 ± 0.007	0.33	0.491 ± 0.05	92.0

The acceptable percent recoveries obtained at 10x LOQs level for As^{+3}, MMA and As^{+5} are consistent with the recommendations of USEPA guidelines (USEPA, 2010). The obtained recoveries show that the analytical procedure is efficient for extraction and quantification of As^{+3}, MMA and As^{+5} in sediments samples. The recovery for DMA has not significantly improved hence the DMA results may not be reliable due to low percent recoveries. The low percentage recoveries of DMA could be due to conversion of it to an identified As species. The RSDs after spiking were found to be 2.1% for As^{+3}, 9.1% for DMA, 7.6% MMA and 10.1% As^{+5}. The RSD in all cases was monitored to assure the precision of the results which showed a high degree of repetitiveness for the analytical procedure (Lou *et al.*, 2014).

The validation for SPE was conducted by spiking-and-recovery procedures. The evaluation of percentage recovery was based on the assessment of the adsorbed As^{+5} which was eluted and quantified using ICP-MS. Briefly, a mixture of 2.0 µg/L As^{+5} and 1.0 µg/L As^{+3} was spiked in water samples and passed through SPE column packed with MWCNTs-BPEI nanocomposites. After SPE procedure, measured value of 1.62 µg/L of As^{+5} was obtained leading to percentage recovery 81.0%. The recovery obtained is consistent with standard guidelines recommendation of USEPA (EPA, 2010). The validated SPE procedure is efficient to separate and quantify As^{+5} in water samples in presence of As^{+3}.

3.7. Speciation of arsenic in water and sediment samples using HPLC/ICP-MS

Arsenic species in water and sediment samples were quantified using HPLC-ICP-MS. Prior to quantification of As species in samples, 20 µg/L As species standards were separately injected into HPLC-ICP-MS to identify retention time for each species. The chromatograms of As^{+3}, DMA, MMA and As^{+5} with the identified retention times are presented in figures 3.1(a)-3.1(d), respectively.

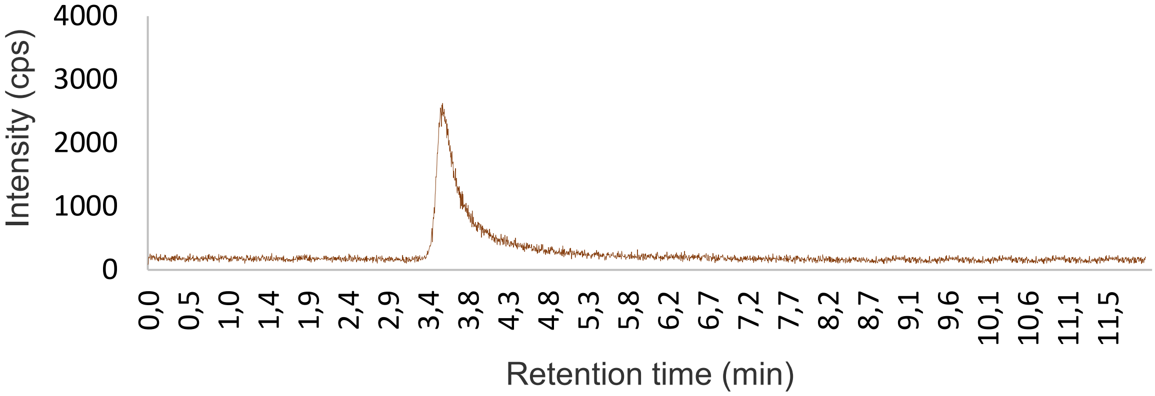

Figure 3.1(a): Chromatogram showing retention time for As^{+3} at 3.52 minutes

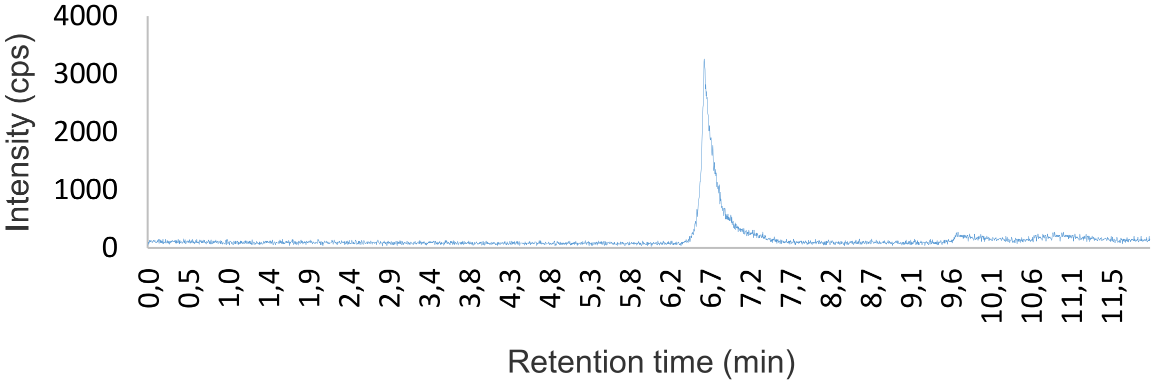

Figure 3.1(b): Chromatogram showing retention time for DMA at 6.71 minutes

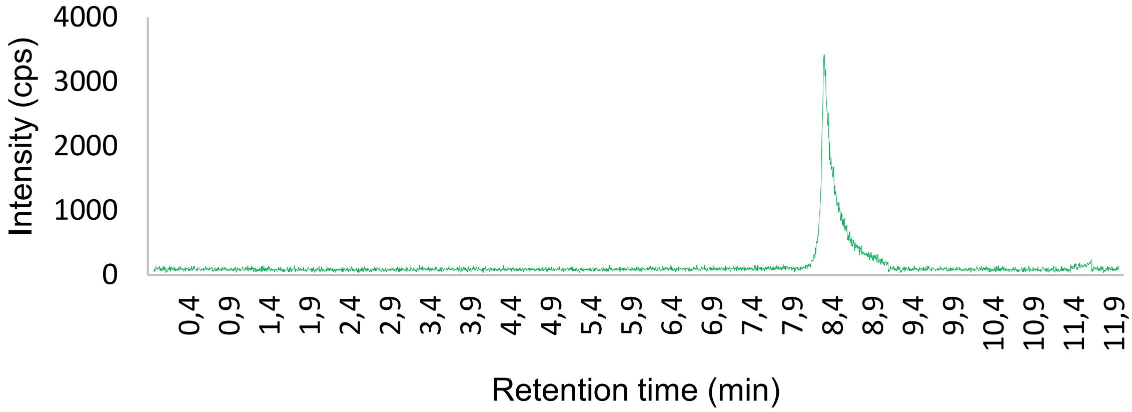

Fig 3.1(c): Chromatogram showing retention time for MMA at 8.31 minutes

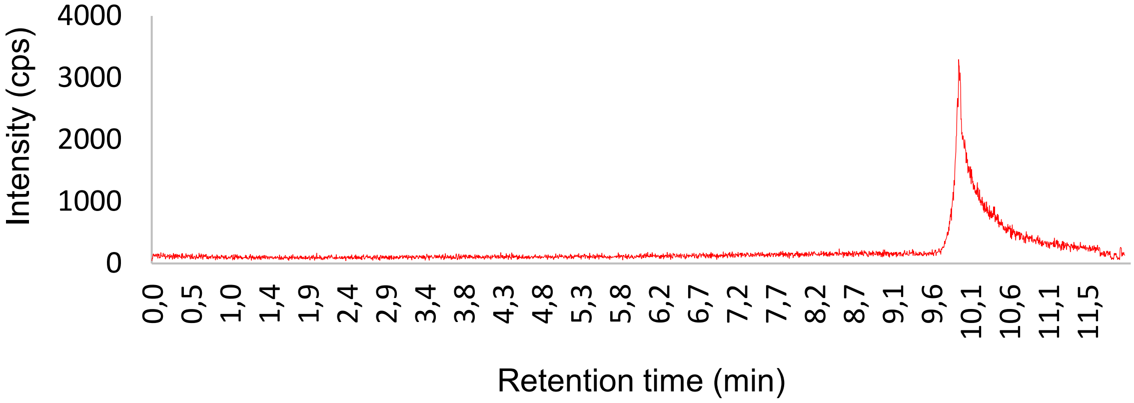

Figure 3.1(d): Chromatogram showing retention time for As^{+5} at 9.95 minutes

The compliance of the retention time with the relative to As species was evaluated by injecting mixture of standards containing As species into HPLC column under the monitored operating conditions. The As species were separated according to their identified retention times. The order of elution of a standard mixture indicates that As^{+3} species is the least retained species in the column while As^{+5} species is strongly retained. Moreover, the chromatogram indicates the efficient communication of HPLC and ICP-MS by allowing synchronous separation and detection of the species. The chromatogram that shows sequentially separated As species is presented in figure 3.2.

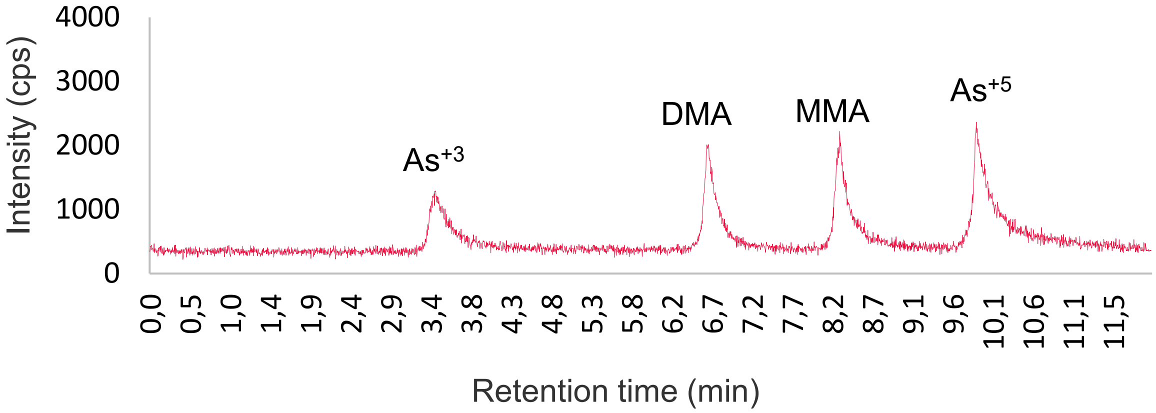

Figure 3.2: Sequential separation of As species in a mixture of standard solutions

The peak intensity is proportional to the increasing concentrations of the analytes. The peaks intensities of native As species were examined at series of mixture of standards after the injection into HPLC column. The observed enhanced signals and intensities clearly demonstrate agreement of the proportionality. The chromatogram (Figure 3.3) shows the relationship between the peak intensities and corresponding different concentrations of As species standards at a constant order of elution. The increasing peak areas were used to plot the linear calibration curves employed for quantification of As species in samples.

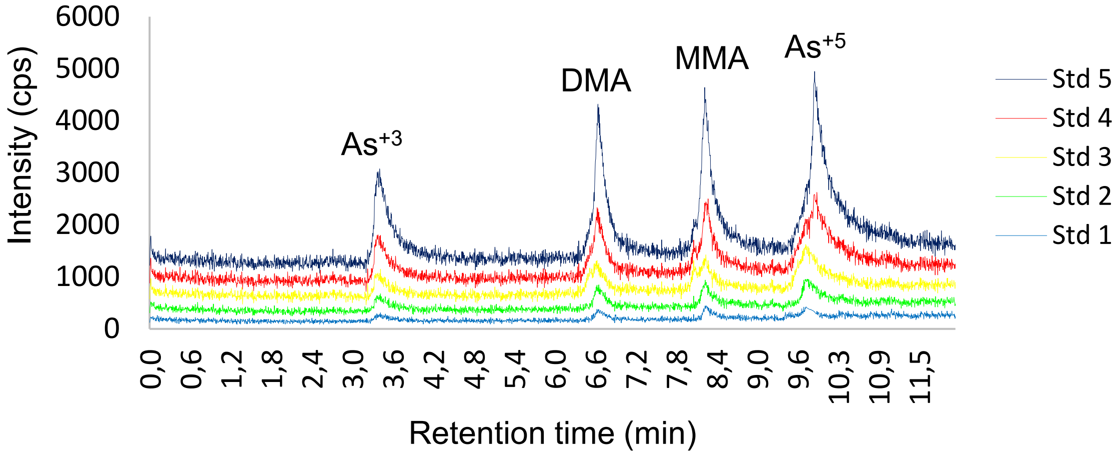

Figure 3.3: Intensified peaks relative to As species standard solutions containing 1.0, 2.5, 5.0, 10 and 20 µg/L of each species on Hamilton PRP-X100 anion exchange column.

The optimisation of chromatographic conditions led to baseline separation of four As species in 12 minutes employing gradient elution with 10 mM NH_4NO_3 (mobile phase A) and 60 mM NH_4NO_3 (mobile phase B) adjusted to pH 8.7 using NH_3. The adoption of NH_4NO_3 mobile phase is due to competency in providing the ionic strength essential in eluting the target ions without any interference as compared to NaH_2PO_4 mobile phase (Martinez-Bravo *et al.*, 2001). Martinez-Bravo *et al.* (2001) observed that NaH_2PO_4 decrease ionisation efficiency of the plasma because of the presence of Na counter-cation, which is readily ionisable. Thus, NaH_2PO_4 or other eluents containing Na are not ideal for the separation of As species based on the reported findings.

The application of different concentration of NH_4NO_3 mobile phase for As species determination was observed with no challenges related to clogging of nebuliser, the sampler and skimmer cones of the ICP-MS. Furthermore, lower concentration of mobile phase A was able to allow the least retained components to be separated while strongly retained components are adsorbed by the stationary phase of the column. However, increasing the concentration to 60 mM NH_4NO_3 (mobile phase B) led to desorption of strongly retained components due to steady increase of competition for the adsorption site (Sun *et al.*, 2015). The stabilised HPLC pump plays a major role in allowing on-line mixing of the mobile phase composition. Thus, making gradient mode of elution most suitable for separation and detection of As species. The gradient elution programme employed for As species determination is indicated in table 3.18.

Table 3.18: Gradient elution programme at 1 mL/min flow rate with the mobile phase A of 10 mM NH_4NO_3 and mobile phase B of 60 mM NH_4NO_3 at pH 8.7.

Time (min)	0	1	1.5	3	3.5	10	12
% A	100	100	50	50	0	0	0
% B	0	0	50	50	100	100	100

Speciation of As in water samples collected from Great Letaba and Mokolo Rivers was successfully conducted using HPLC-ICP-MS. Water samples were preserved by filtration and analysed without acidification. The preservation of As species by acidification cause the interconversion of species. The chromatogram of water sample with most detected species is indicated in figure 3.4. The detection of As^{+3}, MMA and As^{+5} in the water sample shows the successful preservation of the As species by the proposed method.

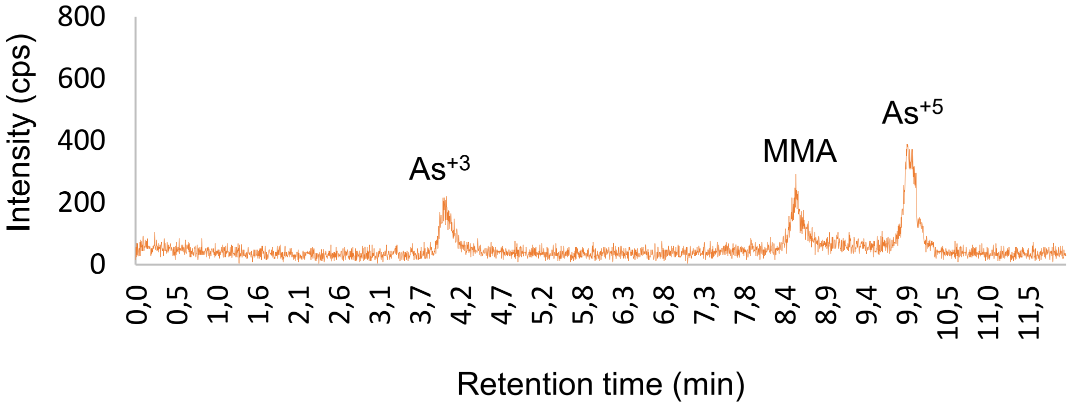

Figure 3.4: The chromatogram showing detected As species in water sample

The As species in water samples collected from the respective rivers were determined using validated analytical procedure. The difference in As species concentrations were influenced by the different factors such as water chemistry, geological area and varied anthropogenic activities. The concentration of As species are presented in tables 3.19-3.21.

Table 3.19: Concentrations of As species in water samples of Great Letaba River.

Sample Id	As^{+3} (µg/L)	DMA (µg/L)	MMA (µg/L)	As^{+5} (µg/L)
GLR-1	< 0.22	< 0.094	< 0.13	< 0.078
GLR-2	< 0.22	< 0.094	< 0.13	< 0.078
GLR-3	< 0.22	< 0.094	< 0.13	< 0.078
GLR-4	< 0.22	< 0.094	< 0.13	0.537 ± 0.0099
GLR-5	< 0.22	< 0.094	< 0.13	< 0.078
GLR-6	< 0.22	< 0.094	< 0.13	0.274 ± 0.013
GLR-7	< 0.22	< 0.094	< 0.13	0.653 ± 0.023
GLR-8	< 0.22	< 0.094	0.459 ± 0.022	1.02 ± 0.057
GLR-9	< 0.22	< 0.094	0.546 ± 0.014	1.05 ± 0.0014
GLR-10	< 0.22	< 0.094	0.437 ± 0.0053	1.27 ± 0.012

The concentrations of As species measured in Great Letaba River water samples vary from site to site. The results in table 3.19 show that As^{+3} and DMA were not detected, MMA was detected at site 8 to 10 and As^{+5} was detected at site 4 and site 6 to 10. The MMA concentration was found to be within the range of 0.437-0.546 µg/L, whereas As^{+5} concentrations ranged from 0.274-1.27 µg/L. The RSDs were less than 10%, thus the precision of the results is adequate. The As species in Great Letaba River could pose a threat to aquatic ecosystem because As is not an essential plant nutrient at any level of concentration (DWAF, 1996). The hippos and fish inhabited in the river and domestic animals (cattle and goat) which drink water directly from Great Letaba River may accumulate As species to toxic level (Le *et al.*, 1998; Rezende *et al.*, 2014). There is no evidence of a beneficial role for any safe dose of As consumption (Le *et al.*, 1998). Therefore, humans may be exposed to As species through the food chain by consumption of As contaminated food like fish as the fisher man was observed during sampling campaign.

The observed concentrations of MMA and As^{+5} may have attributed to the weathering of rocks. Great Letaba River has a rocky bed with a complex geology and effect of weathering of such rocks may have resulted with the minor levels of As^{+5} as revealed by the analysis results. The As contamination as a result of weathering processes does not rapidly elevate As in the environment since the process takes longer time to occur (Winkel *et al.*, 2008). The mining activities found in the proximity of the downstream of Great Letaba River may have also affected the concentration of inorganic As species indirectly. The MMA and DMA concentrations usually affected by microbial metabolism through methylation of inorganic species (Komorowicz and Baralkiewicz, 2011; Chiban *et al.*, 2012).

Table 3.20: Concentration of As species in water samples of Mokolo River during high flow sampling season.

Sample Id	As^{+3} (µg/L)	DMA (µg/L)	MMA (µg/L)	As^{+5} (µg/L)
MOK-1	0.301 ± 0.011	< 0.094	< 0.13	0.951 ± 0.029
MOK-2	< 0.22	< 0.094	< 0.13	1.55 ± 0.21
MOK-3	0.299 ± 0.028	< 0.094	< 0.13	0.681 ± 0.024
MOK-4	< 0.22	< 0.094	0.224 ± 0.01	7.70 ± 0.24
MOK-5	< 0.22	< 0.094	< 0.13	< 0.078
MOK-6	< 0.22	< 0.094	< 0.13	< 0.078
MOK-7	< 0.22	< 0.094	< 0.13	0.0895 ± 0.0036
MOK-8	< 0.22	< 0.094	< 0.13	< 0.078
MOK-9	< 0.22	< 0.094	< 0.13	< 0.078
MOK-10	< 0.22	< 0.094	< 0.13	0.118 ± 0.016

The As species concentrations detected in high flow sampling season also differ per site of samples collected. The As^{+3} was detected in site 1 and site 3 with concentrations of 0.301 and 0.299 µg/L, respectively. The MMA was detected in site 4 with concentration of 0.224 µg/L. The As^{+5} was predominating and concentrations of the detected sites were alternating within the range of 0.0895-7.70 µg/L. The precision of the results is adequate since RSDs were found to be less than 10%. The DMA was not detected in all the sites. Mokolo River is found at the area dominated by variety of anthropogenic activities which may result with the elevated level of As species in the environment. The varied concentration of As species per sampling sites are also affected by the direct exposure of that particular site to As source. For instance, the astonishing concentration of As^{+5} at site 4 may have attributed to the direct deposition of burning fuel released by the motor vehicles. The deposition of burning fuel influenced the rapid accumulation of As at sampling site 4 which samples were collected under the bridge. The As species is not essential nutrient for plants and animals at any concentration so the aquatic ecosystem of Mokolo River is threatened by As contamination.

The sampling campaign at Mokolo River was conducted twice at different seasons to monitor the concentration of As species at each season. The As species concentrations obtained during low flow sampling season are presented in table 3.21.

Table 3.21: Concentrations of As species in water samples of Mokolo River during low flow sampling season.

Sample Id	As^{+3} (µg/L)	DMA (µg/L)	MMA (µg/L)	As^{+5} (µg/L)
LEP-1	< 0.22	<0.094	< 0.13	< 0.078
LEP-2	< 0.22	<0.094	< 0.13	0.449 ± 0.005
LEP-3	< 0.22	<0.094	0.645 ± 0.018	2.03 ± 0.020
LEP-4	< 0.22	<0.094	0.451 ± 0.030	4.99 ± 0.027
LEP-5	< 0.22	<0.094	0.348 ± 0.033	3.24 ± 0.044
LEP-6	< 0.22	<0.094	0.391 ± 0.013	0.920 ± 0.013
LEP-7	< 0.22	<0.094	0.315 ± 0.0051	0.529 ± 0.010
LEP-8	< 0.22	<0.094	< 0.13	0.324 ± 0.027
LEP-9	0.304 ± 0.027	<0.094	< 0.13	0.733 ± 0.031
LEP-10	0.881 ± 0.019	<0.094	0.512 ± 0.072	1.15 ± 0.0013

The As species concentrations obtained in low flow sampling season show the detected As^{+3} site 9 and 10 with the varied concentrations of 0.304 µg/L and 0.881 µg/L, respectively. The MMA was detected at wide range of the sites with the concentrations varied from 0.315-0.645 µg/L. The As^{+5} was predominant at all site with the maximum concentration of 4.99 µg/L found at site 4. The excellent precision of the results was proven by the RSDs which were found below 10%. The DMA was not detected in all sites. The low flow sampling season show higher concentrations of As species as compared to that obtained during high flow sampling seasons. The predominating As^{+5} may have been influenced by the oxidising environmental condition of the river system which occurs at wide range of pH and it favours the dominance of As^{+5} (Rakhunde *et al.*, 2012). The As^{+3} is likely to dominate in the reducing conditions at pH < 9.2, hence As^{+3} was not in favourable conditions and was found at low concentration (Rakhunde *et al.*, 2012). The MMA concentrations show higher microbial activities in Mokolo River during low flow sampling seasons. The microbial activities are known to methylate the inorganic As species and facilitate the oxidation of As^{+3} to As^{+5} resulting with the increased As^{+5} concentration (O'Reilly *et al.*, 2001). The microbial activities are likely to be enhanced by sewage effluents directly or indirectly deposited into the river.

The As species determination in sediment samples was conducted first by investigating a relevant extraction reagents which are incapable of inducing species interconversion. This was because the integrity of the species should be maintained throughout the analytical procedure in order to avoid the incorrect results of the condition of the river systems.

Different analytical procedures were investigated to adopt the suitable procedure in which the reagents used and microwave extraction condition favours the preservation of the integrity of As species. The extraction of As species in sediment samples was attempted using 1.0 M H_3PO_4 and 0.1 M $C_6H_8O_6$ extraction reagents reported by Garcia-Manyes *et al.* (2002). The extraction of As species using phosphate reagent is through ligand exchange, which involves desorption of As species by phosphate. The extracted As species were separated and detected by employing gradient mode of elution using 20 mM and 60 mM NH_4NO_3 at pH 8.7 mobile phase. The chromatogram of As species in sediment samples obtained using the above procedure is indicated in figure 3.5.

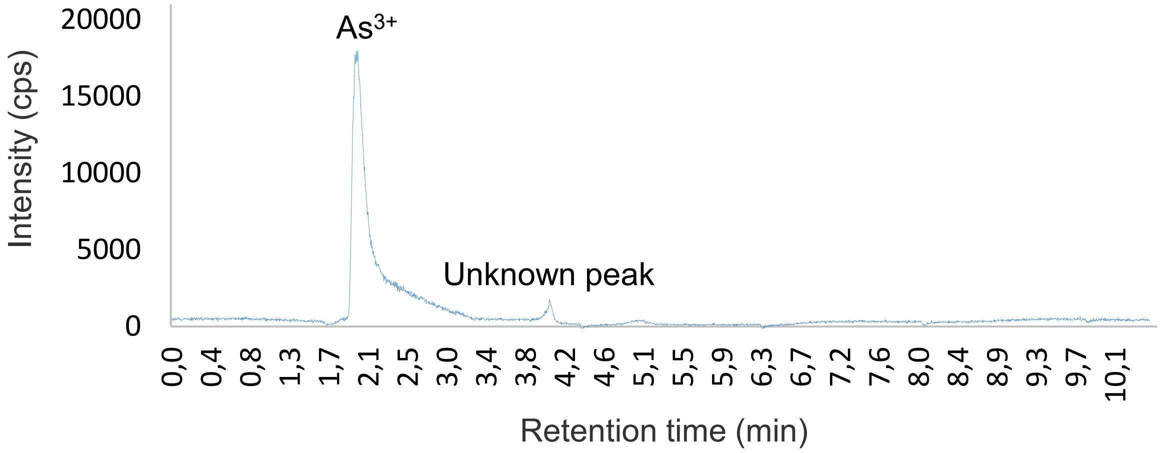

Figure 3.5: Chromatogram of As species for sediment samples obtained using 1.0 M H_3PO_4 and 0.1 M $C_6H_8O_6$

The peaks on the chromatogram were identified as As^{+3} and the unknown peak. The As species obtained using the suggested method show the possibility of reduction of As^{+5} to As^{+3} which may have induced by the use of reducing agent $C_6H_8O_6$.

The $(NH_4)_2HPO_4$ acid and EDTA were investigated for the suitability of extraction of As species in sediment samples. The preliminary analysis of the extracts showed that the capability of the extractant reagents to be used without species interconversion is expected. The $(NH_4)_2HPO_4$ was assayed at different concentrations of 0.1, 0.3 and 1.0 M $(NH_4)_2HPO_4$ with 50 mM EDTA. The extracted species were separated and detected by employing gradient mode of elution using optimised 10 mM NH_4NO_3 and 60 mM NH_4NO_3 at pH 8.7 adjusted with NH_3 solution. The extraction reagents of 0.3 M $(NH_4)_2HPO_4$ with 50 mM EDTA yielded excellent results which were further investigated for testing the applicability of the proposed analytical procedure for monitoring of As species in sediments samples. The chromatogram of mostly extracted As species in sediment samples using the developed analytical procedure is indicated in figure 3.6.

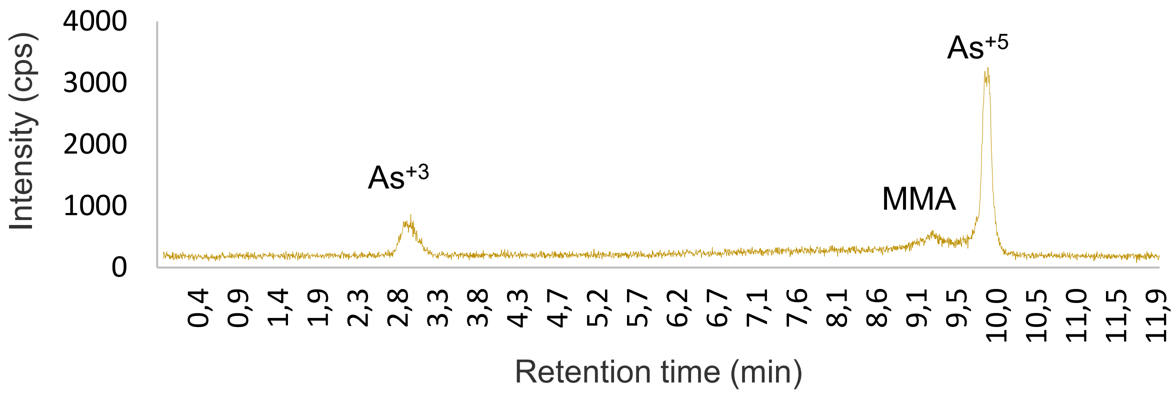

Figure 3.6: Chromatogram of As species for sediment samples

The As species concentrations in sediments of the river systems were extracted and monitored with a suitable procedure. The species concentrations in sediment samples are indicated in tables 3.22-3.24.

Table 3.22: Concentrations of As species in sediment samples of Great Letaba River.

Sample Id	As^{+3} (ng/g)	DMA (ng/g)	MMA (ng/g)	As^{+5} (ng/g)
GLR-1	74.0 ± 2.0	< 0.07	97 ± 5.5	457 ± 27
GLR-2	337 ± 1.7	< 0.07	401 ± 1.1	881 ± 42
GLR-3	1190 ± 16	< 0.07	449 ± 6.3	1150 ± 49
GLR-4	630 ± 14	< 0.07	318 ± 28	903 ± 43
GLR-5	482 ± 6.1	< 0.07	261 ± 2.1	601 ± 16
GLR-6	340 ± 2.1	< 0.07	159 ± 14	312 ± 39
GLR-7	< 0.11	< 0.07	132 ± 3.0	291 ± 9.2
GLR-8	< 0.11	< 0.07	< 0.09	152 ± 12
GLR-9	< 0.11	< 0.07	< 0.09	< 0.03
GLR-10	< 0.11	< 0.07	311 ± 5.4	189 ± 5.4

The detected As species in Great Letaba River sediments were in the range of 74-1190 ng/g for As^{+3}, 97-449 ng/g for MMA and 152-1150 ng/g for As^{+5}. The DMA was not detected in all sites. The results were precise with RSDs of less than 10%. The highest concentration was observed at site 3 and may have been attributed to the weathering processes of rocks. Various types of rocks were dominated in site 3 and as such, As containing rocks may be converted to inorganic As species which is then dissolved in water and further adsorbed into river sediments (Winkel *et al.*, 2008). The activities of micro-organisms in sediments methylate the inorganic species to organic species (O'Reilly *et al.*, 2001). Therefore, MMA concentrations were resulted by the effects of metabolic activities of micro-organisms. The As species concentrations in sediment samples are higher than in water samples. The underlying sediments protect water quality of the river system through adsorption of water contaminant (Terlecka, 2005). Thus, higher As species concentration were observed in sediment samples.

The As species concentrations of Mokolo River samples obtained during different seasons are presented in tables 3.23 and 3.24.

Table 3.23: Concentrations of As species in sediment samples of Mokolo during high flow sampling season.

Sample Id	As^{+3} (ng/g)	DMA (ng/g)	MMA (ng/g)	As^{+5} (ng/g)
MOK-1	4350 ± 450	< 0.07	1600 ± 90	13000 ± 92
MOK-2	2560 ± 74	< 0.07	2280 ± 74	13100 ± 160
MOK-3	7950 ± 500	< 0.07	< 0.09	12800 ± 1200
MOK-4	3760 ± 160	< 0.07	< 0.09	15600 ± 85
MOK-5	2580 ± 140	< 0.07	935 ± 87	2580 ± 140
MOK-6	3920 ± 140	< 0.07	2060 ± 120	6160 ± 590
MOK-7	3930 ± 220	< 0.07	1870 ± 53	4120 ± 120
MOK-8	2890 ± 59	< 0.07	1710 ± 180	4110 ± 230
MOK-9	3140 ± 99	< 0.07	1850 ± 280	4060 ± 200
MOK-10	3350 ± 100	< 0.07	1610 ± 62	4420 ± 190

During high flow sampling season, highest concentration of 7950 ng/g As^{+3} was found in site 3, 2280 ng/g for MMA was observed in site 2 and 15600 ng/g As^{+5} was observed in site 4. During low flow sampling season (Table 3.24), the highest concentration of 8870 ng/g As^{+3} was found in site 3, 1860 ng/g for MMA was found in site 9 and

9630 ng/g As^{+5} was observed in site 4. The precision of the results were monitored in all the cases and RSDs of less than 10% obtained show good precision. The DMA was not detected in both sampling season.

Table 3.24: Concentrations of As species in sediment samples of Mokolo River during low flow sampling season.

Sample Id	As^{+3} (ng/g)	DMA (ng/g)	MMA (ng/g)	As^{+5} (ng/g)
LEP-1	311 ± 9.9	< 0.07	1320 ± 22	9260 ± 18
LEP-2	3920 ± 480	< 0.07	1030 ± 110	8170 ± 640
LEP-3	8870 ± 510	< 0.07	1370 ± 160	7730 ± 200
LEP-4	6610 ± 130	< 0.07	1400 ± 93	9630 ± 100
LEP-5	6780 ± 360	< 0.07	832 ± 95	7900 ± 290
LEP-6	6440 ± 31	< 0.07	959 ± 100	6590 ± 340
LEP-7	7020 ± 340	< 0.07	1600 ± 11	1490 ± 170
LEP-8	3380 ± 180	< 0.07	728 ± 94	1750 ± 78
LEP-9	3350 ± 140	< 0.07	1860 ± 56	1570 ± 110
LEP-10	3640 ± 330	< 0.07	1810 ± 110	1410 ± 48

The concentration of As^{+3} was higher during low flow sampling season whereas As^{+5} was higher during high flow sampling season. This may have been attributed by redox processes and geochemical nature of sediments (O'Reilly *et al.*, 2001). The anthropogenic and microbial activities also affect the levels of As species. The metabolic activities of micro-organisms in sediments methylate inorganic As species to MMA and DMA. Hence levels of MMA were observed in sediments of both sampling seasons. The highest concentration of particular inorganic species in water and sediment samples were predominating the site 4 of the river in both sampling seasons.

Mokolo River has higher concentration of As than Great Letaba River. There is lack of reports on As species in water and sediments from South Africa. Thus, comparison has been made with the reported levels from other countries. Ellwood and Maher (2003) reported the range of As^{+3} and As^{+5} concentrations of 230-2430 ng/g and

110-7930 ng/g, respectively in marine sediments obtained from Lake Macquari, Australia using HPLC-ICP-MS. The concentrations of As^{+3} and As^{+5} in sediments reported by Ellwood and Maher (2003) are lower than data obtained from Mokolo River in both sampling seasons. However, the levels reported by these authors were comparable with data obtained from Great Letaba River. Chen *et al.* (2006) detected 72.9 µg/g for As^{+5} in soil sample using IC-ICP-MS which is higher than As^{+5} concentrations reported in this study. The levels of As species could vary depending on the source and environmental conditions. The main anthropogenic sources of As are from use of arsenical pesticides, fertilisers, irrigation, ash from the burning of fossil fuels, and leachates from industrial waste such as mine tailings.

3.8. Solid phase extraction of As^{+5} in water using multi walled carbon nanotubes with branched polyethyleneimine

The SPE technique was adopted for this study due to faster operation, pre-concentration efficiency, merit of satisfactory recovery and easier compatibility with analytical instruments (Chen *et al.*, 2014). The SPE technique was used to pre-concentrate As^{+5} in water samples by employing MWCNTs-BPEI as the adsorbent materials.

3.8.1 Characterisation of adsorbent material

The control MWCNTs, oxidised MWCNTs and MWCNTs-BPEI were characterised using XRD, FTIR and TGA to verify the successful modification of the nanocomposite before use as adsorbent.

The characterisation using XRD was employed for phase identification and crystallinity through the modification process of MWCNTs with BPEI polymer. The XRD spectrum of control MWCNTs, oxidised MWCNTs and MWCNTs-BPEI are shown in figure 3.7.

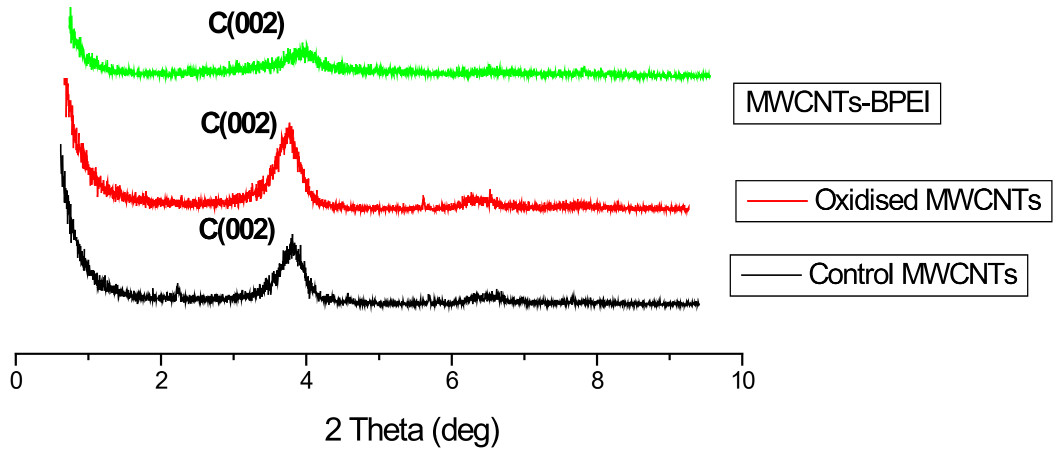

Figure 3.7: The XRD patterns for control MWCNTs, oxidised MWCNTs and MWCNTs-BPEI

The XRD profile shows a peak in the control MWCNTs which is identified as graphitic carbon indexed to C(002) plane reflections of hexagonal graphite (Mkhondo and Magadzu, 2014). The intensified graphitic peak of the oxidised-MWCNTs is attributed to formation of sp^3 hybridised carbon (C-H) due to effects of acid treatment as compared to sp^2 hybridised carbon (C=C) of the untreated or control MWCNTs (Malikov *et al.*, 2014). The enhanced peak on the oxidised MWCNTs further indicates a formation of more ordered structure of MWCNTs with the walls remaining intact without significant damage. The impurities present in the control MWCNTs are due to thin layer of amorphous carbon on the nanotube surface and the encapsulated iron catalyst residue (Stobinskia *et al.*, 2010). A decrease of graphitic carbon indexed to C(002) plane reflection of the MWCNTs-BPEI shows the successful interaction of MWCNTs with BPEI polymer. The attenuation of the graphitic peak intensity of MWCNTs-BPEI observed on the XRD pattern occurred as a result of physisorption of a thin layer of amorphous BPEI coating on the surface of oxidised MWCNTs (Malikov *et al.*, 2014). The XRD pattern of BPEI polymer (Figure 3.8) was investigated for identification of BPEI peaks on the XRD spectrum of MWCNTs-BPEI.

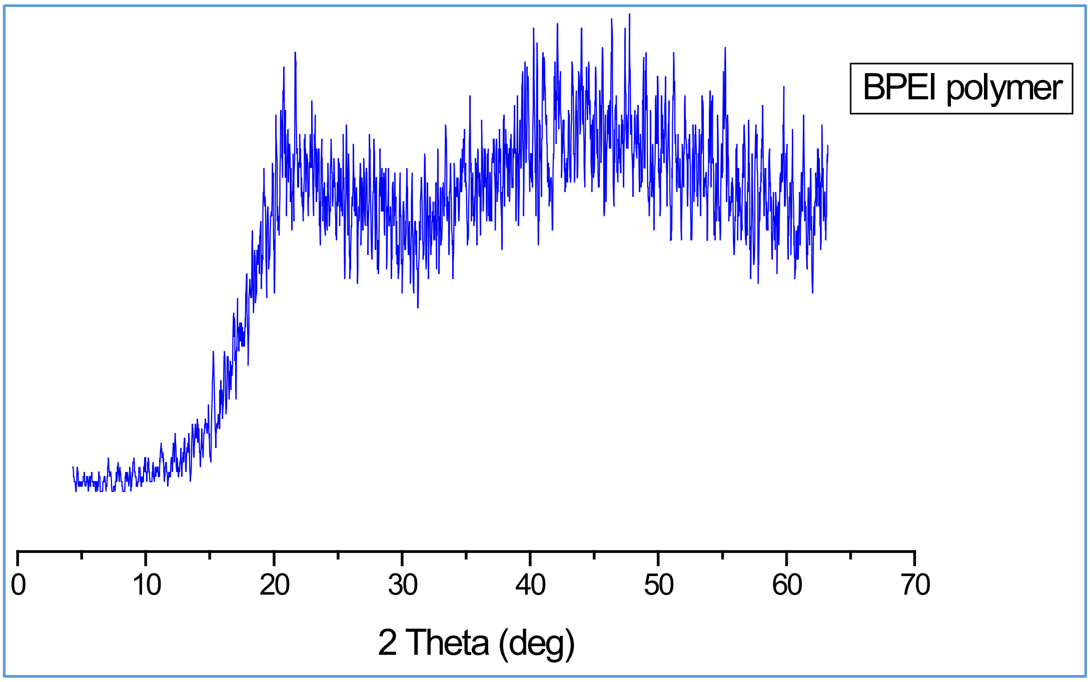

Figure 3.8: The XRD pattern for BPEI polymer

To understand the nature of functional groups at each step in the chemical functionalisation, the FTIR spectra of control MWCNTs and acid-treated MWCNTs (oxidised) shown in Figure 3.9 and MWCNTs-BPEI composite shown in Figure 3.10 were measured. In Figure 3.9, control MWCNTs spectrum shows weak absorption peaks on the spectrum. The peaks at 3722 cm^{-1} and 1740 cm^{-1} correspond to the characteristic stretching vibrations of the O-H bond in hydroxyl groups, carboxyl groups and absorbed water (Fuente *et al.*, 2003; Yan *et al.*, 2007; Bergeret *et al.*, 2008; Naseh *et al.*, 2010). The peaks at 2927 cm^{-1} and 1534 cm^{-1} are assigned to C-H and C=C vibration modes, respectively in graphitic structure of MWCNTs and are strongly dependent on the nature and concentration of surface oxides (Bergeret *et al.*, 2008; Naseh *et al.*, 2010).

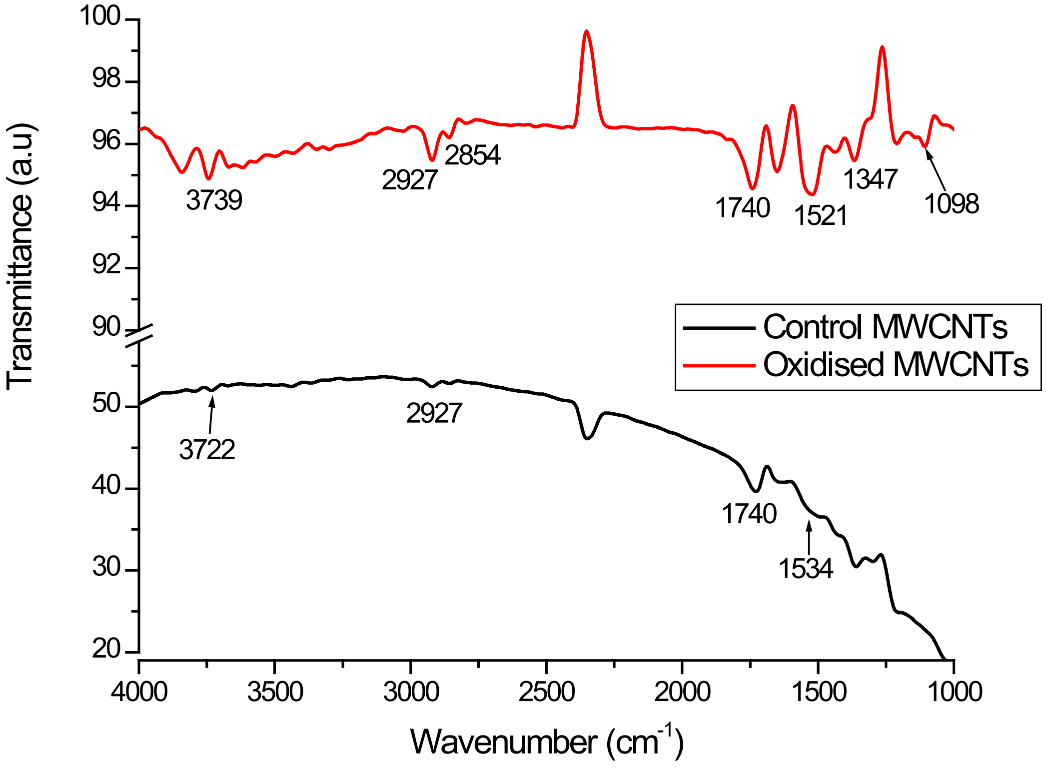

Figure 3.9: The FTIR spectra of control MWCNTs and oxidised MWCNTs

The spectrum of oxidised MWCNTs shows appearance of the enhanced peaks intensities as compared to intensities of the peaks on the spectrum of control MWCNTs. The absorption peaks at 3739 and 1740 cm^{-1} correspond to stretching vibrations of O-H and C=O, respectively (Zhang *et al.*, 2003). The peak at 1740 cm^{-1} indicates that carboxylic groups, which are formed due to the oxidation of carbon atoms on the surfaces of the MWCNTs by HNO_3 and H_2SO_4 acid mixture (Moradiana *et al.*, 2014). Two weak peaks also emerged at 1347 and 1098 cm^{-1} which are due to the O-H bending deformation of carboxylic acid group and acidic C-O stretching, respectively (Mkhondo and Magadzu, 2014). In addition, peaks at 2854 and 2927 cm^{-1} could be attributed to asymmetric and symmetric CH_2 stretching, whereas peak at 1534 cm^{-1} becomes clearer and it corresponds to C-H stretching vibrations (Fuente *et al.*, 2003). The intensities of the peaks on oxidised MWCNTs spectrum were greatly influenced by the concentration of carboxyl groups attached to the control MWCNTs, which could be attributed to the oxygen-containing groups (-COOH, -OH) (Yan *et al.*, 2007; Naseh *et al.*, 2010). This is due to the increase in the dipole moment associated with graphene vibrations (Bergeret *et al.*, 2008; Moradiana *et al.*, 2014). This result confirms that a sufficient number of oxygen-containing functional groups were produced on the surface of MWCNTs by acid treatment.

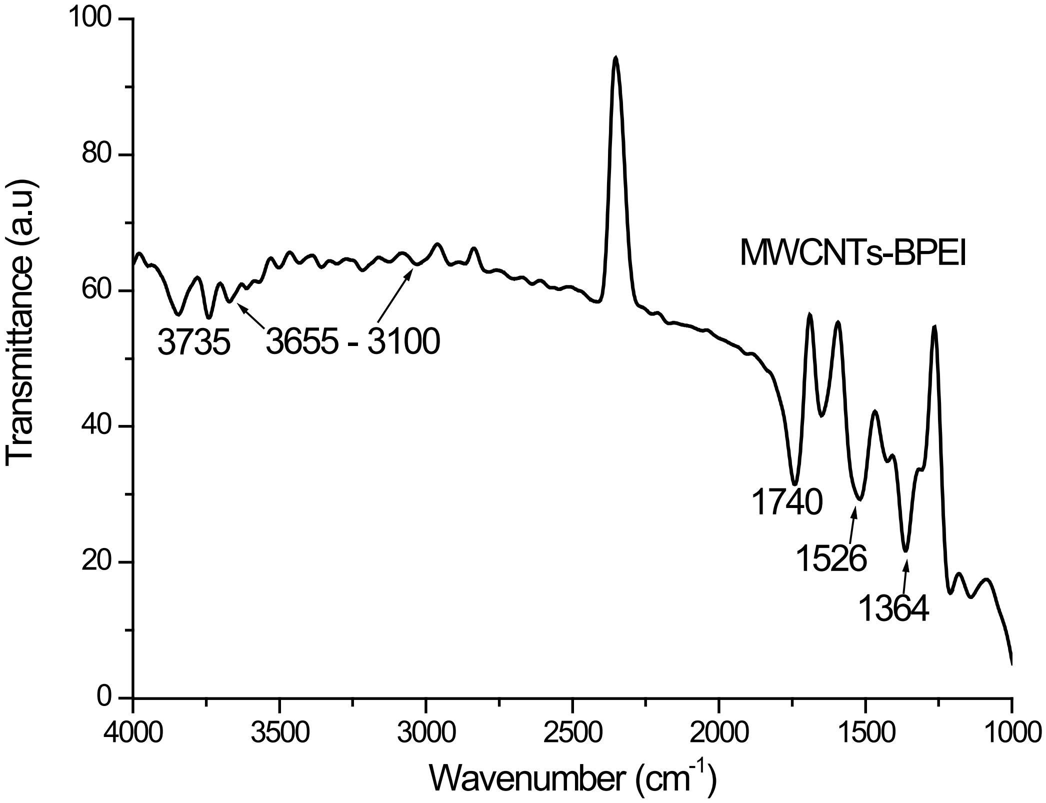

Figure 3.10: The FTIR spectrum of MWCNTs-BPEI

The spectrum of MWCNTs-BPEI (Figure 3.10) reveals the absorption of BPEI polymer non-covalently immobilised on the MWCNTS through the induced surface oxides (Shen *et al.*, 2009). In Figure 3.10, absorption peak located at 3735 cm^{-1} could be attributed to the O-H vibrations in BPEI and MWCNTs (Singh *et al.*, 2005). The absorption peaks at 3100-3655 cm^{-1} are assigned to the stretching vibrations of N-H of the BPEI (Chen *et al.*, 2013; Zhaoa *et al.*, 2013). The peak at 1740 cm^{-1} indicates the absorption characteristic of N-C=O bond formation between amine and carboxylic group of the MWCNTs-BPEI (Singh *et al.*, 2005; Moradiana *et al.*, 2014). In addition, peaks located at 1526 and 1364 cm^{-1} can be assigned to N-H bending formation and C-N stretching vibrations of the composite (Singh *et al.*, 2005; Shen *et al.*, 2009; Wang *et al.*, 2013; Zhaoa *et al.*, 2013; Moradiana *et al.*, 2014). The FTIR spectrum of MWCNTs-BPEI demonstrates successful non-covalent immobilisation of BPEI onto the side walls of the oxidised MWCNTs leading to formation of nanocomposite.

The modification of MWCNTs can be further supported by Raman analysis presented in Figure 3.11. The main graphitic bands present on the spectra are assigned as D band located at 1342 cm^{-1} and G band at 1572 cm^{-1} (Bokobza *et al.*, 2012; Zhaoa *et al.*, 2013; Zhou *et al.*, 2014). The D band is usually activated by the presence of disorder in carbon systems and characteristic of G band strongly correspond to in-plane C-C symmetric stretching vibrations in graphene sheets (Zhou *et al.*, 2014). The Raman spectra also exhibits a band at 2691 cm^{-1} called the G' band and attributed to the overtone of the D band. The degree of structural defects or disorders in sp^2-based carbon can be evaluated by the intensity ratio of the D and G bands in the spectra (Bokobza *et al.*, 2012; Wang *et al.*, 2013). The relative intensity ratio of these bands (I_D/I_G) is known as a ratio of sp^3-hybridised carbon atoms (amorphous/disordered carbon) relative to sp^2-bonded carbon atoms (graphitic carbon) (Baik *et al.*, 2004; Zhang *et al.*, 2004).

In Figure 3.11, Raman spectra have different I_D/I_G ratios, which is an indication of disruption of the sp^2-bonded carbon atoms to sp^3-hybridised carbon atoms. As expected, the I_D/I_G ratios of oxidised MWCNTs and MWCNTs-BPEI are relatively higher than that of control MWCNTs, suggesting that some moieties are covalently introduced onto the surfaces of MWCNTs (Baik *et al.*, 2004). Furthermore, a debundling also occurs by incorporation of BPEI polymer chains into oxidised MWCNTs aggregates during composite processing, which resulted with low I_D/I_G ratio of MWCNTs-BPEI as compared to oxidised MWCNTs. Raman spectrum of the composite (MWCNTs-BPEI) is dominated by the weakly absorbed BPEI polymer bands covalently immobilised of the walls of oxidised MWCNTs. This confirms successful functionalisation of MWCNTs-BPEI.

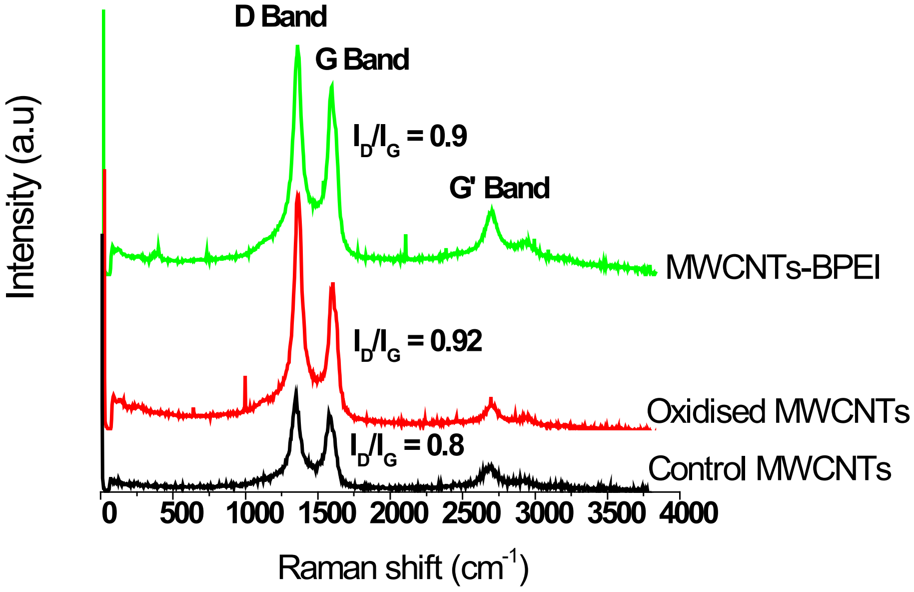

Figure 3.11: The Raman spectra of control MWCNTs, oxidised MWCNTs and MWCNTs-BPEI

The modified MWCNTs were explored using TGA to investigate thermal stability, purity and decomposition temperature. The TGA profile of the modified MWCNTs is presented in Figure 3.12. The TGA profiles reveal a slight decomposition at around a temperature of 100°C, is mainly due to loss of water from materials. The stability of the MWCNTs could be attributed to the aromatic bonding within the structure, composition of catalyst and other materials such as amorphous carbon and graphitic particles (Yu *et al.*, 2007). The absence of non-oxidisable compound for approximately 150 to 490°C in control MWCNTs indicated no destruction of aromatic carbon ring as a functionalised group (Bom *et al.*, 2002). The losses from 490 to 580°C could be attributed to decomposition of amorphous carbon. A further weight loss from 580 to 800°C may have attributed to residual mass of metal catalyst Fe used to manufacture the nanotubes as well as the oxidation products of the catalyst (Bom *et al.*, 2002).

The MWCNTs were treated with acid mixture to eliminate impurities as well as to change the thermal behaviour of hexagonal carbon ring. The oxidisable compounds from 100 to 525°C in the thermogram of oxidised MWCNTs are attributed to the induced surface oxides during the acid treatment process (Bom *et al.*, 2002). Debundling graphitic carbon in MWCNTs and reduction of metal catalyst impurities through acid treatment provided a weight loss shifted from 586°C in thermogram of control MWCNTs to decomposition temperature of 630°C in the oxidised MWCNTs. The zero percent weight loss in the oxidised MWCNTs from 630°C indicates that the Fe catalyst was completely degraded at the high temperature applied. The stability of oxidised MWCNTs at high temperature revealed that no defects occurred during functionalisation, hence the materials achieve high thermal stability compared to control MWCNTs (Geng *et al.*, 2015). There is a significant weight loss from 100 to 543°C in the thermogram of MWCNTs-BPEI which is ascribed to the presence of BPEI interacted with surface oxides grafted on the walls of the oxidised MWCNTs (Bom *et al.*, 2002; Yu *et al.*, 2007). The oxidised MWCNTs indicated a further weight loss at 630°C while decomposition of BPEI happened at 543°C (Bom *et al.*, 2002). This clearly demonstrated the non-covalent immobilisation of BPEI on MWCNTs and resulted in a coating amount of BPEI of 18%.

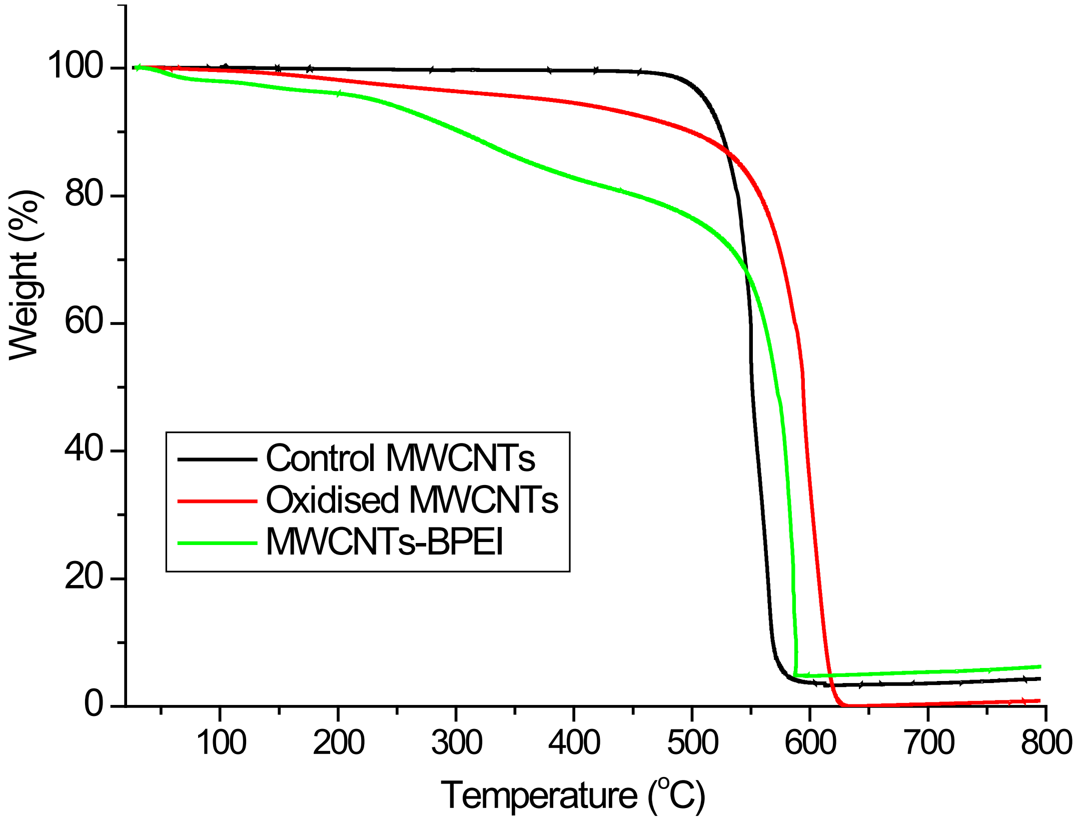

Figure 3.12: The TGA profiles for control MWCNTs, oxidised MWCNTs and MWCNTs-BPEI

3.8.2 Concentrations of As^{+5} in water samples obtained using solid phase extraction

The MWCNTs functionalised with BPEI exhibit excellent sorbent material for the selective retention of As^{+5} in the presence As^{+3} in the aqueous samples. The successful modification of MWCNTs-BPEI led to validation of SPE analytical procedure and the pre-concentration factor of 23.3, with adequate percentage RSDs achieved using off-line mode. The results for SPE procedure are comparable with HPLC-ICP-MS as shown in Table 3.25

The results obtained by SPE procedure are in good agreement with the HPLC-ICP-MS results. This agreement show that MWCNTs-BPEI composites exhibit a favourable adsorption efficiency for As^{+5} in water samples. The SPE has the capability to provide the samples which are concentrated enough for detection. Due to the interaction between the adsorbent material, analyte of the interest and eluent, the SPE procedure is reliable to resolve the interferences of polyatomic and matrices (Zwir-Ferenc and Biziuk, 2006).

The SPE procedure showed potential for the routine speciation analysis of As^{+5} in aqueous matrices. This was attributed to MWCNTs-BPEI composites for providing the potential approach of monitoring As^{+5} in water samples. The accuracy and precision of the results show the efficiency of SPE procedure for sample pre-treatment.

Table 3.25: Concentrations of As^{+5} in water samples of Mokolo River during low flow sampling season.

Sample Id	As^{+5} [a] (µg/L)	As^{+5} [b] (µg/L)
LEP-1	0.0612 ± 0.0032	< 0.078
LEP-2	0.307 ± 0.029	0.449 ± 0.005
LEP-3	1.85 ± 0.12	2.03 ± 0.020
LEP-4	3.65 ± 0.22	4.99 ± 0.027
LEP-5	2.27 ± 0.14	3.24 ± 0.044
LEP-6	0.702 ± 0.04	0.920 ± 0.013
LEP-7	0.367 ± 0.038	0.529 ± 0.010
LEP-8	0.153 ± 0.043	0.324 ± 0.027
LEP-9	0.493 ± 0.067	0.733 ± 0.031
LEP-10	0.762 0.087	1.15 ± 0.0013

[a] denotes analysis using ICP-MS after separation by SPE

[b] denotes analysis using HPLC-ICP-MS

The study conducted by Chen *et al.* (2013) reported As^{+5} concentrations of 1.52 µg/L in snow water and 2.04 µg/L in rain water with the pre-concentration factor of 16.3 when using AFS detection system after the SPE procedure. The results obtained in a study by Chen *et al.* (2013) are comparable with the results obtained in this study. However, concentration of As^{+5} in water samples differ with respect to the potential sources of As in water sample. The chemistry and pH of water also play a crucial role on the influence of the existence of As species in water.

3.9. Determination of Cr(VI) in water using GF-AAS

Concentration of Cr(VI) was measured using GF-AAS after separating through the column. Quantitative recovery of 90.0% was obtained for method validation of SPE procedure for Cr speciation. The use of alizarin solution prevented oxidation of Cr(III) to Cr(VI) at pH 5.5. The LOD and LOQ for the analysis of water samples after SPE by GF-AAS were found to be 0.105 µg/L and 0.351 µg/L, respectively.

The total Cr and Cr(VI) concentrations were quantified using GF-AAS. The measured concentrations of total Cr and Cr(VI) together with the percentage of Cr(VI) in water samples collected from Blood River are given in Table 3.26. The percentage of Cr(VI) in water samples collected from Blood River ranged from 3.51 to 32.5%.

Table 3.26: Percentage of Cr(VI) in water samples collected from Blood River.

Site	**Total Cr (µg/L)**	**Cr(VI) (µg/L)**	**%Cr(VI)**
1	3.73	0.131	3.51
2	1.56	0.169	10.8
3	4.57	0.572	12.5
4	6.12	1.99	32.5
5	5.68	1.45	25.5
6	5.37	0.320	5.97
7	< 0.31	0.443	-
8	< 0.31	0.408	-
9	1.84	0.228	12.4
10	3.55	1.02	28.8

Similarly, the concentrations of total Cr and Cr(VI) in water samples collected from Mokolo River were measured using GF-AAS. The concentrations of total Cr and Cr(VI) along with the percentage of Cr(VI) in water samples collected from Mokolo River are given in Table 3.27. The percentage of Cr(VI) in water samples collected from Mokolo River ranged from 9.59 to 24.5%.

Table 3.27: Percentage of Cr(VI) in water samples collected from Mokolo River.

Site	**Total Cr (µg/L)**	**Cr(VI) (µg/L)**	**%Cr(VI)**
1	< 0.31	0.322	-
2	3.52	0.455	12.9
3	1.33	0.319	23.9
4	2.25	0.553	24.5
5	1.37	0.133	9.73
6	2.35	0.435	18.5
7	3.43	0.705	20.5
8	2.55	< 0.105	-
9	1.63	0.456	27.9
10	2.49	0.238	9.59

The levels of Cr(VI) in water samples from Blood and Mokolo Rivers ranged from 0.131 to 1.99 µg/L and 0.133-0.553 µg/L, respectively. These levels were low and couldn't pose risks to human beings, aquatic plants and animals. The highest level of Cr(VI) was detected in Blood River, whereas the recorded lowest level of Cr(VI) was the same in both rivers. This is in agreement with the levels of total Cr in water samples collected from both rivers. Vasilatos *et al.* (2012) reported Cr(VI) concentrations as high as 80 µg/L in surface and ground water used for public water supply in Greece. The highest concentration of 1.99 µg/L, in this study, is 40 times lower than the level reported by Vasilatos *et al.* (2012). The comparison of the levels of Cr(VI) in water samples from both rivers is presented in figure 3.13.

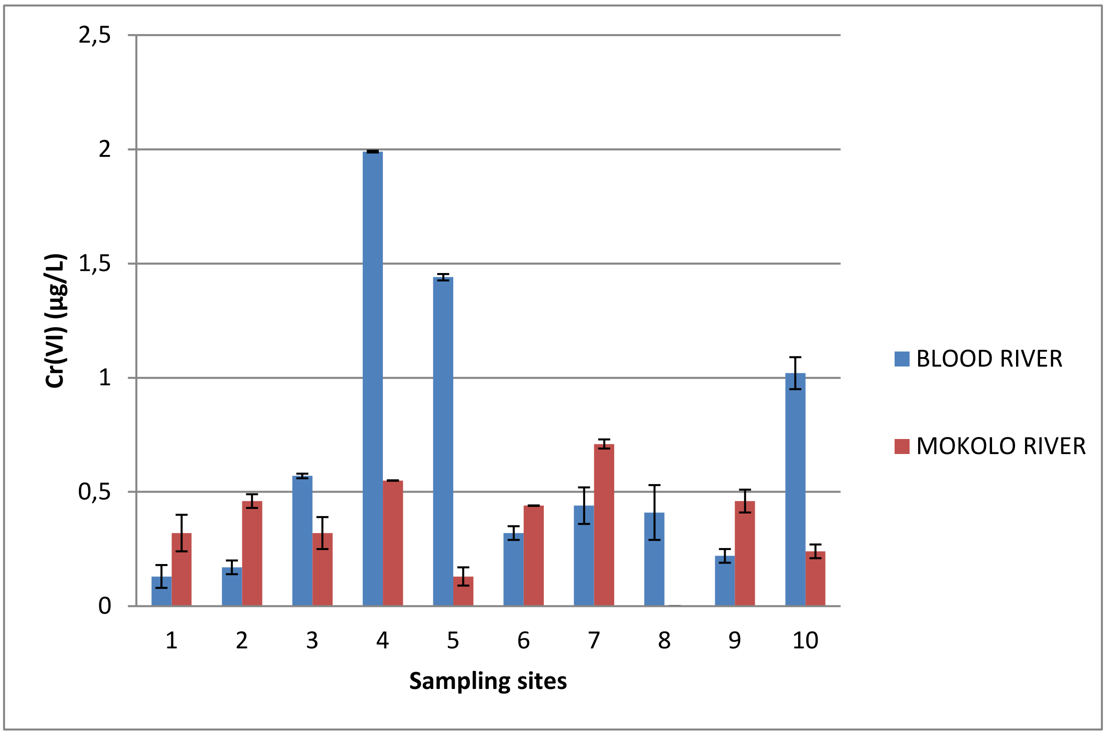

Figure 3.13. Comparison of the levels of Cr(VI) in water samples collected from Blood and Mokolo Rivers

The stability of Cr(VI) solution was investigated by analysing the extracted solution in a week interval. After seven days the percent recovery of 94.2% was recorded. The percent recoveries of Cr(VI) after 14 and 21 days were 62.7% and 58.6%, respectively. This reveals that the stability of Cr(VI) has been substantially decreased after 14 days. Therefore, we have analysed the separated Cr(VI) within a week in this study.

3.10. Determination of Cr(VI) in sediment samples

Concentrations of Cr(VI) in sediment samples were measured using GF-AAS. Percentage recovery of 99.9% was obtained for method validation of Cr(VI) determination procedure by spiking the sample before extraction using 0.1 M Na_2CO_3.

The LOD and LOQ for Cr(VI) quantification method by GF-AAS were found to be 0.0306 ng/g and 0.102 ng/g, respectively.

The total Cr and Cr(VI) concentrations in sediment samples were measured using GF-AAS. The measured concentrations of total Cr and Cr(VI) together with the percentage of Cr(VI) in sediment samples collected from Blood River are given in Table 3.28. The percentage of Cr(VI) in sediment samples collected from Blood River ranged from 0.308 to 0.977%. Hexavalent Cr represented only a little fraction of the total Cr in sediments, with the highest value of 0.977%.

Table 3.28: Percentage of Cr(VI) in sediment samples collected from Blood River.

Site	**Total Cr (µg/g)**	**Cr(VI)** (µg/g)	**%Cr(VI)**
1	131	1.28	0.977
2	146	0.450	0.308
3	135	0.610	0.452
4	219	0.930	0.425
5	183	1.02	0.557
6	129	0.410	0.318
7	183	0.820	0.448
8	253	1.32	0.522
9	152	0.720	0.474
10	164	0.540	0.329

Similarly, the total Cr and Cr(VI) concentrations in sediment samples from Mokolo River were measured using GF-AAS. The measured concentrations of total Cr and Cr(VI) together with the percentage of Cr(VI) in sediment samples collected from Mokolo River are given in Table 3.29. The percentage of Cr(VI) in sediment samples collected from Mokolo River ranged from 0.197 to 1.67%. The fraction of Cr(VI) in sediment samples is lower than its fraction in water samples. However, the presence of Cr(VI) in sediments represent a permanent environmental risk (Elci *et al.*, 2010).

Table 3.29: Percentage of Cr(VI) in sediment samples collected from Mokolo River.

SITE	**Total Cr** (µg/g)	**Cr(VI) (µg/g)**	**%Cr(VI)**
1	73.7	0.361	0.489
2	91.1	0.180	0.197
3	108	0.332	0.307
4	25.7	0.430	1.67
5	63.4	0.312	0.492
6	52.6	0.580	1.10
7	193	1.04	0.539
8	156	0.761	0.488
9	99.2	0.202	0.204
10	53.0	0.815	1.54

The comparison of the levels of Cr(VI) in sediment samples from both rivers are dine in figure 3.14.

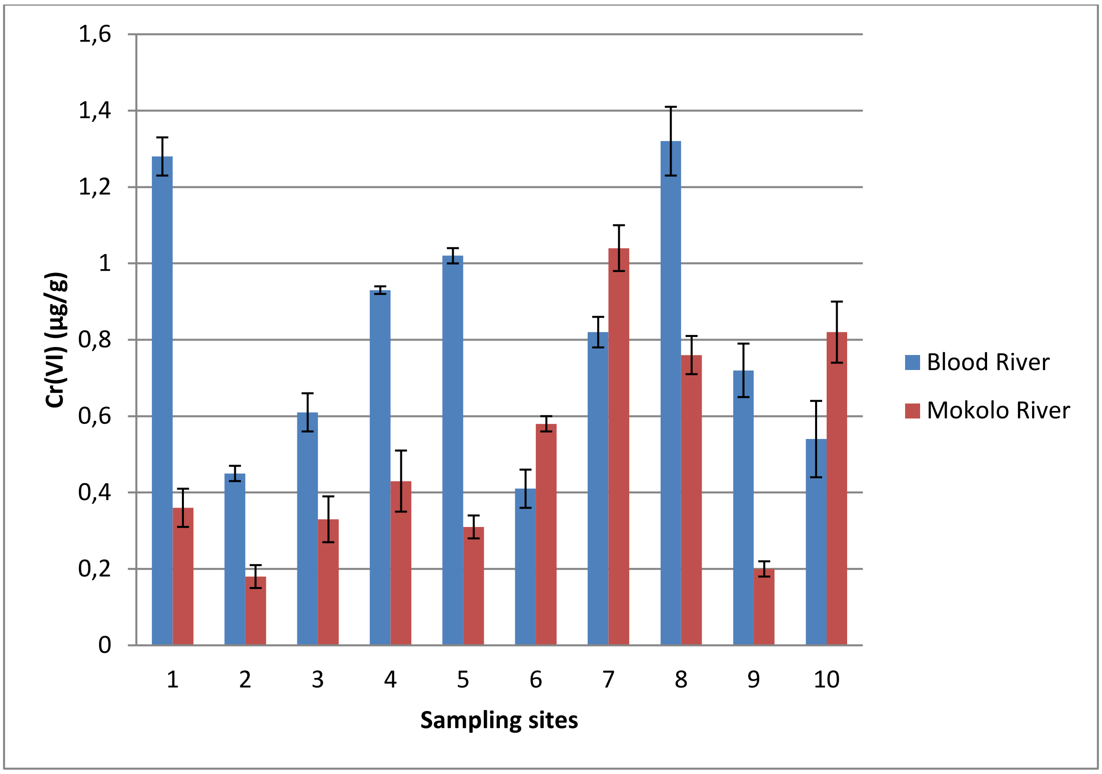

Figure 3.14. Comparison of the levels of Cr(VI) in sediment samples collected from Blood and Mokolo Rivers

Aquatic ecosystems surrounded by catchments with a known history of mining, near artisanal and small scale mining operations, and expanding agricultural and urban developments are often exposed to varied sources of metal contaminants. These are common sources in Blood and Mokolo Rivers. Historical trends of Cr(VI) levels in sediments are not available in these rivers. Sediment samples from Blood River contained Cr(VI) concentrations ranging from 0.410 to 1.32 µg/g. These measured values are relatively higher than those detected in Mokolo River (0.202-1.04 µg/g). Sediments of Mokolo River were sandy while those collected from Blood River were flocculent muddy. These differences in types of sediments together with the environmental conditions could have attributed to the differences in recorded concentrations.

Mandiwana (2008) used 0.01 M Na_3PO_4 for extracting Cr(VI) in soil samples. We evaluated the method for extraction of Cr(VI) in sediments. The measured concentrations of Cr(VI) after microwave-assisted extraction by 10 mL of 0.01 M Na_3PO_4 are presented in table 3.30 along with the levels obtained by extraction with Na_2CO_3. The extraction method using Na_2CO_3 showed more efficient extraction of Cr(VI) in sediments than the extraction method employing Na_3PO_4.

Table 3.30: Comparison of concentrations of Cr(VI) measured in sediment samples obtained from Blood River after extraction following two methods.

Site	Cr(VI)^a µg/g ± SD	Cr(VI)^b µg/g ± SD
1	1.28 ± 0.05	0.09 ± 0.02
2	0.45 ± 0.02	< 0.06
3	0.61 ± 0.05	< 0.06
4	0.93 ± 0.01	< 0.06
5	1.02 ± 0.02	0.061 ± 0.03
6	0.41 ± 0.05	< 0.06
7	0.82 ± 0.04	< 0.06
8	1.32 ± 0.09	< 0.06
9	0.72 ± 0.07	0.062 ± 0.001
10	0.54 ± 0.10	0.07 ± 0.003

^{a} denotes concentration of Cr(VI) extracted using 0.1 M Na_2CO_3; ^{b} denotes concentration of Cr(VI) extracted using 0.01 M Na_3PO_4

Similarly, a Na_3PO_4 extraction procedure has been applied for extraction of Cr(VI) in sediment samples collected from Mokolo River. Similar results have been observed by analysing sediment samples collected from Mokolo River (Table 3.31). The Na_2CO_3 extraction procedure found to be more efficient than the Na_3PO_4 extraction procedure. Oxidation state of Cr(VI) was not altered during the leaching processes using Na_2CO_3 as extractant (Panichev *et al.*, 2005). Thus, we recommend the use of Na_2CO_3 extraction method for quantitative extraction of Cr(VI) in sediments.

Table 3.31: Comparison of Cr(VI) levels in sediment samples of Mokolo River by Na_2CO_3 and Na_3PO_4 extraction procedures.

SITE	Cr(VI)[a] µg/g ± SD	Cr(VI)[b] µg/g ± SD
1	0.36 ± 0.05	< 0.06
2	0.18 ± 0.03	< 0.06
3	0.33 ± 0.06	< 0.06
4	0.43 ± 0.08	< 0.06
5	0.31 ± 0.003	< 0.06
6	0.58 ± 0.02	< 0.06
7	1.04 ± 0.06	< 0.06
8	0.76 ± 0.05	< 0.06
9	0.20 ± 0.02	< 0.06
10	0.82 ± 0.08	< 0.06

[a] denotes concentration of Cr(VI) extracted using 0.1 M Na_2CO_3; [b] denotes concentration of Cr(VI) extracted using 0.01 M Na_3PO_4

3.11. Sequential extraction of potentially toxic elements in sediments

3.11.1. Determination of limit of detection for sequential extraction procedure

The LODs for sequential extraction procedure are presented in table 3.32.

Table 3.32: The LODs in mg/kg obtained for the determination of potentially toxic elements in sediments by ICP-OES employing sequential extraction procedure.

Analyte		Stage 1	Stage 2	Stage 3	Residual
Cd		0.008	0.038	0.0064	0.125
Cr		0.218	0.040	0.0064	0.041
Cu		0.008	0.013	0.0742	0.022
Fe		0.087	0.008	0.0573	0.005
Ni		0.017	0.004	0.0658	0.003
Pb		0.276	0.169	0.503	0.026
Zn		0.023	0.004	0.0806	0.041

The LODs for the exchangeable, reducible, oxidisable and residual stages ranged from 0.008 to 0.276, 0.004 to 0.169, 0.0064 to 0.503 and 0.003 to 0.125 mg/kg, respectively. The LODs reported by Ciceri *et al.* (2008) were 0.066, 0.23, 0.018, 0.41, 0.026 and 0.0059 mg/kg in the first stage, 0.16, 0.18, 0.016, 0.11, 0.0069 and 0.0010 mg/kg in the second stage and 0.50, 0.14, 0.023, 0.76, 0.0076 and 0.043 mg/kg in the third stage for Cr, Ni, Cu, Zn, Cd and Pb, respectively. This values were found to be higher that the detection limits obtained in this study.

3.11.2. Validation of analytical procedure for sequential extraction

The accuracy of sequential extraction procedure was validated by analysing BCR 701 certified reference material. The percent recoveries for this procedure are presented in table 3.33. The obtained percent recoveries were within the acceptable ranges for all stages.

Table 3.33: Percent recoveries of potentially toxic elements in sequentially extracted lake sediment certified reference material (BCR 701).

Stage	**Analyte**	**Measured value**	**Certified value**	**Percent recovery**
		Mean ± SD (mg/kg)	Mean ± SD (mg/kg)	
Stage 1	Cd	7.13±0.25	7.30±0.40	98
	Cr	2.69±0.050	2.26±0.16	119
	Cu	52.7±3.0	49.3±1.7	107
	Ni	13.2±0.28	15.4±0.9	86
	Pb	2.87±0.092	3.18±0.21	90
	Zn	223±3.5	205±6.0	109
Stage 2	Cd	3.05±0.36	3.77±0.28	81
	Cr	50.3±1.0	45.7±2.0	110
	Cu	126±4.0	124±3.0	101
	Ni	25.8±2.3	26.6±1.3	97
	Pb	107±18	126±3.0	85
	Zn	126±9.3	114±5.0	111
Stage 3	Cd	0.218±0.010	0.27±0.06	81
	Cr	110±4.0	143±7.0	77
	Cu	63.1±2.1	55.0±4.0	115
	Ni	18.2±0.78	15.3±0.9	119
	Pb	9.25±0.49	9.30±2.0	99
	Zn	46.5±2.7	46.0±4.0	101

3.11.3. Fractionation of potentially toxic elements in the sediment samples as determined by the three-step BCR procedure

The concentrations of potentially toxic elements in different fractions of sediment samples collected from Blood River in high flow sampling season were determined using ICP-OES. The levels of Cd in sequentially extracted sediment samples are given in figure 3.15. Furthermore, the total concentrations which are obtained by adding the concentrations of Cd in the four stages of sequential extraction procedure are compared with pseudo-total concentrations determined after microwave-assisted acid digestion (Figure 3.16).

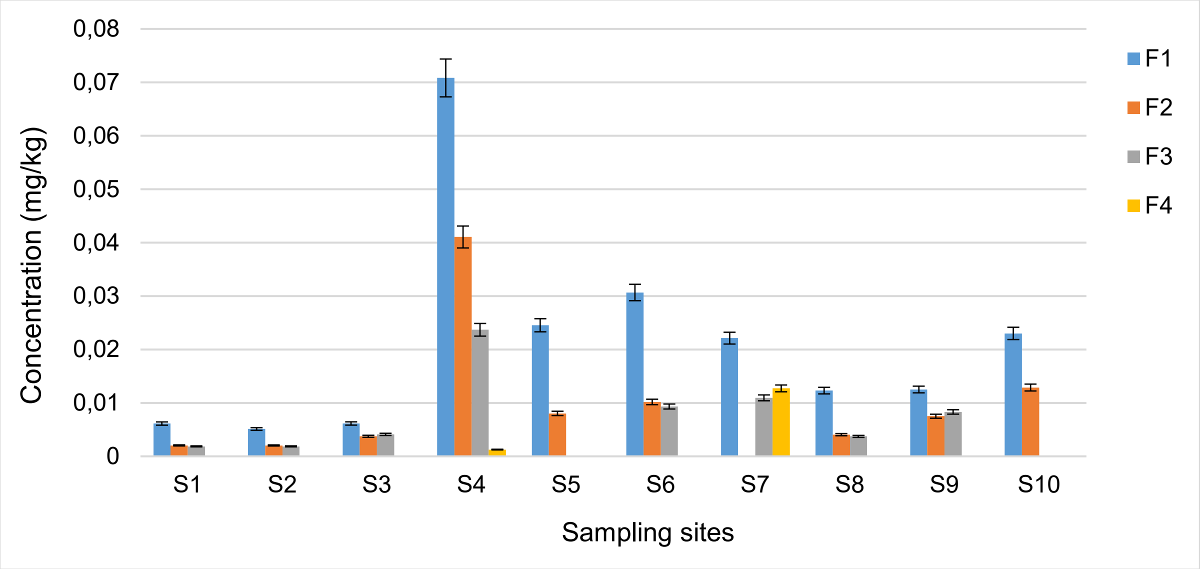

Figure 3.15: Concentrations of Cd in different fractions of sediment samples

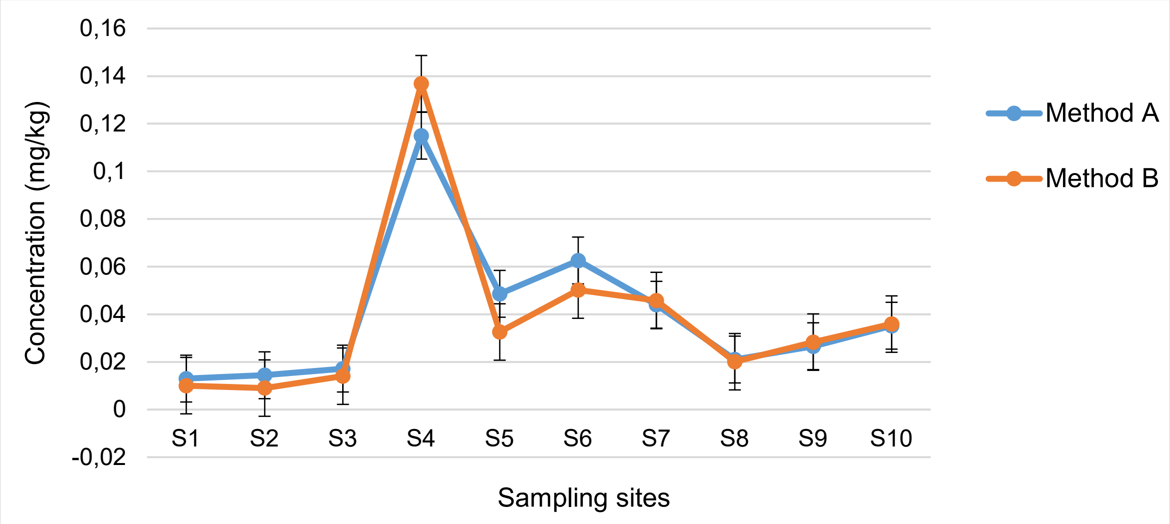

Figure 3.16: Comparison of total concentrations of Cd (method B) with pseudo-total concentrations of Cd (method A)

The partitioning trend of Cd was similar in all sites (Figure 3.15). The concentrations detected in the sites were highly favourable in the exchangeable stage. A study carried out by Shozi (2015) emphasised Cd as a mineral that is very rare in the Earth's crust and associated its existence in the rivers with anthropogenic activities. This statement is in good agreement with the highest concentration of Cd obtained in this study at site 4. Site 4 of the Blood River was found to be adjacent to an illegal dumping site. The domestic wastes could have contributed to the elevated levels of Cd in the river sediment. For most of the sampling sites, Cd in the residual stage was below the LOD value of 0.125 mg/kg. The fractionation pattern of Cd followed the order F1>F2>F3>F4. The highest level of Cd in labile fraction in all sites compared to other fractions might bring risk to the water ecological system and should be paid more attention to.

Figure 3.16 shows the trend between the total concentrations of extracted Cd and pseudo-total Cd concentrations in digested sediment samples. The total concentration of Cd obtained from extraction exceeded the pseudo-total concentration from digestion method employed at site 4. In most sites, the total concentrations and pseudo-total concentrations of Cd are in good agreement.

Similarly, the concentrations of Cr in sequentially extracted sediment samples are presented in figure 3.17. Moreover, the total concentrations of Cr are compared with pseudo-total concentrations determined after microwave-assisted acid digestion (Figure 3.18).

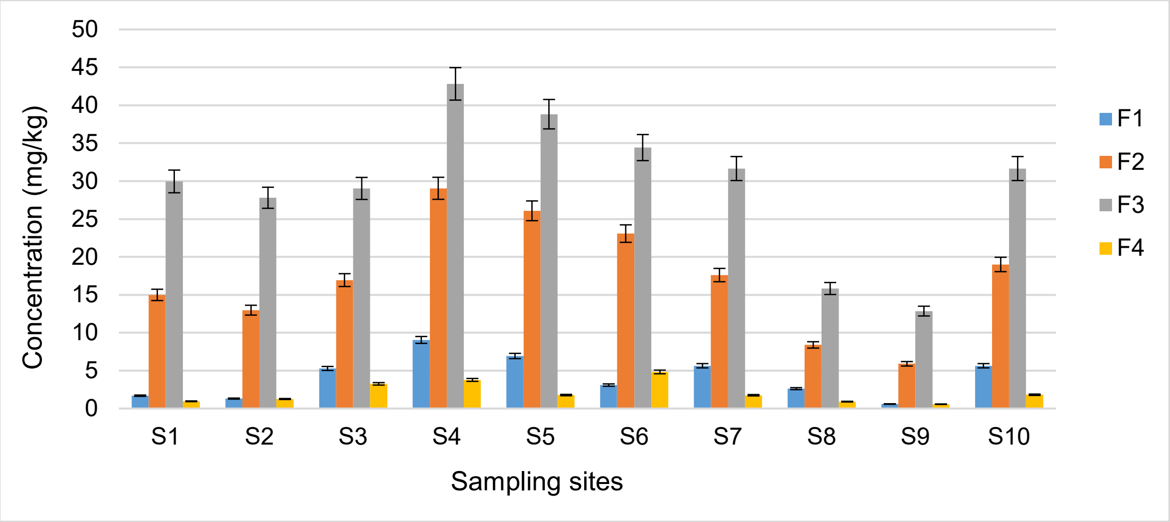

Figure 3.17: Concentrations of Cr in different fractions of sediment samples

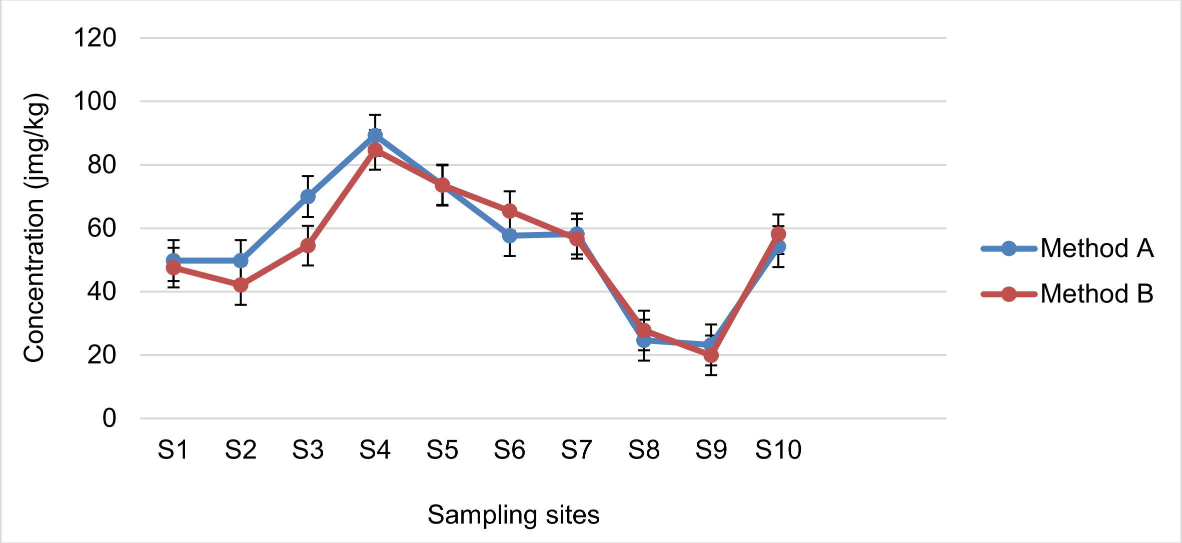

Figure 3.18: Comparison of total concentrations of Cr (method B) with pseudo-total concentrations of Cr (method A)

The partitioning pattern of Cr was similar in all the sites. The highest concentration was measured in oxidisable fraction. A classical study by Martin and Meybeck (1979) introduced the need for the fourth stage and categorised it as the residual stage. They reported the importance of the stage in relation to determination of contamination factors. In this study, Cr was detected in residual fraction in all the sites (Figure 3.17). The pattern of Cr levels in different fractions were F3>F2>F1>F4.

Reliability of the results obtained in the sequential extraction method B was checked by comparison with the pseudo-total digestion concentrations (Method A). A good agreement between the two methods was shown by in figure 3.18.

The concentrations of Cu in sequentially extracted sediment samples are presented in figure 3.19. Furthermore, the total concentrations of Cu are compared with pseudo-total concentrations determined after microwave-assisted acid digestion (Figure 3.20).

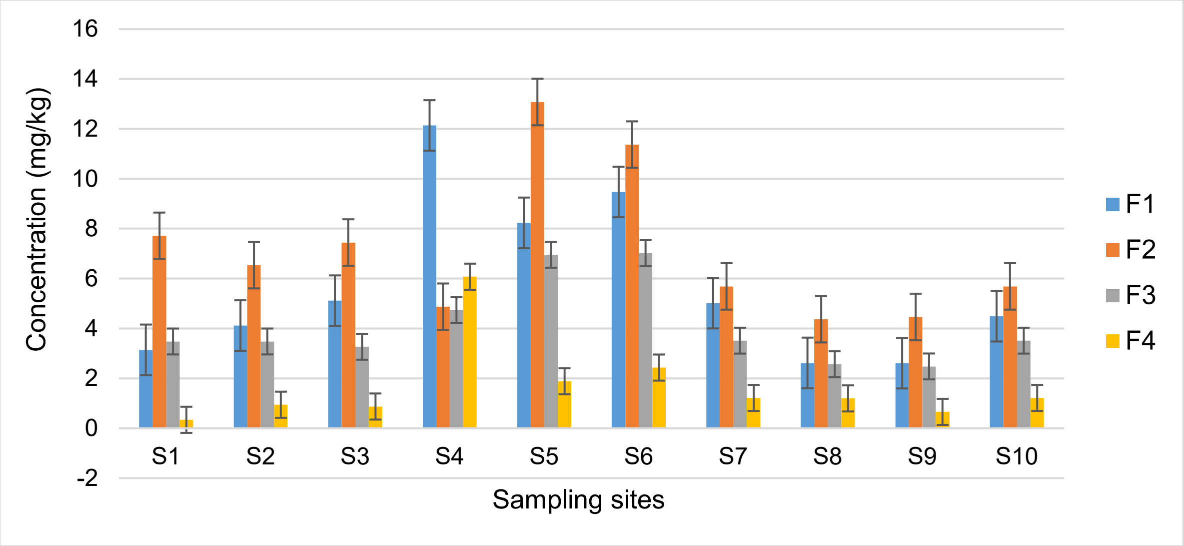

Figure 3.19: Concentrations of Cu in different fractions of sediment samples

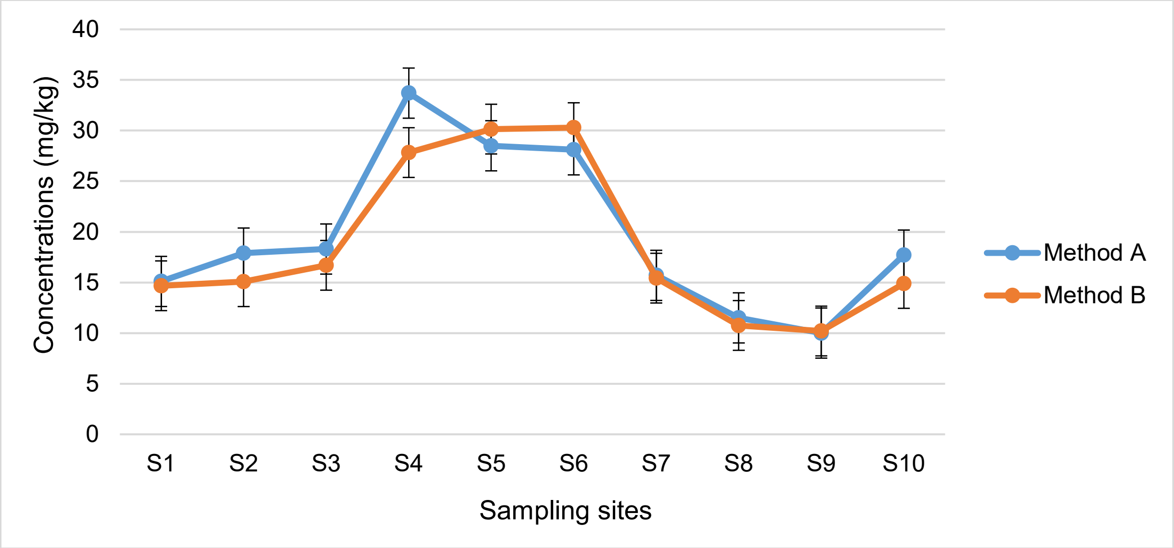

Figure 3.20: Comparison of total concentrations of Cu (method B) with pseudo-total concentrations of Cu (method A)

The partitioning pattern of Cu in the reducible fraction was highly favourable in all the sites except site 4 (Figure 3.19). Copper was primarily associated with the reducible fraction, followed by the exchangeable, oxidisable and lastly the residual fraction. The sum of Cu concentrations in three fractions plus residual was in good agreement with the pseudo-total concentrations as shown in figure 3.20.

The concentrations of Ni in different extraction fractions of sediment samples are presented in figure 3.21. The sum of concentrations of Ni in different extraction fractions plus residual are compared with pseudo-total concentrations determined after microwave-assisted acid digestion in figure 3.22.

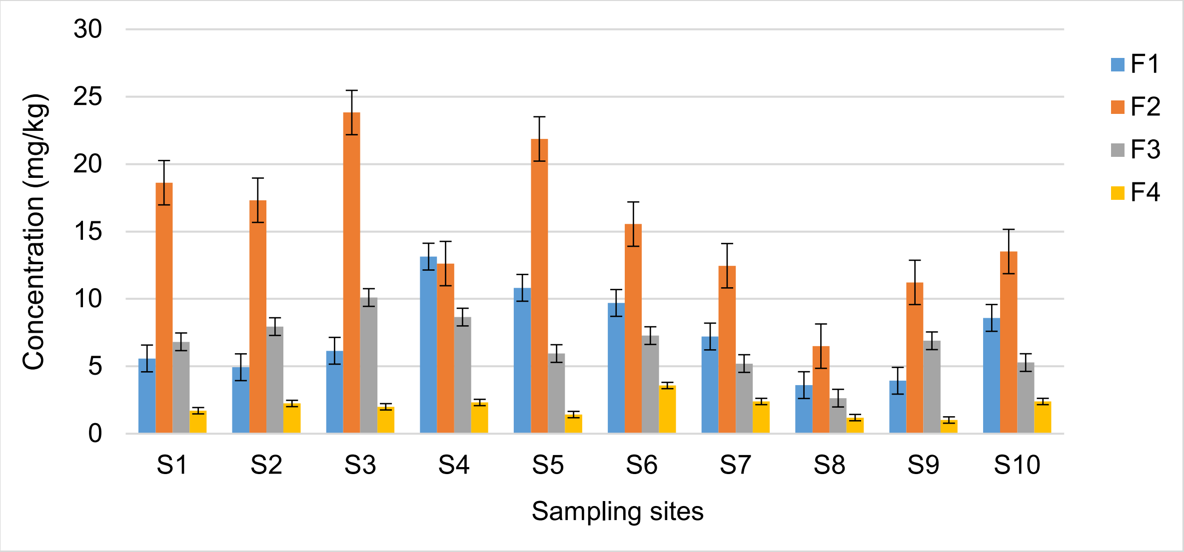

Figure 3.21: Concentrations of Ni in different fractions of sediment samples

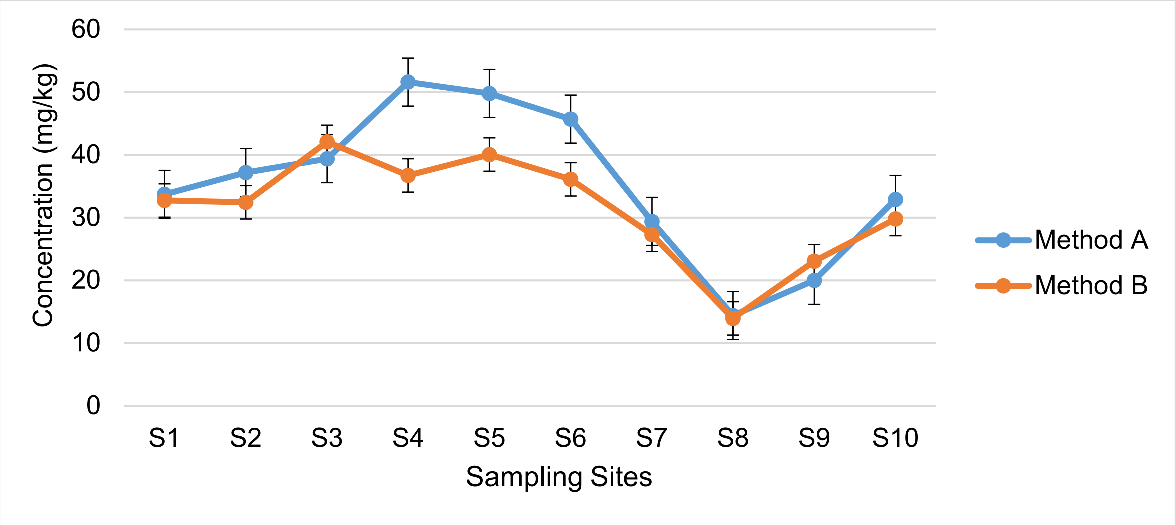

Figure 3.22: Comparison of total concentrations of Ni (method B) with pseudo-total concentrations of Ni (method A)

The second fractionation stage represents the elements which can easily bind to Fe and Mn oxides. These elements may leach from sediments to the water course when subjected to more reductive conditions (Nemati *et al.*, 2011). The fractionation pattern of Ni followed the order F2>F1>F3>F4. Nickel showed a similar partitioning pattern between the four fractions. The metal was mostly associated with the reducible fraction. The total concentration obtained from addition of the extraction fractions plus residual was lower than the pseudo-total concentration determined by the digestion method. This difference was elevated in site 4 to site 6.

The concentrations of Pb in different extraction fractions of sediment samples are shown in figure 3.23. The sum of concentrations of Pb in different extraction fractions plus residual are compared with pseudo-total concentrations determined after microwave-assisted acid digestion in figure 3.24.

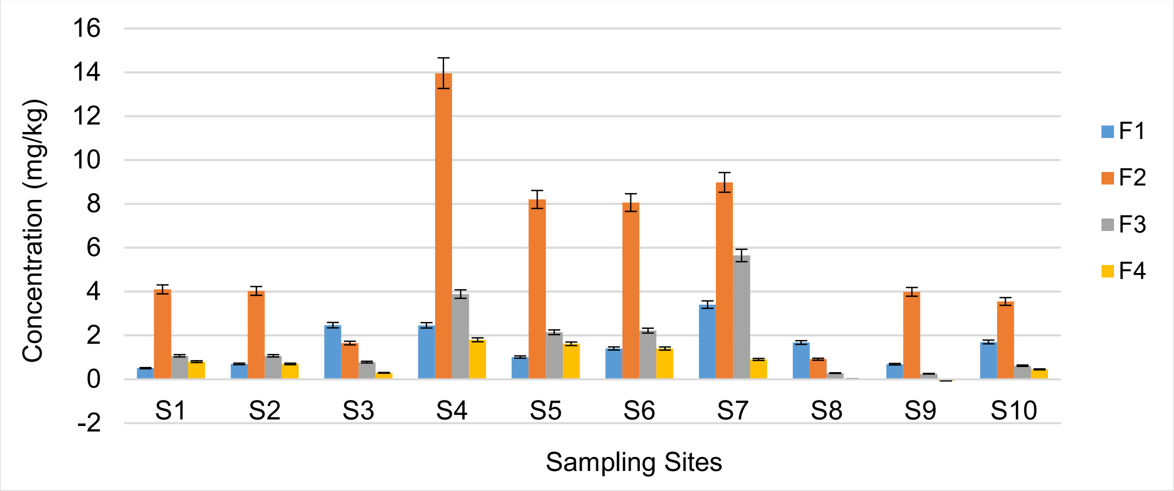

Figure 3.23: Concentrations of Pb in different fractions of sediment samples

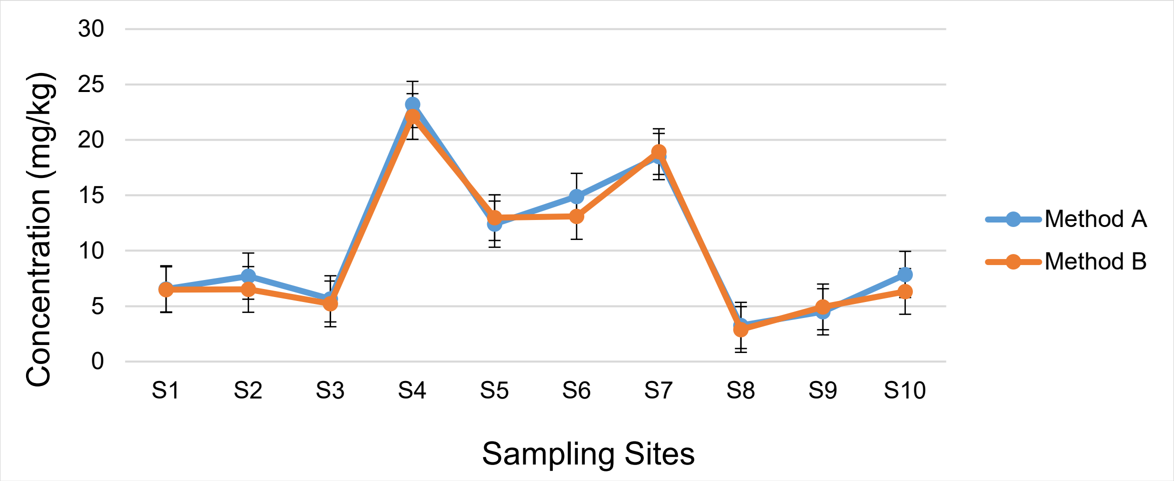

Figure 3.24: Comparison of total concentrations of Pb (method B) with pseudo-total concentrations of Pb (method A)

Naturally occurring Pb minerals are not very mobile under normal environmental conditions, the sources of Pb are likely anthropogenic in nature (Jain, 2004). Elevated Pb concentrations were expected in the Fe-Mn (reducible) fraction. Fe-Mn oxyhydroxides are important scavengers of Pb in sediments and Pb is able to form stable complexes with Fe-Mn oxyhydroxides (Li *et al.*, 2001; Wong *et al.*, 2007). In this study, high concentration of Pb was observed in reducible fraction for most sites. The fractionation pattern of Pb followed the order F2>F3>F1>F4, except in sites 3 and 8. Sites 3 and 8, showed a different trend where Pb was dominant in the exchangeable fraction. The highest level of Pb in labile fraction in these sites compared to other fractions might bring high risk to the aquatic biota. In figure 3.10, sampling sites in the middle stream S4-S7 are adjacent to a residential area of Seshego Township and elevated levels of Pb in S4-S7 could be attributed to domestic wastes dumped near these sites. In general, the sum of the concentrations of Pb in different fractions and pseudo-total concentrations of Pb are in good agreement (Figure 3.24).

The concentrations of Zn in different extraction fractions of sediment samples are given in figure 3.25. The sum of concentrations of Zn in sequentially extracted fractions plus residual are compared with pseudo-total concentrations determined after microwave-assisted acid digestion in figure 3.26.

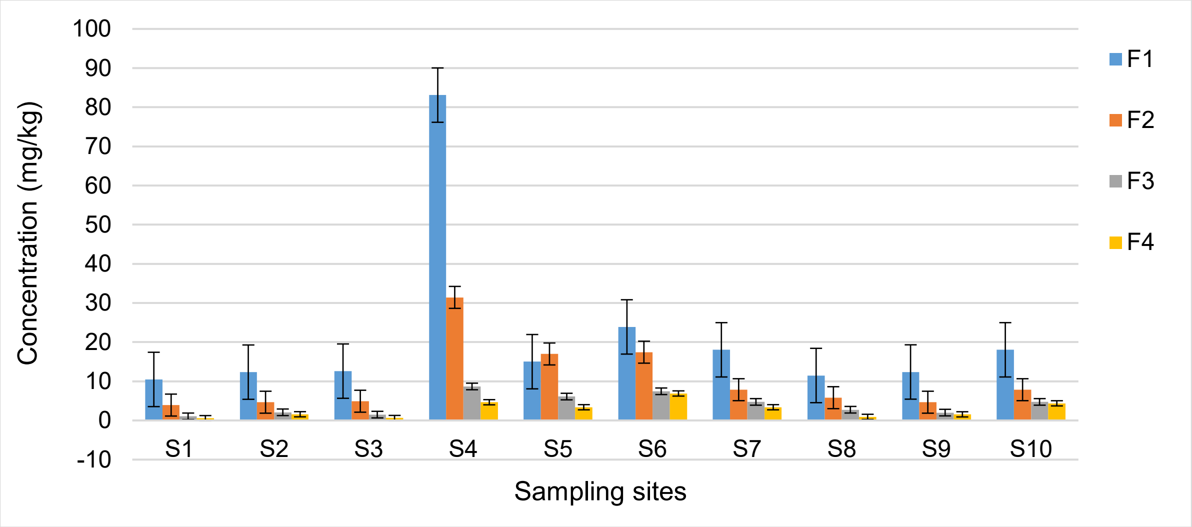

Figure 3.25: Concentrations of Zn in different fractions of sediment samples

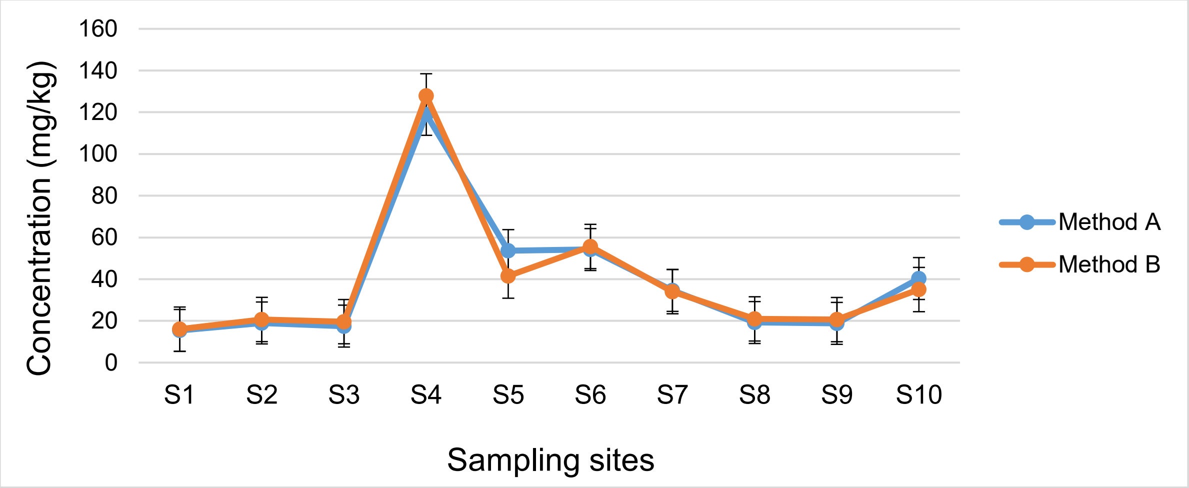

Figure 3.26: Comparison of total concentrations of Zn (method B) with pseudo-total concentrations of Zn (method A)

Zinc showed to be weakly bound and easily leachable by soluble salts and ions, thus the high levels observed in the exchangeable fraction in this study. The high levels of Zn at site 4 may have resulted from the release of exchangeable Zn associated with the illegal dumping near to Blood River. Zinc partitioning followed the order F1>F2>F3>F4. In general, the sum of the concentrations of Zn in different fractions and pseudo-total concentrations of Zn are in good agreement (Figure 3.26).

The levels of Fe in different extraction fractions of sediment samples are shown in figure 3.27. The sum of concentrations of Fe in sequentially extracted fractions plus residual are compared with pseudo-total concentrations measured after microwave-assisted acid digestion in figure 3.28.

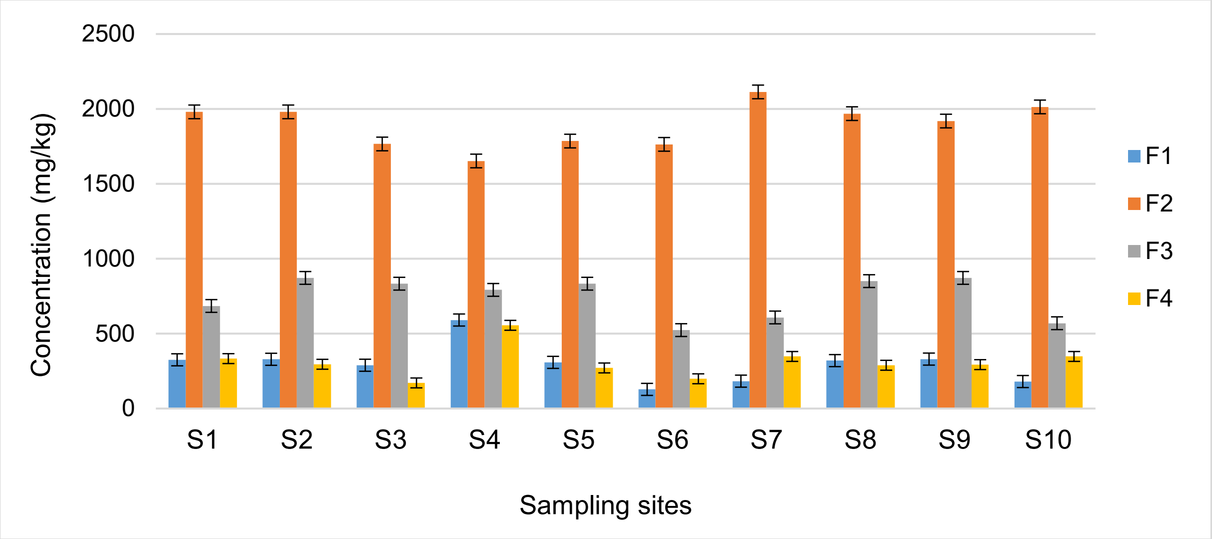

Figure 3.27: Concentrations of Fe in different fractions of sediment samples

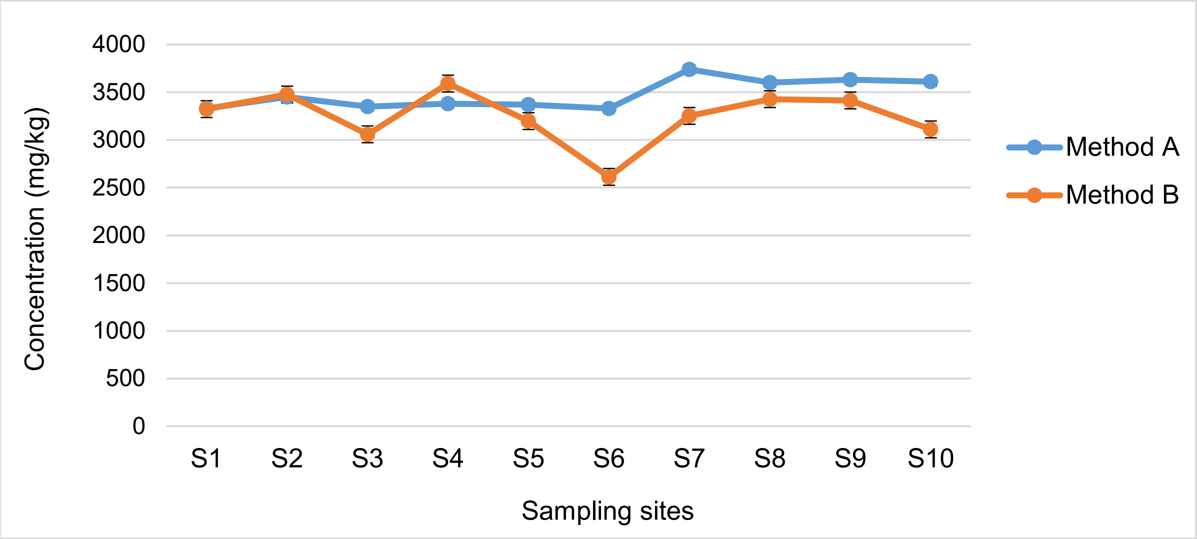

Figure 3.28: Comparison of total concentrations of Fe (method B) with pseudo-total concentrations of Fe (method A)

Concentrations of Fe in the sediments from different sites followed the order F2>F3>F4>F1. Due to lack of certified value for Fe in the BCR-701 reference material, validation of the analytical results was done by comparing the sum of sequentially extracted concentrations of Fe with the pseudo-total concentrations determined after digestion using microwave digestion system. The agreement of results obtained using two methods, validated the levels of Fe obtained by the sequential extraction method. Iron is one of the most important and abundant elements in the Earth. The continuous increase in the Fe concentration along the sampling sites may be due to the contribution of anthropogenic factors.

3.12. Environmental Implications

The determination of contamination factor (Cf) of potentially toxic elements is an important aspect that indicates the degree of potentially toxic elements risk to the environment in relation with its retention time. A high Cf of potentially toxic elements indicates a high risk to the environment and low retention time (Nemati *et al.*, 2011). The individual contamination factor (ICF) and the global contamination factor (GCF) have been used to assess the environmental risks and estimate possible damage to aquatic organisms and environment caused by contaminated sediments and water (Nemati *et al.*, 2011; Nasr *et al.*, 2015). This is based on the potentially toxic elements being able to bind to different sediment fractions that determines the bioavailability of the elements from the sediments to the water and the environment (Jain, 2004).

3.12.1. Individual Contamination Factor and Global Contamination Factor

The ICF and GCF values were calculated following the method by Nemati *et al.* (2011). The ICFs for the different sediments were obtained by dividing the sum of the non-residual fractions (F1 + F2 + F3) by the residual fraction (F4) of each sample.

$$\text{ICF} = \frac{[F1+F2+F3]}{F4}$$

The GCF for each site was calculated by summing the ICF of all the metals obtained for the sediment samples (Ikem *et al.*, 2003).

$$\text{GCF} = \Sigma\ \text{ICF}$$

The ICF and GCF classifications were discussed following the interpretation by Zhao *et al.* (2012) where, ICF < 0 and GCF < 6 indicates low contamination, 1 < ICF < 3 and 6 < GCF < 12 indicate moderate contamination. Additionally, when 3 < ICF < 6 and

12 < GCF < 24, which indicates considerable contamination. Lastly, ICF > 6 and GCF>24 is classified as high contamination. The ICF and GCF values for the ten studied sites are calculated and given in table 3.34.

Table 3.34: Individual contamination and global contamination factors of Blood River during the low flow period obtained employing method B.

Element	**ICF**										
	S1	S2	S3	S4	S5	S6	S7	S8	S9	S10	Average
Cd	0.0802	0.0724	0.112	108	0.260	0.402	2.600	0.161	0.227	0.287	11.4
Cr	48.9	33.7	15.7	21.4	40.4	12.5	31.4	29.6	34.0	31.1	29.9
Cu	42.4	15.0	18.2	3.6	15.0	11.5	11.7	7.97	14.6	11.2	15.1
Fe	8.98	10.8	16.9	5.5	10.8	12.1	8.3	10.9	10.7	7.9	10.3
Ni	18.1	13.5	20.0	14.8	27.2	9.10	10.4	10.6	21.8	11.4	15.7
Pb	7.05	8.27	16.5	11.3	7.02	8.35	19.9	188	190	13	46.9
Zn	26.6	1.06	30.4	26.5	11.3	7.08	9.05	21.9	12.2	7.0	15.3
GCF	152	82	118	191	112	61	93	269	283	82	144

Based on the calculated values of ICF, low contamination by Cd in S1, S2, S3, S5, S6, S8, S9 and S10, and S7 showed a moderate contamination by Cd, whereas site 4 had an ICF value of 108, indicating a high contamination risk of Cd to the environment. This was based on the anthropogenic activities that were dominant at

S4. The values of ICF for Cr and Cu were above the maximum threshold for high contamination, which shows the risk associated with these elements.

The ICF values of Fe in all the sites were in the high contamination level, except for S3, which was classified as moderate contaminant. However, with continuous pollution occurring in the area, the Fe level in S3 will likely increase.

The ICF values of Ni in all sites were in the high contamination level. Monitoring of the element should be carried out to control possible threat to the aquatic system.

The Pb was classified under high contamination level in all the sites since the ICF values exceeding the ICF of 6 from S1-S10. Owing to the high toxicity of Pb, the calculated values represent a potential risk of contamination to the water phase, or to the biota, in the sediment samples. Similarly, Zn was also classified as high contamination risk to the river system based on the ICF values, with an exception in S2, which was under the moderate contamination level.

Overall, the risk assessment showed high possibility of Cr, Cu, Fe, Ni, Pb, and Zn to be released from the sediments to overlying water with the average ICF values of 29.9, 15.1, 10.3, 15.7, 46.9 and 15.3, respectively. The average ICF values followed the order: Pb, Cr, Ni, Zn, Cu, Cd and Fe. Although Cd was under the low classification in most of the sites, it was overall classified under high-risk contamination level based on the average ICF value of 11.2 (Table 3.34).

The residual concentration of any element is considered a non-mobile fraction and is an important partition influencing the mobility of the elements, while the non-residual fractions are considered mobile. The results showed Cr, Cu, Fe, Ni, Pb, and Zn have high potential mobility. The mobility of the elements shows the increased possible risk of these elements to the surrounding environment and aquatic organisms.

The GCF values of the analytes were greater than 24 in all the sites, indicating high possibility of these elements to be released to water. Thus, the analysed elements in sediments pose high risks to the ecosystem. The GCF values were 152, 82, 118, 191, 112, 61, 93, 269, 283 and 82 from S1 to S10, orderly. The average GCF value was 114, thus classified as high contamination level. The combined effect of the elements and with potential high mobility reveal the increased possible risk of these potentially toxic elements to the ecosystem.

3.12.2. Risk Assessment Code

The risk assessment code (RAC) was first introduced by Perin *et al.* (1985), and was applied to assess the mobility and bioavailability of potentially toxic elements in surface sediments (Mortazavi *et al.*, 2016). The RAC value of each analyte is calculated by the following equation:

$$\text{RAC} = \frac{F1}{\Sigma F1 - F4} \text{ x } 100$$

The RAC classifications followed the interpretation by Perin *et al.* (1985), where RAC value of <1 indicates No risk, between 1 and 10 indicates low risk, 11 to 30 is medium risk, 31 to 50 is high risk and finally, >50 is classified very high risk. Table 3.35 shows the calculated percent RAC values of the analytes in the sediments of Blood River.

Table 3.35: Risk assessment code of potentially toxic elements in sediments from Blood River during low flow season.

Element	**RAC (%)**										
	S1	S2	S3	S4	S5	S6	S7	S8	S9	S10	Average
Cd	4.54	3.81	4.42	51.7	89.1	17.5	48.4	8.48	8.15	14.3	25.0
Cr	3.55	3.02	9.70	10.7	9.41	4.72	9.95	9.45	2.98	9.70	7.32
Cu	21.4	27.3	30.6	43.5	27.3	31.2	32.5	24.3	25.6	30.1	29.4
Fe	9.78	9.46	9.44	16.5	9.62	4.90	5.63	9.33	9.66	5.79	9.01
Ni	17.1	15.2	14.6	35.7	27.0	26.9	26.4	25.9	17.1	28.8	23.5
Pb	7.85	10.8	47.5	11.1	7.85	10.8	18.0	58.0	13.9	26.9	21.3
Zn	65.4	33.2	64.2	65.0	36.2	43.0	53.0	54.8	60.1	51.5	52.6

Following the contamination assessment evaluated by ICF and GCF values, the RAC is applied to assess the risk based on the percentage of metal in exchangeable fraction or bound to carbonate (Saeedi *et al.*, 2013). Based on the calculated RAC values in table 3.35, an average of 52.6% of total Zn of the study sites was either adsorbed to exchangeable, or carbonate bound. Thus, it is in the high to very high-risk category to aquatic and non-aquatic environment and can easily enter into the food chain. The RAC values ranged between 33.2 and 65.45 in the sites, indicating high risk in S2, S5 and S6 and very high risk in S1, S3, S4, S7, S8, S9 and S10.

Chromium and Fe were classified under the low risk category indicating lower availability from which they cannot be easily leached out to the aquatic environment. The RAC values of Cr ranged between 2.98 and 10.7% with an average value of 7.32%. An average RAC for Fe was 9.01%, ranging from 4.90% in S6 to 16.5% in S4, which falls under the moderate risk category.

Although the concentration of Cd was significantly low in the sediments of Blood River, the RAC value indicated it as a potential risk to the aquatic and surrounding environment of the river. The average RAC value in the sediments was 25.0% indicating medium risk, while the RAC ranged between 3.81% (low risk) and 89.1% (very high risk). Cadmium in S1, S2, S3, S8 and S9 was classified as high risk and in S6 and S10 as moderate risk.

The average RAC values of Cu (29.4%), Ni (23.4%) and Pb (21.3%) classified the elements as medium risk to the environment. The RAC values of Cu ranged from 21.4% in S1 to 43.5% in S4. Although Cu was classified under the medium risk category, S3, S4, S6, S7 and S10 were classified under the high risk. The presence of Ni in the non-residual fraction categorised its existence in the sediments as medium risk to the environment in the sites with an exception in S4 (35.7%) which was of high risk. Partitioning of Pb in the sediments resulted in the RAC values of Pb ranging from 7.85% in sites 1 and 5 to 58.0% in S8. The existence of this element in S3 and S8 indicates that it poses high risk to the aquatic organisms in the Blood River. Overall, the analyte was classified under the low (S1, S2, S5 and S6) to medium risk (S4, S7, S9 and S10).

These findings indicate potential risks to the human health of residents surrounding the Blood River. These may be caused by direct exposure to the water and indirect exposure via food chain. The risk assessment of Blood River followed the decreasing order of Zn > Cu > Cd > Ni > Pb > Fe > Cr.

3.13. Microwave-assisted sequential extraction of potentially toxic elements in sediments

3.13.1. Determination of Limit of detection for microwave-assisted sequential extraction procedure

The LODs for microwave-assisted sequential extraction procedure are presented in Table 3.36.

Table 3.36: Limit of detection in mg/kg for the microwave-assisted sequential extraction procedure obtained by ICP-OES.

Analyte		Stage 1	Stage 2	Stage 3	Residual
Cd		0.0070	0.0038	0.0006	0.0019
Cr		0.0034	0.0204	0.0043	0.0002
Cu		0.0021	0.0025	0.0250	0.0011
Fe		0.0019	0.0156	0.0021	0.0008
Ni		0.0212	0.0015	0.0658	0.0007
Pb		0.0106	0.0006	0.0010	0.0008
Zn		0.0021	0.0036	0.0008	0.0011

For the exchangeable stage, the LOD values followed the trend: Ni>Pb>Cd>Cr>Cu≥Zn>Fe ranging from 0.0019-0.0212 mg/kg. The LODs in the reducible stage ranged from 0.0006-0.0204 mg/kg, following the order: Cr>Fe>Cd>Zn>Cu>Ni>Pb. The LODs for the oxidisable and residual stages ranged from 0.0006-0.0658 mg/kg and 0.0002-0.0.0018 mg/kg, respectively. The order of the LODs in the oxidisable fractionation and residual stage were as follows: Ni>Cu>Cr>Fe>Pb>Zn>Cd and Cd>Cu≥Zn>Fe≥Pb>Ni>Cr.

3.13.2. Validation of microwave-assisted sequential extraction procedure

The accuracy of microwave-assisted sequential extraction procedure was validated by analysing BCR 701 certified reference material. The percent recoveries for this procedure are presented in table 3.37.

Table 3.37: Percent recoveries of potentially toxic elements in microwave-assisted sequentially extracted lake sediment certified reference material (BCR 701).

Fraction	**Element**	**Measured value**	**Certified value**	**Recovery**
		Mean±SD (mg/kg)	Mean±SD (mg/kg)	(%)
F1	Cd	5.81±0.036	7.30±0.40	80
	Cr	1.86±0.032	2.26±0.16	82
	Cu	40.5±2.1	49.3±1.7	82
	Ni	10.6±0.063	15.4±0.9	69
	Pb	2.39±0.054	3.18±0.21	75
	Zn	213±3.5	205±6.0	104
F2	Cd	2.55±0.015	3.77±0.28	68
	Cr	48.6±0.70	45.7±2.0	106
	Cu	114±0.89	124±3.0	92
	Ni	26.3±0.45	26.6±1.3	99
	Pb	103±1.3	126±3.0	81
	Zn	122±1.4	114±5.0	107
F3	Cd	0.212±0.0011	0.27±0.06	79
	Cr	110±0.71	143±7.0	77
	Cu	63.1±0.71	55.0±4.0	115
	Ni	17.9±0.028	15.3±0.9	117
	Pb	9.22±0.025	9.30±2.0	99
	Zn	45.0±0.67	46.0±4.0	98

Percent recoveries for most elements were within the acceptable range of 75-125%. Low recovery was observed for Cd (68%) in stage 2.

3.13.3. Determination of concentrations of potentially toxic elements in sediments by microwave-assisted sequential extraction procedure

Sediment samples collected from Blood River during low flow sampling season were analysed by applying microwave-assisted sequential extraction procedure. The concentrations of potentially toxic elements determined by microwave-assisted sequential extraction procedure (method C), modified BCR method (method B) and pseudo-total concentrations determined after digestion (method A) are presented in this section. The comparison of the concentrations of Cd determined by three methods are presented in figure 3.29. The concentrations of Cd determined by three methods are in good agreement except in site 5. In site 5, digestion method showed higher concentration of Cd than the two sequential extraction methods, which could be attributed to the strength of the reagents used for mineralisation of sediments.

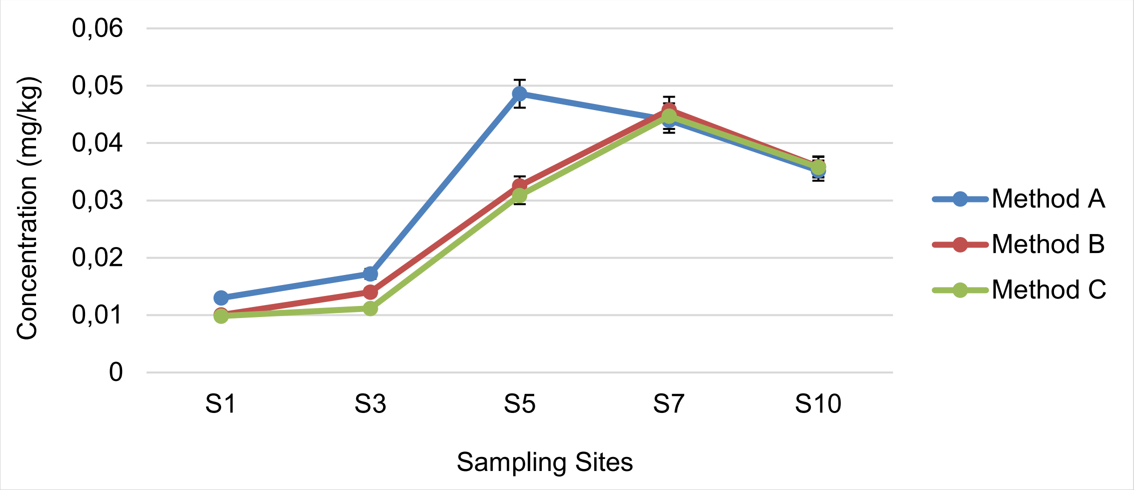

Figure 3.29: Comparison of concentrations of Cd determined by methods A, B and C

The comparison of the concentrations of Cr determined by three methods are presented in figure 3.30. The concentrations of Cr measured by three methods are in good agreement except in site 3, which the pseudo-total concentration was higher than the concentrations determined by the extraction methods.

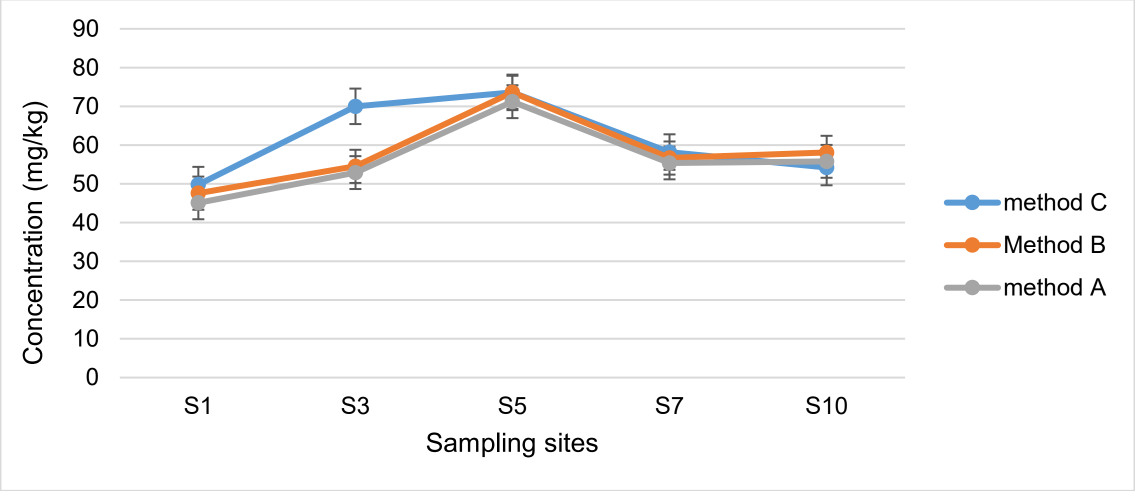

Figure 3.30: Comparison of concentrations of Cr determined by methods A, B and C

The two sequential extraction methods showed similar results. Thus, microwave-assisted sequential extraction method can be used to lessen the sample preparation time.

The comparison of the levels of Cu determined by three methods are shown in figure 3.31. The microwave-assisted sequential extraction method is reliable since the results obtained by both extraction methods are comparable (Figure 3.31).

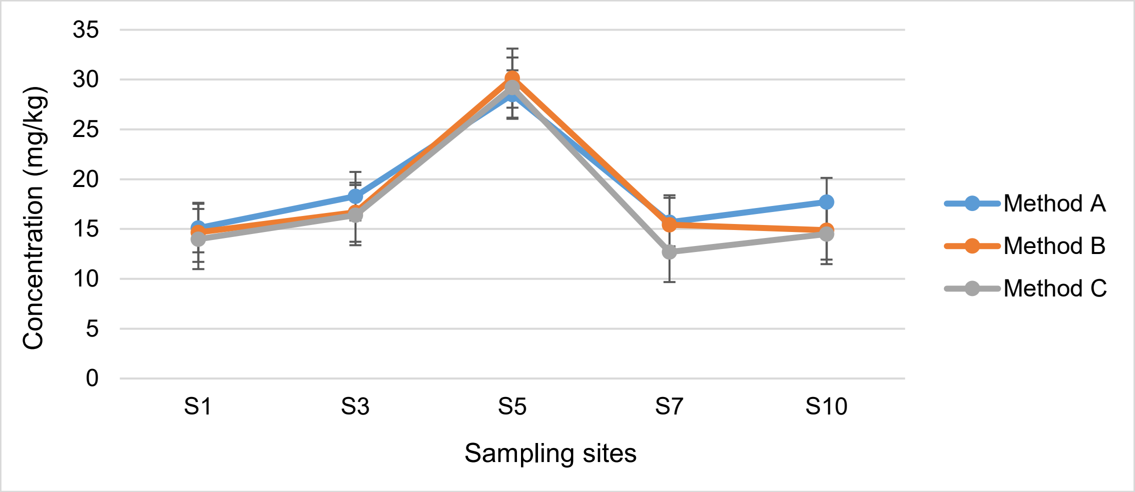

Figure 3.31: Comparison of concentrations of Cu determined by methods A, B and C

The concentrations of Fe determined by three methods are compared in figure 3.32. The total concentrations of Fe determined by sequential extraction methods (methods

B and C) were comparable to the pseudo-total concentration (method A) in all the sites (Figure 3.32).

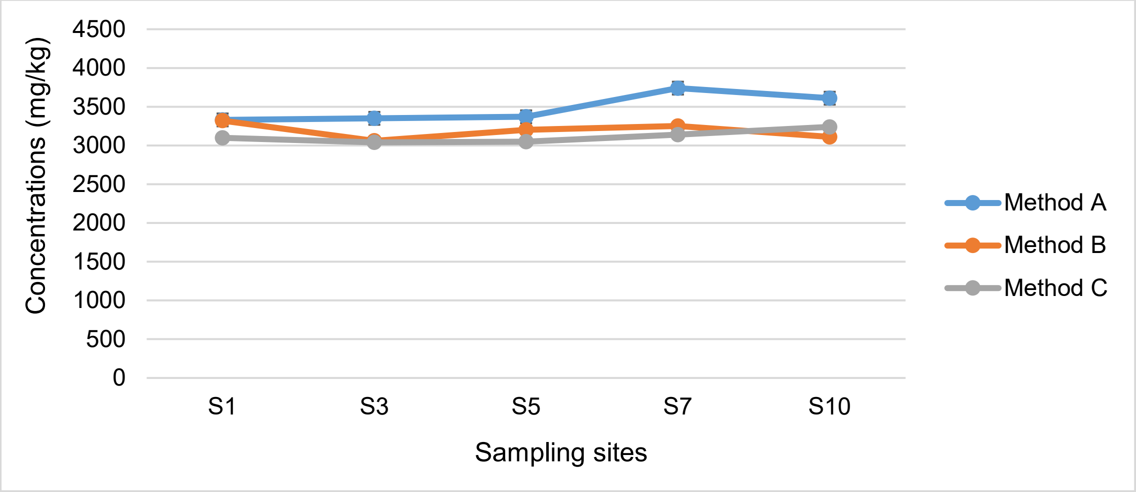

Figure 3.32: Comparison of concentrations of Fe determined by methods A, B and C

The concentrations of Ni measured by three methods are compared in figure 3.33. The levels of Ni determined by sequential extraction methods (methods B and C) were in good harmony with the pseudo-total concentration (method A) in all the sites (Figure 3.33) except in site 5. Again, this may be attributed to the strength of the reagents employed in method A as compared to the extraction reagents used in methods B and C. Sequential extraction of Ni in sediments can be done by method C to shorten the extraction time and use less volume of reagents.

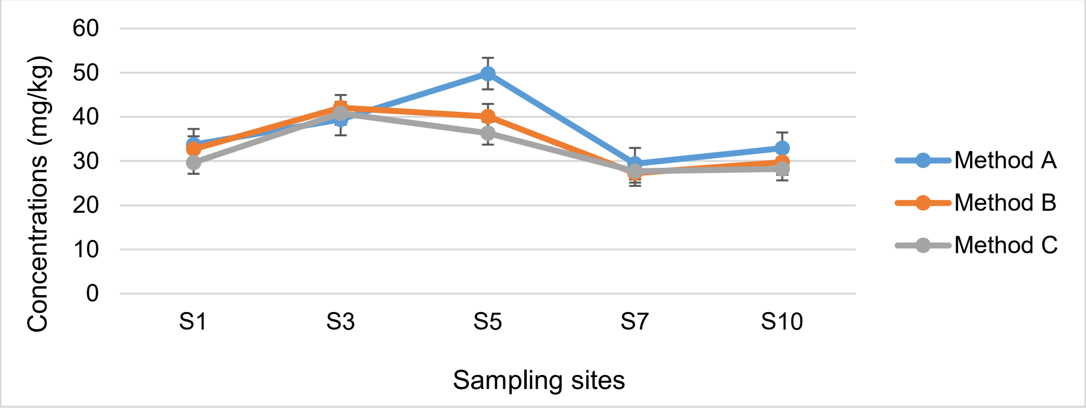

Figure 3.33: Comparison of concentrations of Ni determined by methods A, B and C

The concentrations of Pb measured by three methods are compared in figure 3.34. The concentrations of Pb obtained by both sequential extraction methods are in good agreement with the pseudo-total concentrations of Pb.

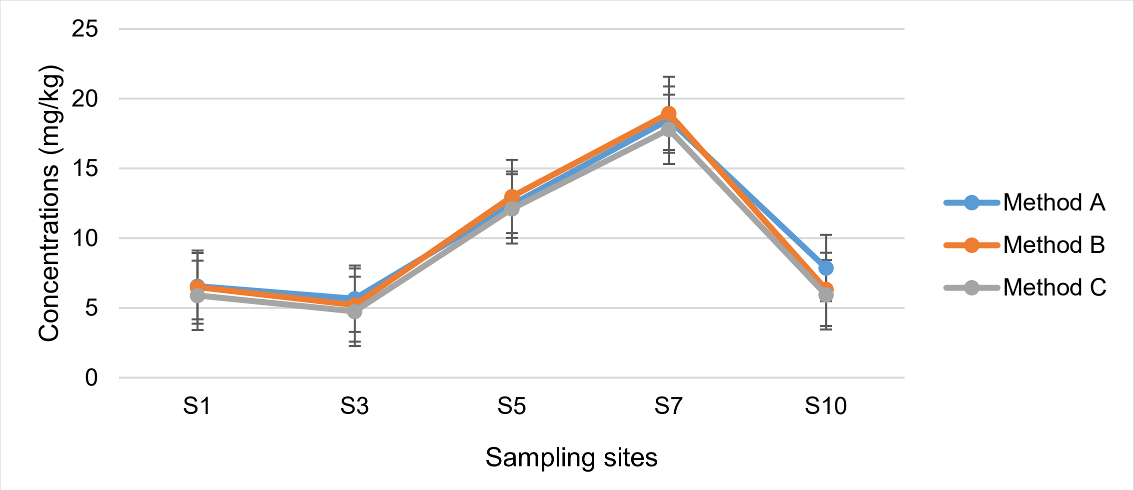

Figure 3.34: Comparison of concentrations of Pb determined by methods A, B and C

The concentrations of Zn determined by three methods are presented in figure 3.35. The concentrations of Zn determined by sequential extraction methods (methods B and C) were in good agreement with the pseudo-total concentration (method A) in all the sites (Figure 3.35) except in site 5.

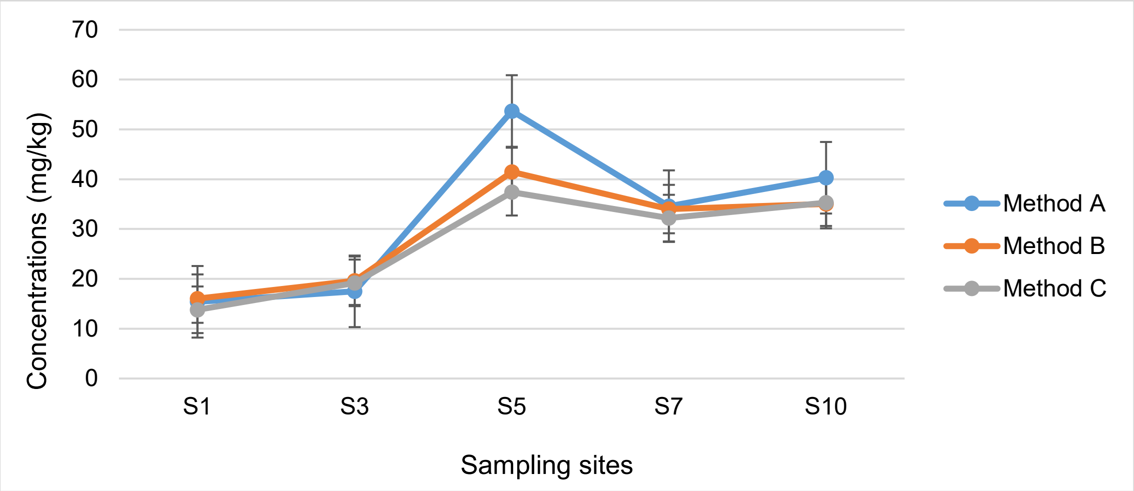

Figure 3.35: Comparison of concentrations of Zn determined by methods A, B and C

3.14. Removal of selected metal ions from contaminated water

3.14.1. The effect of pH on the adsorption of metal ions

The pH is one of the parameters that plays a vital role in the adsorption process of metal ions since it affects the solubility of metal ions. To have an effective adsorption, ionic charges of the adsorbate and adsorbent need to correspond. To this effect, 0.1 M NaOH and 0.1 M HCl were used to adjust pH to desired values. The concentration and form of soluble metal species affect hydrolysis and precipitation of metal ions (Adil *et al.*, 2000). It was further stated that hydrolysis of these metals become significant around pH 5-8 (Weijie *et al.*, 2013). The effect of pH on adsorption of metal ions by MWCNTs nanocomposites (raw MWCNTs, MWCNT/EDA, MWCNTs/PVA1, MWCNTs/PVA2 and MWCNTs/PAMAM) was studied and is illustrated in figures 3.36 to 3.38. The removal of three metal ions (Cr(VI), Pb(II) and Cu(II)) from simulated solutions were investigated by comparing five nanocomposites affinity to adsorb the metal ions. It can be observed in figures 3.36 to 3.38 that the adsorption of Pb (II) and Cu (II) revealed similar trend of percentage removal that increases with an increase in pH. The maximum percentage removal was found to be at pH 6.5 for both Pb(II) and Cu(II) while for Cr(VI) was at pH 2 by employing the investigated nanocomposites.

It was discovered that at low pH minimum removal was obtained for Pb(II) and Cu(II). This is due to the surface protonation of the adsorbent at low pH since high concentrations of H^+ ions are in competition with metal ions for available binding active sites (Mohammad *et al.*, 2013). Relatively higher adsorption was observed from pH 5.5 to 8.5 with maximum adsorption at 6.5 for both metal ions. This is due to the interaction of the metal ions with unprotonated groups such as amine and carbonyl groups at high pH values. A decrease in adsorption was observed from pH of 8.5 in basic conditions. This could be attributed to an increase in concentrations of OH^- at higher pH. This could lead to formation of metal hydroxides that result in precipitates. Similar findings were reported in the study conducted by Mohammad *et al.* (2013).

The adsorption process of Cr(VI) was different from Pb(II) and Cu(II) since high adsorption capacity of nanocomposites for Cr(VI) was found to be at pH 2. This might be explained by considering the three forms in which Cr(VI) exists ($HCrO_4^-$, $Cr_2O_7^{2-}$ and CrO_4^{2-}) (Wengiang, 2018). The author stated that in acidic condition the transformation of CrO_4^{2-} from $HCrO_4^-$ occurs. Therefore, negatively charged adsorbent surface are neutralized by H^+ at low concentration which in turn favours the electrostatic attraction between Cr(VI) in the form of $HCrO_4^-$ and surface charge (Mohan and Pittman, 2006). Similar outcomes were also reported by other researchers (Singh and Tiwari, 1997; Enniyaa *et al.*, 2018). The MWCNTs/PAMAM composite yielded higher percentage removal for Pb(II), whereas MWCNTs/PVA1 composite material yielded higher percentage removal for Cu(II) and Cr(VI).

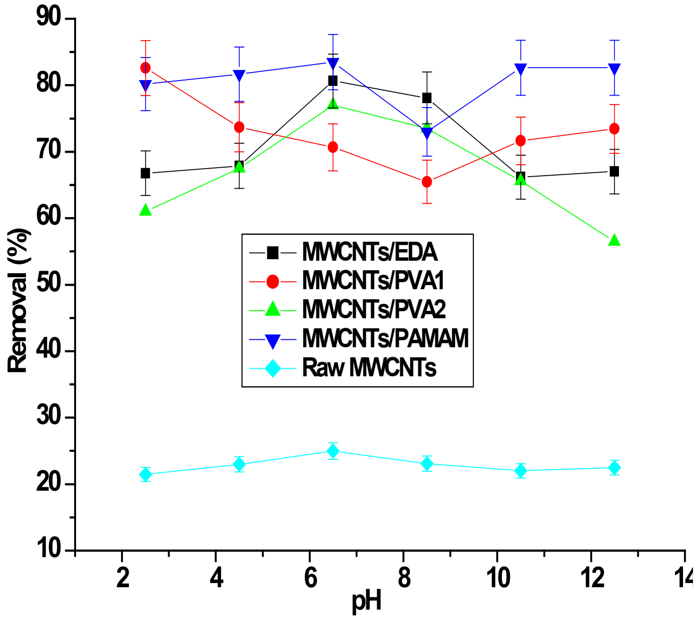

Figure 3.36: Effect of pH on Pb(II) adsorption by different MWCNT nanocomposites

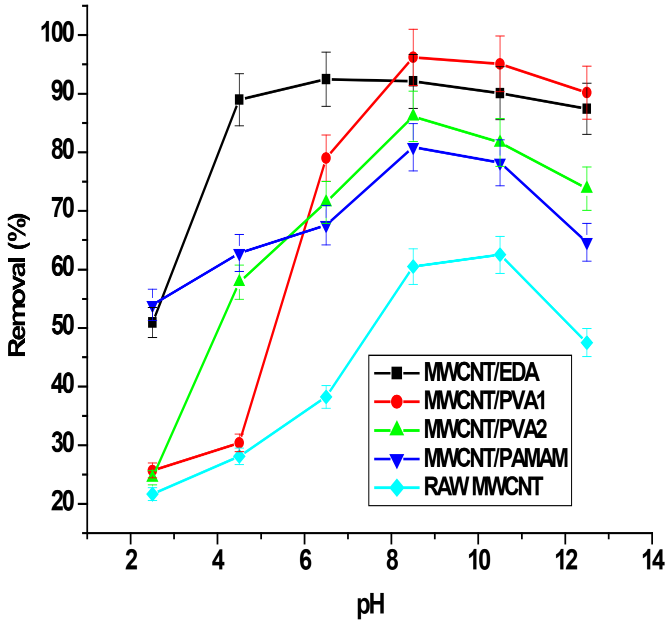

Figure 3.37: Effect of pH on Cu(II) adsorption by different MWCNT nanocomposites

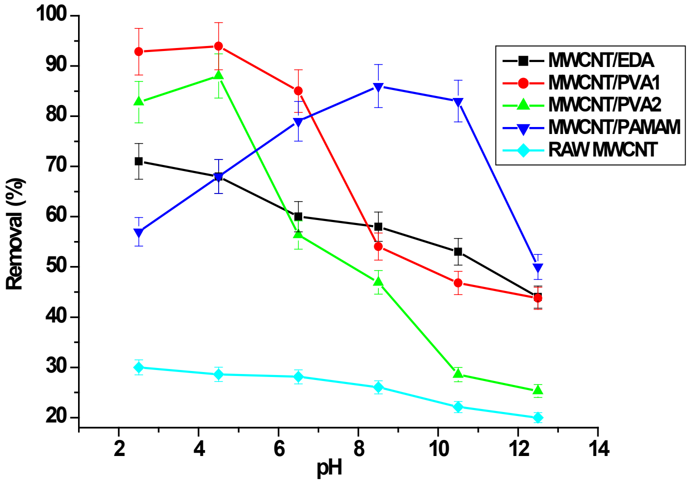

Figure 3.38: Effect of pH on Cr(VI) adsorption by different MWCNT nanocomposites

3.14.2. The effect of initial concentration on the adsorption of metal ions

Solutions of metal ions with varying concentrations were used to investigate the effect of initial metal ions concentrations by employing optimum pH. The effect of initial metal ions concentrations was assessed for three metal ions (Cu(II), Pb(II) and Cr(VI)) using MWCNTs/nanocomposites. The experimental studies revealed that percentage removal of Cu(II) and Pb(II) increased with an increase in metal ions concentration and reached equilibrium at 40 mg/L as shown in figures 3.39 and 3.40. A similar trend was reported by Kosa *et al.* (2012) using MWCNTs modified with 8-hydroxyquinoline (8-HQ-MWCNTs) adsorbent for removal of Cu (II), Pb (II) and Zn (II) metal ions.

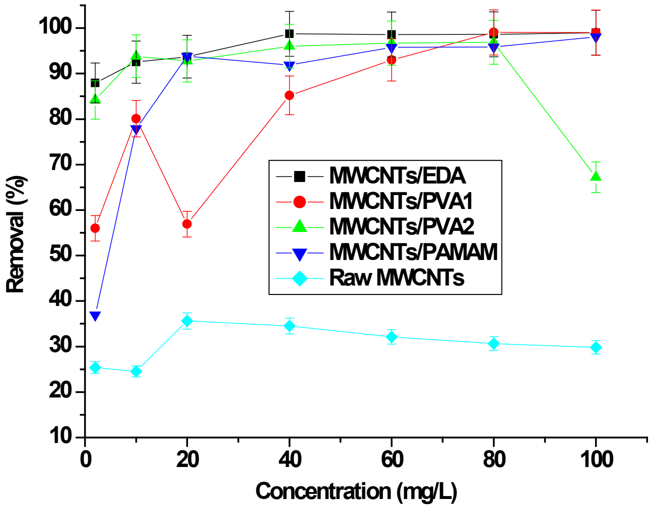

Figure 3.39: Effect of concentration on Pb(II) adsorption by different MWCNTs nanocomposites

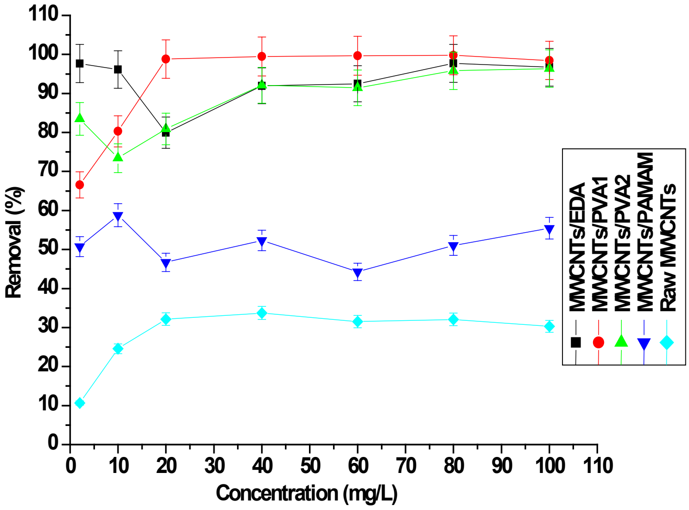

Figure 3.40: Effect of concentration on Cu(II) adsorption by different MWCNTs nanocomposites

The adsorption capacity of MWCNTs/EDA and MWCNTs/PAMAM for Cr(VI) decreased with an increase in metal ion concentration presumably due to rapid saturation of the surface charge on adsorbent. Metal adsorption depends on initial metal ion concentration because specific sites are available at low metal ion concentration and become saturated at high metal ion concentration, which results in less available sites for adsorption (Kosa *et al.*, 2012). The results obtained in this study are in agreement with the reports from other studies (Al-Asheh & Duvnjak, 1996; Al-Asheh & Duvnjak, 1997; Al-Asheh & Banat, 2001; Wong *et al.*, 2003; Rahman, 2007). However, MWCNT/PVA composite showed increased percentage removal with an increase in metal ion concentration and became stable at concentration of 20 mg/L. In this study, MWCNTs/PVA1 appeared to be the best nanocomposite for Cr(VI) adsorption (Figure 3.41).

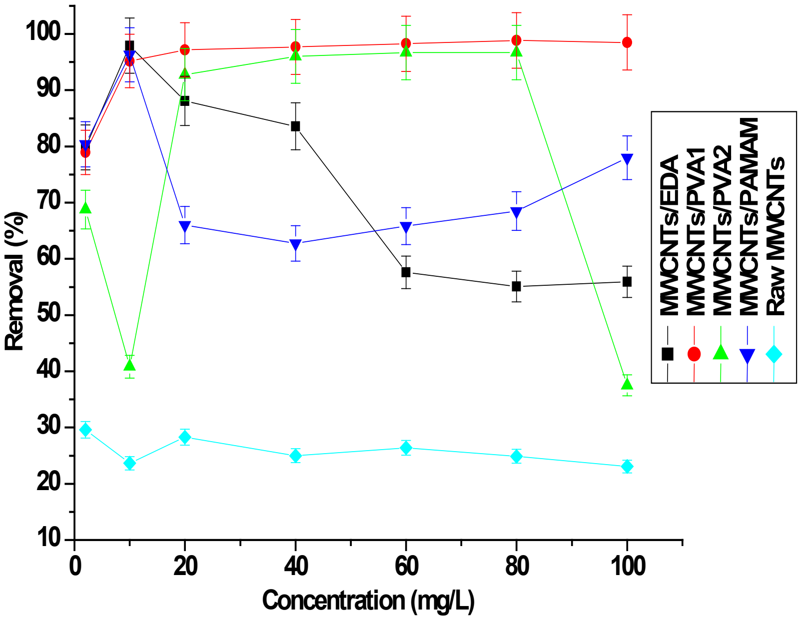

Figure 3.41: Effect of concentration on Cr(VI) adsorption by different MWCNTs nanocomposites

3.14.3. The effect of contact time on the adsorption of metal ions

To determine fast and quantitative adsorption rate, the effect of contact time was investigated. The effect of contact time was investigated in the time range of 30 to 150 minutes. Figures 3.42 to 3.44 illustrate removal efficiency of nanocomposites versus contact time. Equilibrium was reached during the first 30 minutes almost for all metal ions and nanocomposites, it then remained constant for all the metal ions. Similar observation was observed in the study by Li *et al.* (2011). The findings of this study revealed that PVA_1-MWCNTs as the possible adsorbent of choice for Cu(II), whereas PVA_2-MWCNTs and PAMAM-MWCNTs showed high adsorption capacity for Pb(II) and Cr(VI), respectively. However, to achieve quantitative adsorption for Cr(VI) using MWCNTs/PAMAM it required 2 h. The raw MWCNTs revealed a low percentage removal for all metal ions.

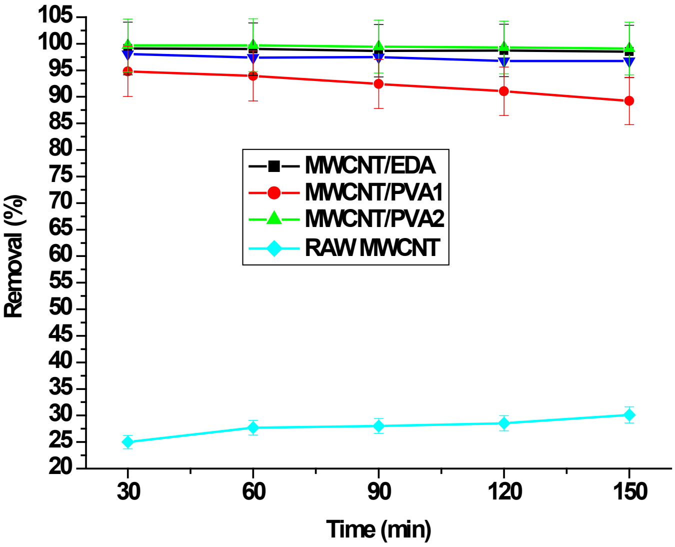

Figure 3.42: Effect of contact time on Pb(II) adsorption by different MWCNT nanocomposites

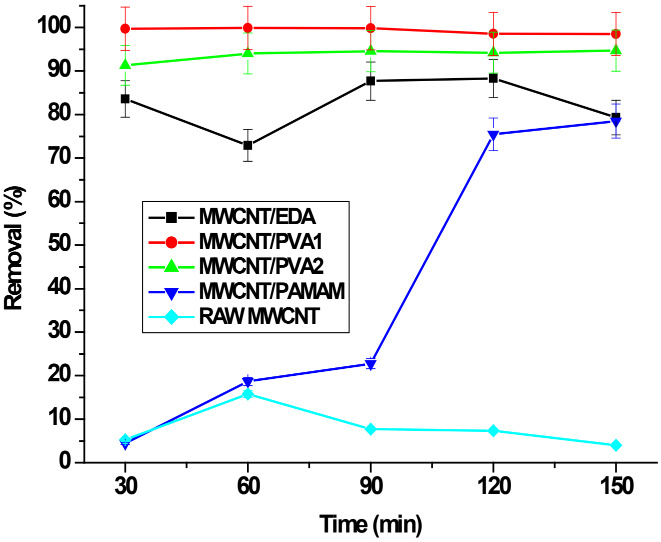

Figure 3.43: Effect of contact time on Cu(II) adsorption by different MWCNT nanocomposites

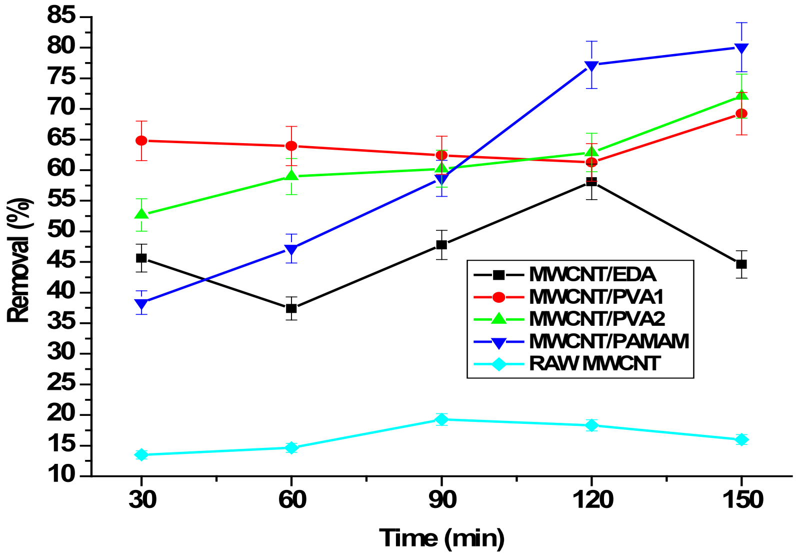

Figure 3.44: Effect of contact time on Cr(VI) adsorption by different MWCNT nanocomposites

3.14.4. The effect of adsorbent dosage on the adsorption of metal ions

Figures 3.45 to 3.47 show the influence of the adsorbent dosage on the adsorption of metal ions. In the adsorption studies of Cu(II) and Pb(II), a high removal efficiency was observed from low adsorbent dosage to high adsorbent dosage showing little variation with the change in masses of nanocomposites. A similar trend was reported by Mohammad *et al.* (2013) where maximum percentage removal was found at low adsorbent dosage of 0.03 g to be 95% for Pb(II) and Cu(II) ions. The adsorption of Cr(VI) in all nanocomposites increases with an increase in adsorbent dosage. Its maximum removal was 85% for 0.13 g of adsorbent dosage which is due to less active sites availability. This study is also in agreement with the study by Lia *et al.* (2003).

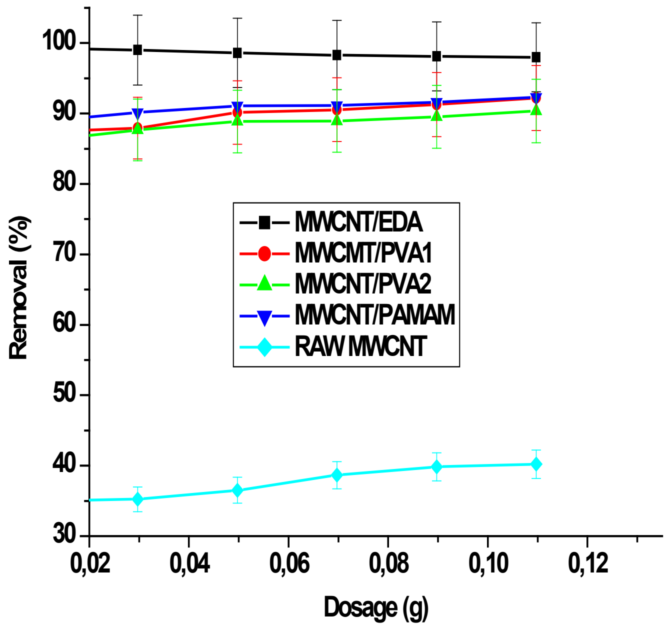

Figure 3.45: Effect of adsorbent dosage on Pb(II) adsorption by different MWCNT nanocomposites

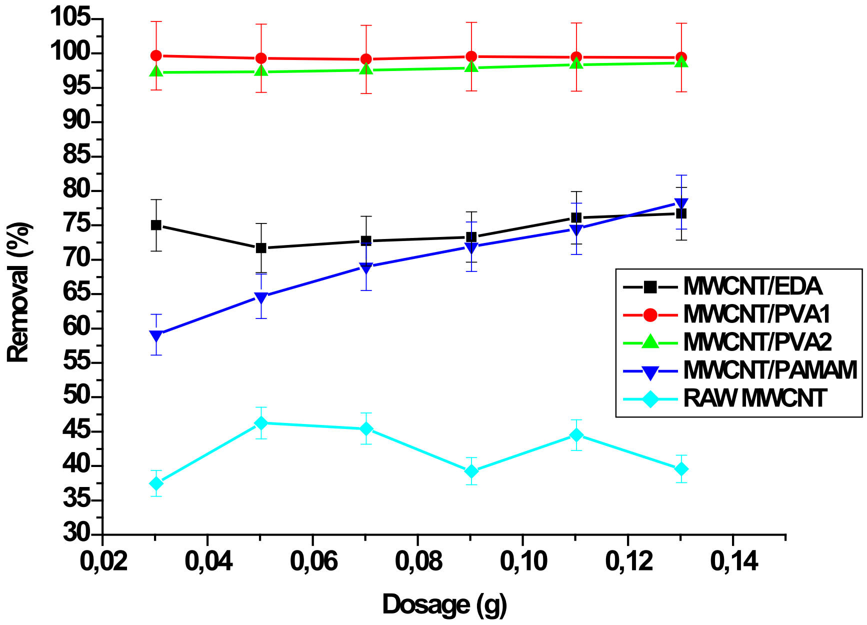

Figure 3.46: Effect of adsorbent dosage on Cu(II) adsorption by different MWCNT nanocomposites

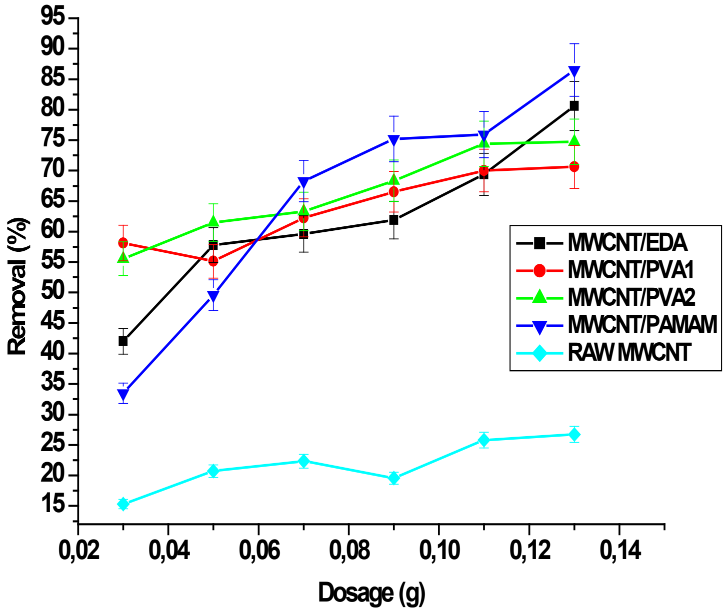

Figure 3.47: Effect of adsorbent dosage on Cr(VI) adsorption by different MWCNT nanocomposites

3.15. Characterisation of synthesised nanomaterials

3.15.1. Characterisation by FTIR spectrometry

The MWCNTs functional groups were observed using FTIR spectrometry. Figure 3.48 shows the spectra of raw MWCNTs (a) and oxidised MWCNTs (b). There are no clear peaks in the raw MWCNT which is expected since there are no additional groups attached. There are no characteristics peaks of -OH and -COOH functional groups observed. However, a very weak peak at 1625 cm^{-1} is observed which might be due to the C=C bond of MWCNTs aromatic rings and it was also reported by Ren *et al.* (2013).

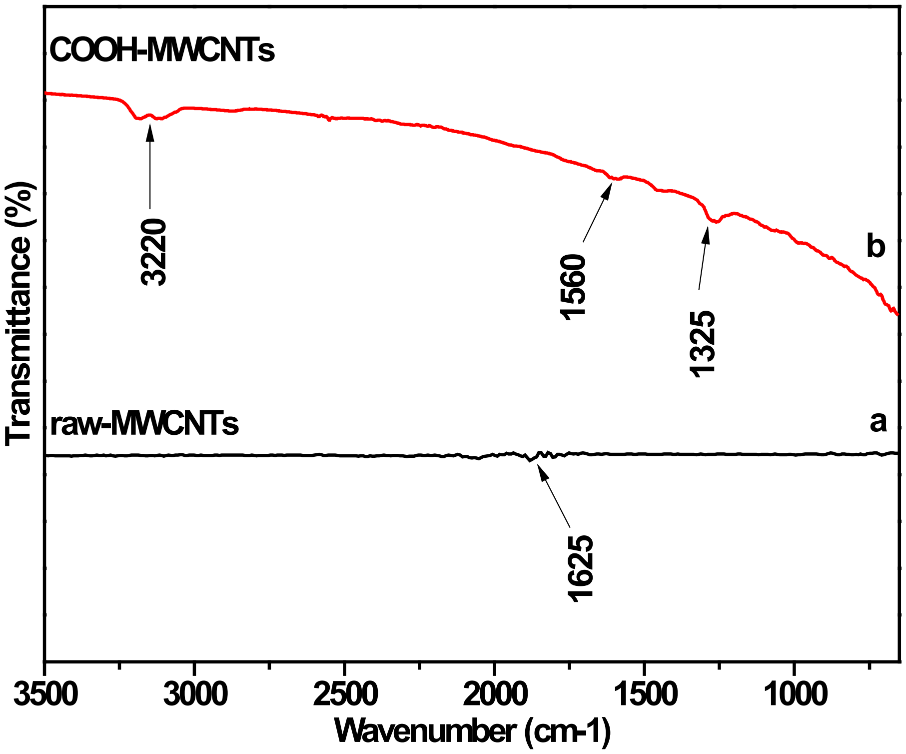

Figure 3.48: FT-IR spectra of (a) raw MWCNT and (b) MWCNT/COOH

Oxidation of MWCNTs brought up hydroxyl and carbonyl groups on nanomaterial surface. The stretching band at 3220 cm^{-1} could be associated to O-H functional groups. An aromatic ring peak attributed to C=C was also observed at 1560 cm^{-1}. The appearance of peak 1325 cm-1 is associated with C-O stretching vibrations of carboxylated group. Similar findings were reported by other researchers (Mohammad *et al.*, 2013; Weijie *et al.*, 2013).

The MWCNTs/EDA and MWCNTs/PAMAM modified nanocomposites spectra are illustrated in figure 3.49 (c) and (d), respectively. The sharp peaks in MWCNTs/PAMAM showed succesful modificatio of nanocomposites. The peak at 1750 cm^{-1} could be due to stretching band of amine. The band at 1682 cm^{-1} is attributed to amide C=O stretching. Furthermore, the band at 1420 cm^{-1} corresponds to amide group bending and the peak at 1210 cm^{-1} is attributed to C-N-H group. The charecteristc peak of C-N group is observed at 1009 cm^{-1} that shows a family of

PAMAM/dendrimer which was reported by Barakat *et al.*(2013) and Afshin *et al.* (2016).

The internsified peaks were observed after modification of MWCNTs with EDA. A weak band at 3250 cm^{-1} is attributed to the primary amine stretching vibration incorporated while peak at 1729 cm^{-1} is assigned to -NH$_2$ vibrations (Rahimpour *et al.*, 2011). The peak at 1520 cm^{-1} corresponds to N-H, whereas the peak at 1250 cm^{-1} shows C-N bond stretching of amide groups, which is in agreement with the study by Jimino *et al.* (2009).

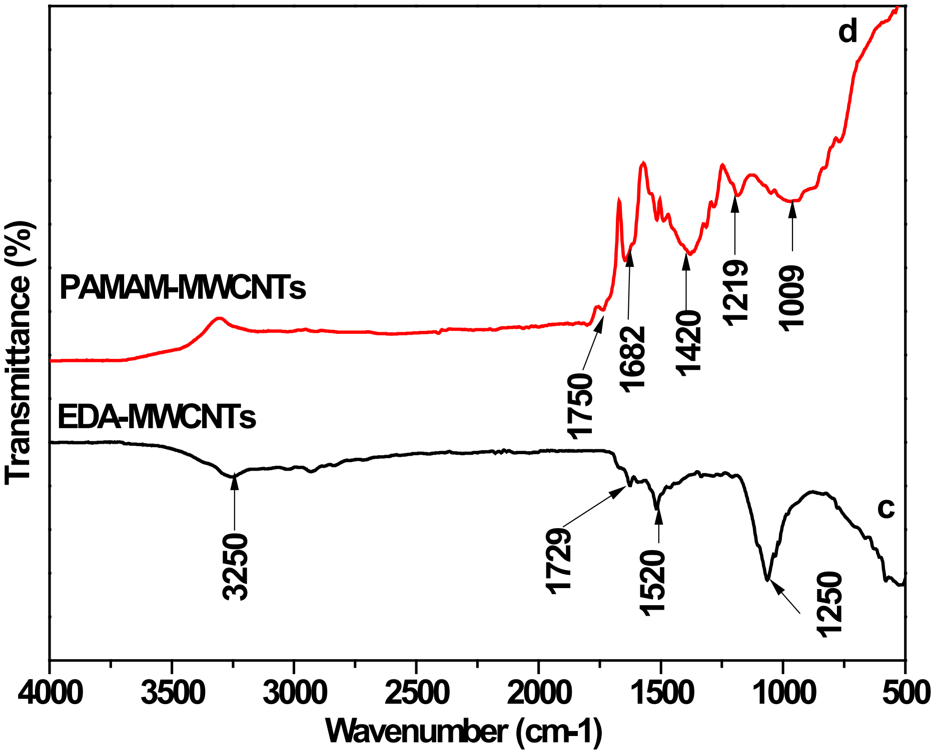

Figure 3.49: FT-IR spectra of (c) MWCNT/EDA and (d) MWCNT/PAMAM

The FTIR spectra of MWCNTs modified with PVA are shown in figure 3.50. The PVA shows an absorption band of hydrogen bonded O-H peak above 3000 cm^{-1} when the alcohol is not dissolved in a solvent (Elbadawy *et al.*, 2015) . However, in this study, the O-H peak is very weak because when MWCNTs were modified with PVA, PVA was dissolved in high boiling point solvent (DMSO) and further washed with excess deionised water until neutral pH. Thus, the hydrogen bonded O-H peak has been weakened. The observed peaks are very weak as shown in figure 3.50.

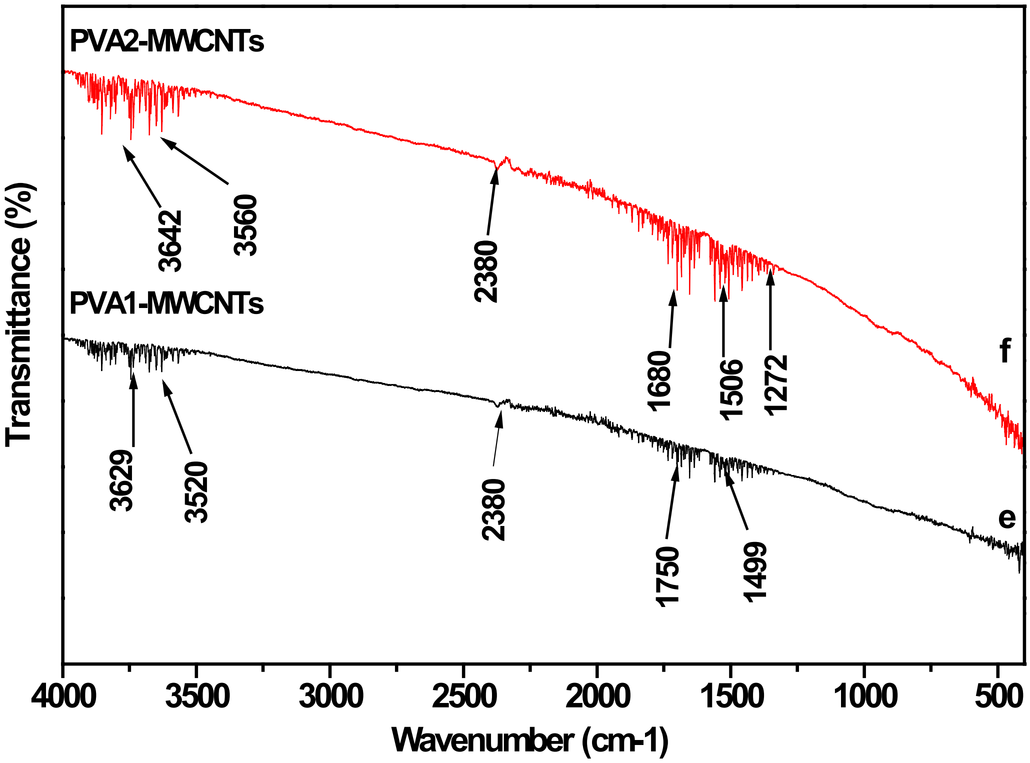

Figure 3.50: FT-IR spectra of (e) MWCNT/PVA1 and (f) MWCNT/PVA2

The FTIR spectra of raw PVA with different molecular weights are displayed in figure 3.51. There are peaks exhibited at 3500, 3100, 3515 and 3250 cm^{-1}. These are due to the stretching vibrations of -OH groups. Such observation was also reported by Thien *et al.* (2008). The peaks located at 1789 and 1732 cm^{-1} are assigned to C=O stretching while C-O stretching bands of PVA polymer are located at 1050 and 1018 cm^{-1}. One of the properties of PVA is crystallinity, therefore important peaks that attributed to the crystallinity of this polymer has been identified between 1500 and 1000 cm^{-1} (Afshari *et al.*, 2016). These characteristic peaks were observed, in this study corresponding to C-O stretching bands located at 1489, 1429, 1050 and 1018 cm^{-1}. Similar findings were reported elsewhere (Krimm *et al.*, 1956; Afshari *et al.*, 2016).

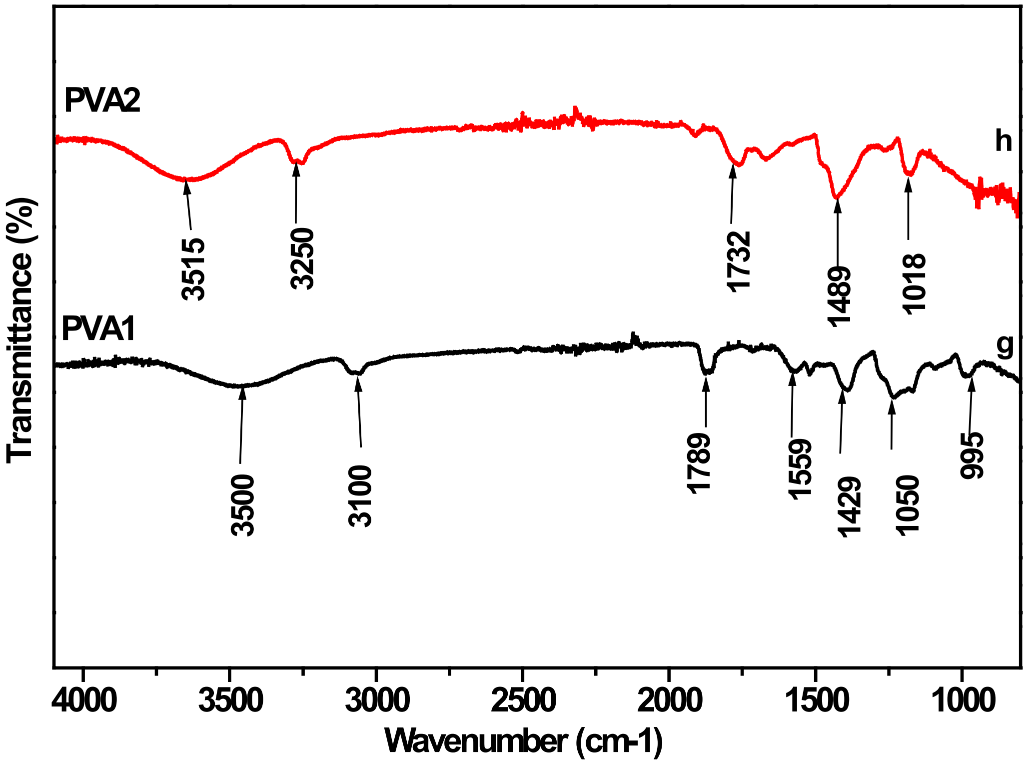

Figure 3.51: FTIR spectra of (g) PVA1 and (h) PVA2

3.15.2. Charecterisation by TGA

TGA analysis curves of prestine MWCNT and modified MWCNTs are presented in figure 3.52. The thermal degradation of modified MWCNTs is greater than pristine and oxidised MWCNTs.

Raw and oxidised MWCNTs were stable and a sign of decomposition was not observed. For oxidised MCWNTs a smaller weight loss was discovered from 100°C and is might be due to evaporation of water adsorbed. Similar behaivor was reported in the study of Canete-Rosales *et al.* (2014). The weight loss between 100°C and 400°C could be associated to evolution of CO_2 of the carboxylic group.

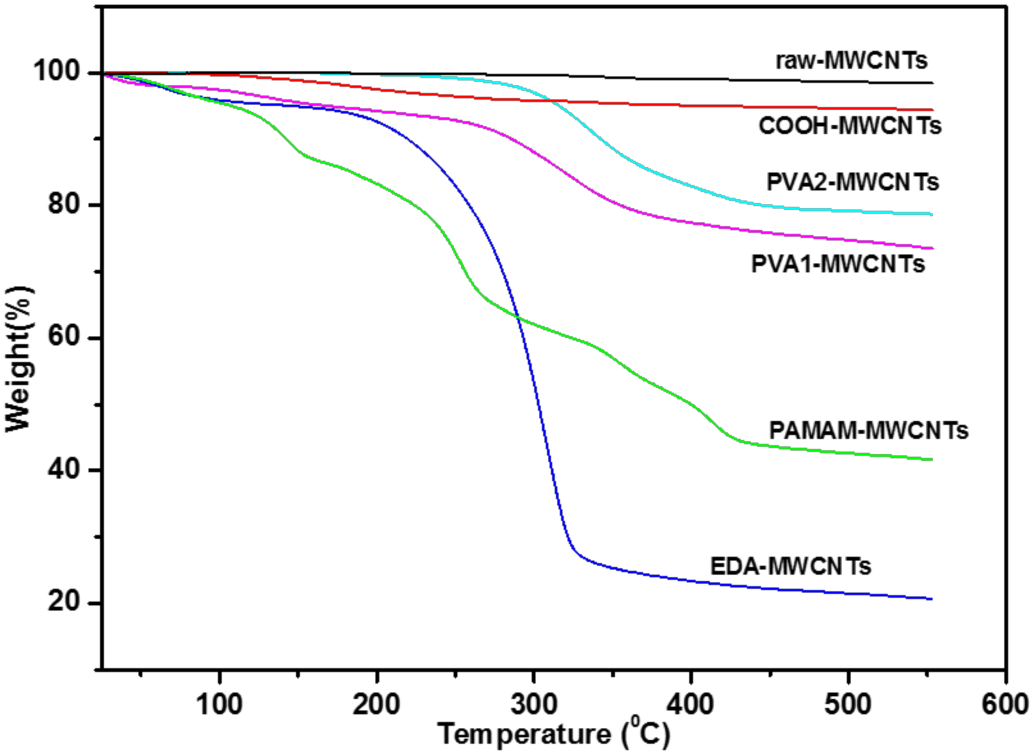

Figure 3.52: The TGA profiles for raw MWCNT, MWCNT/COOH, MWCNT/EDA, MWCNT/PAMAM, MWCNT/PVA1 and MWCNT/PVA2

A sequential weight loss is detected for MWCNTs/EDA and it could be associated to the covalently bonded amide to the walls of MWCNTs. It has been reported that EDA has a lower decomposition temperature, hence in the current study, MWCNTs/EDA shows a drastic decomposition from 60°C, which is attributed to the organic functional groups added on the surface of MWCNTs (Mehdi *et al.*, 2011). The added functional groups were thermally unstable as shown from 220°C to 360°C, which exhibited by high weight loss due to breakdown of amine groups attached to MWCNTs. The elimination of functional groups attached during modification were reported (Mehdi *et al.*, 2011).

The covalent bond between carbon nanomaterials and EDA was disrupted as observed through thermal decomposition from 360°C to 600°C. Similar findings were reported by Hadavifar *et al.* (2014).

A sequential weight loss was detected for PAMAM-MWCNTs and it can be associated to the number of generations of PAMAM covalently bonded walls of MWCNTs. It has been reported that the number of generations of PAMAM/dendrimer increases the quantity of PAMAM on the walls of MWCNTs, hence in this study PAMAM-MWCNTs showed a drastic decomposition from 60°C to 340°C. This could be attributed to additional organic moieties (Yuan *et al.*, 2008). Furthermore, the elimination of functionalities attached during modification are seen to be degrading from 350°C to 600°C, which was also reported by Pan *et al.* (2006).

The thermal stability of PVA-MWCNTs was investigated and compared to the stability of raw MWCNTs. Two thermograms of PVA-MWCNTs with different molecular weights portrayed similar trend with different decomposition temperatures. Moreover, the low molecular weight polymer (PVA1) revealed lower decomposition temperature than the high molecular weight polymer (PVA2). This might be due to the increased number of chains which results in stronger covalent bonds in the PVA2 that hinder decomposition process. Similar phenomena was reported by Jeon *et al.* (2010). The moisture vaporisation weight loss peak was observed at 50°C to 110°C, thermal degradation steepness was at 150°C to 300°C and the byproduct formation of PVA was at 380°C to 600°C. Similar results were reported by Park *et al.* (2012).

3.15.3. The XRD patterns of raw MWCNTs, COOH-MWCNTs, EDA-MWCNTs and PAMAM-MWCNTs

The crystallinity and phase identification of different nanocomposites were conducted using XRD. Figures 3.53 and 3.54 show the XRD profiles of the nanocomposites. It has been reported that the main XRD diffractograms of MWCNTs strongly exhibits graphite characteristics due to their intrinsic nature (Aqel *et al.*, 2012). The indexed peaks on the nanocomposites at 2θ of 26°, 38º and 42º are due to (002), (100) and (101) planes, respectively. It further corroborates that they are a reflection of hexagonal graphite. The COOH-MWCNTs and EDA-MWCNTs XRD patterns are similar with that of raw MWCNTs. However, the peaks become lower intense than those of raw MWCNTs, which indicates the removal of impurities and presence of poor crystallinity. Similar findings were reported by Rashidi *et al.* (2015).

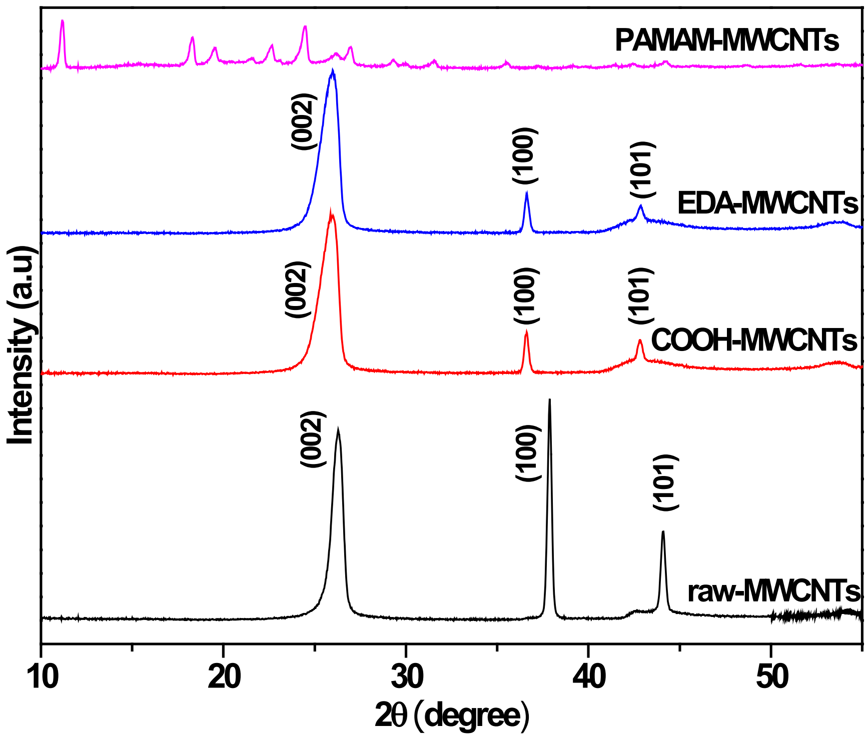

Figure 3.53: XRD patterns for raw MWCNT, COOH-MWCNT, EDA-MWCNT and PAMAM-MWCNT

The diffraction angle of EDA-MWCNTs and PAMAM-MWCNTs shows that the crystallinity of raw MWCNTs has been affected due incorporation of polymers. Peak characteristics of MWCNTs in PAMAM-MWCNTs are not visible on XRD patterns and this could be attributed to insufficient content of MWCNTs hence the decrease in intensity of peaks. Furthermore, diffraction peaks are exhibited in the range of 2θ of 13.5° to 27.8º. Veerapandian *et al.* (2015) reported similar results.

The diffraction patterns of pure PVA and PVA modified MWCNTs are shown in figure 3.54. The PVA is one of the crystalline polymers known, thus the broad sharp diffraction peak at 2θ= 21.4° is a characteristic peak of PVA crystalline structure. The intensity of characteristic peaks of nano composites in both molecular weights weakened significantly, which could be attributed to change in crystalline structure of pure PVA after introduction of MWCNTs (Ma *et al.*, 2012).

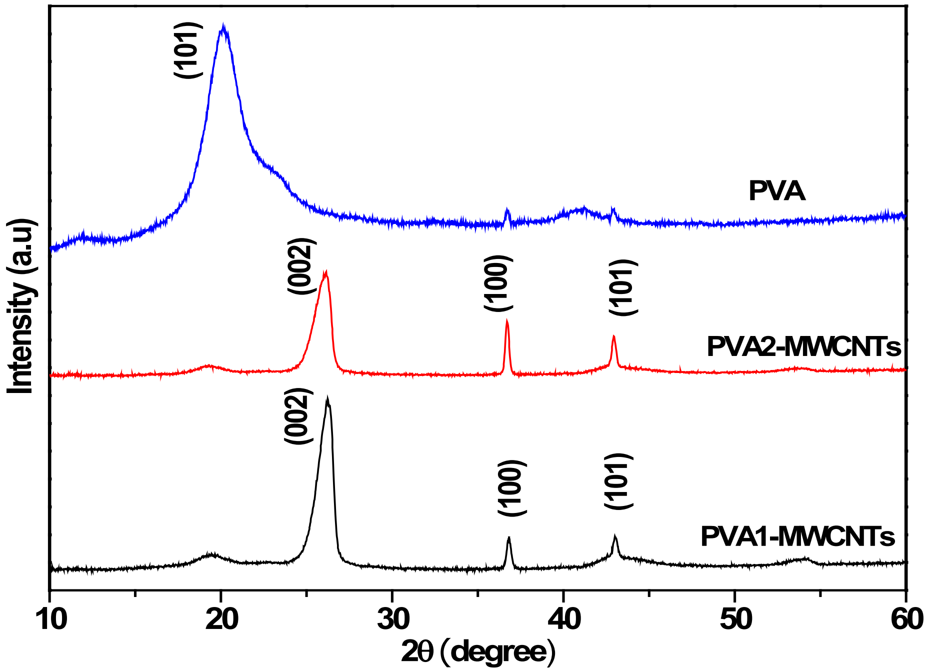

Figure 3.54: The XRD patterns of PVA1-MWCNTs, PVA2-MWCNTs and raw PVA

3.15.4. Characterisation of raw MWCNTs and nanocomposites by SEM

The morphology of the nano composites were further characterised by SEM. Two SEM images per nano composite were taken at different magnifications. Figures 3.55 and 3.56 show raw and oxidised MWCNTs SEM images, respectively. The accumulated irregular raw MWCNTs are illustrated in figure 3.55(a) and (b). It contains some surface of carbonaceous species such as amorphous carbon (Sun *et al.*, 2012). Hence raw MWCNTs have disordered debris with entangled like structures.

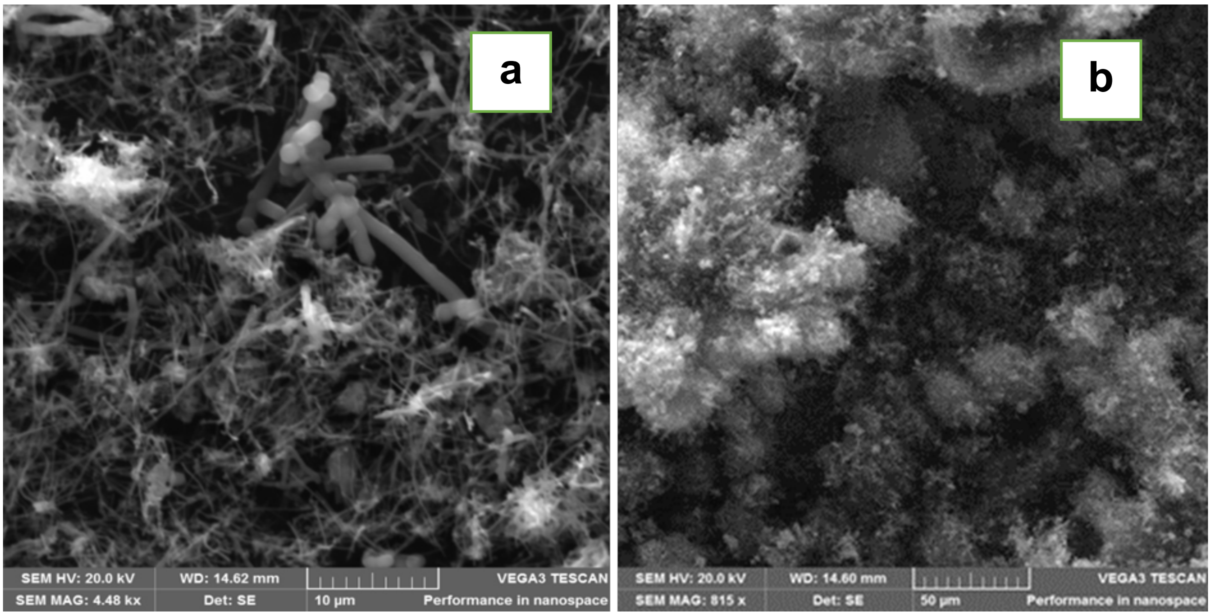

Figure 3.55: SEM images of raw MWCNTs at different magnifications (a) 10 µm and (b) 50 µm

The surface of MWCNTs was cleaned during oxidation process by removing carbonaceous species. Moreover, compact stacking morphology was exhibited and improvement of slightly thinner MWCNTs was observed. Oxidised MWCNTs showed a better dispersion as compared to raw MWCNTs. Similar observation has been made by Safo *et al.* (2018).

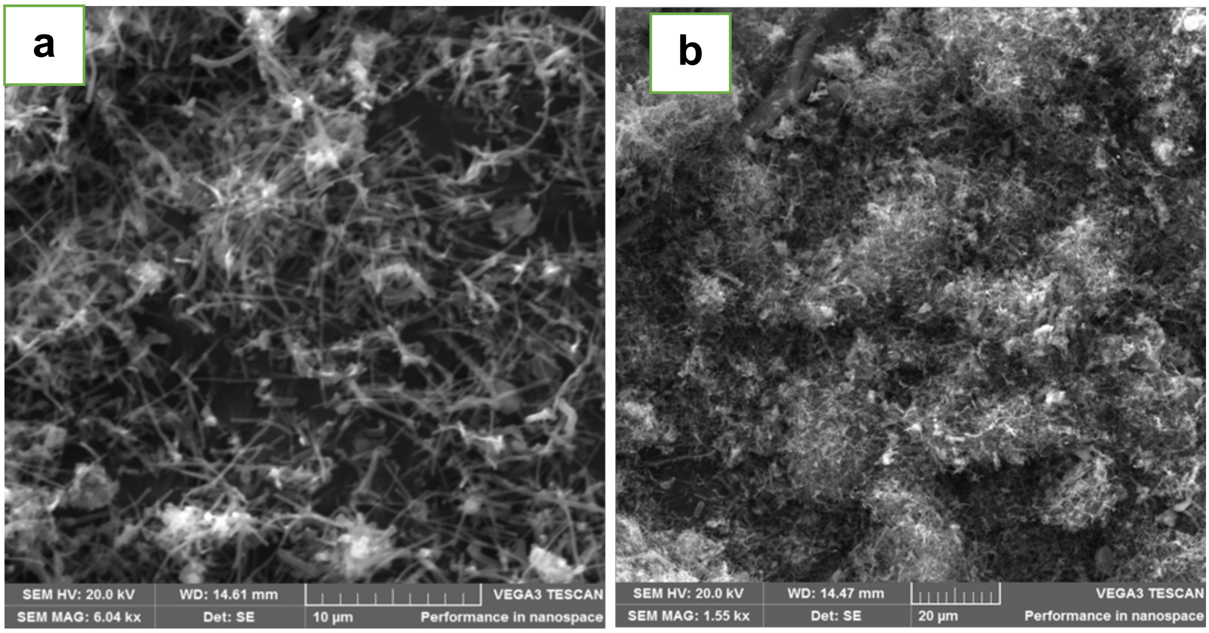

Figure 3.56: SEM images of oxidised MWCNTs at different magnifications (a) 10 µm and (b) 20 µm.

The SEM micrograms of EDA-MWCNTs and PAMAM-MWCNTs are illustrated in figure 3.57. In EDA-MWCNTs nano composite (figure 3.57(a) and (b)), there have been some improvement without agglomeration, which could be attributed to the grafting of amino group on the surface of the MWCNTs. Moreover, the EDA-MWCNTs nano composite appear to be brighter than raw and oxidised MWCNTs. This might be due to exposure to EDA, which increases the activity of adsorbent surface areas due to functionalisation as mentioned by Hadavifar *et al.* (2014).

The PAMAM-MWCNTs micrograms in figure 3.57 (c) and (d) show the smooth surface of nano composites. It can further be noted that the length and the diameter have a wide distribution due to more additional generation of PAMAM on the surface of MWCNTs. A dense polymeric matrix can slightly be seen in the background of the nano composite, which attributes grafting of PAMAM (Zheng *et al.*, 2013).

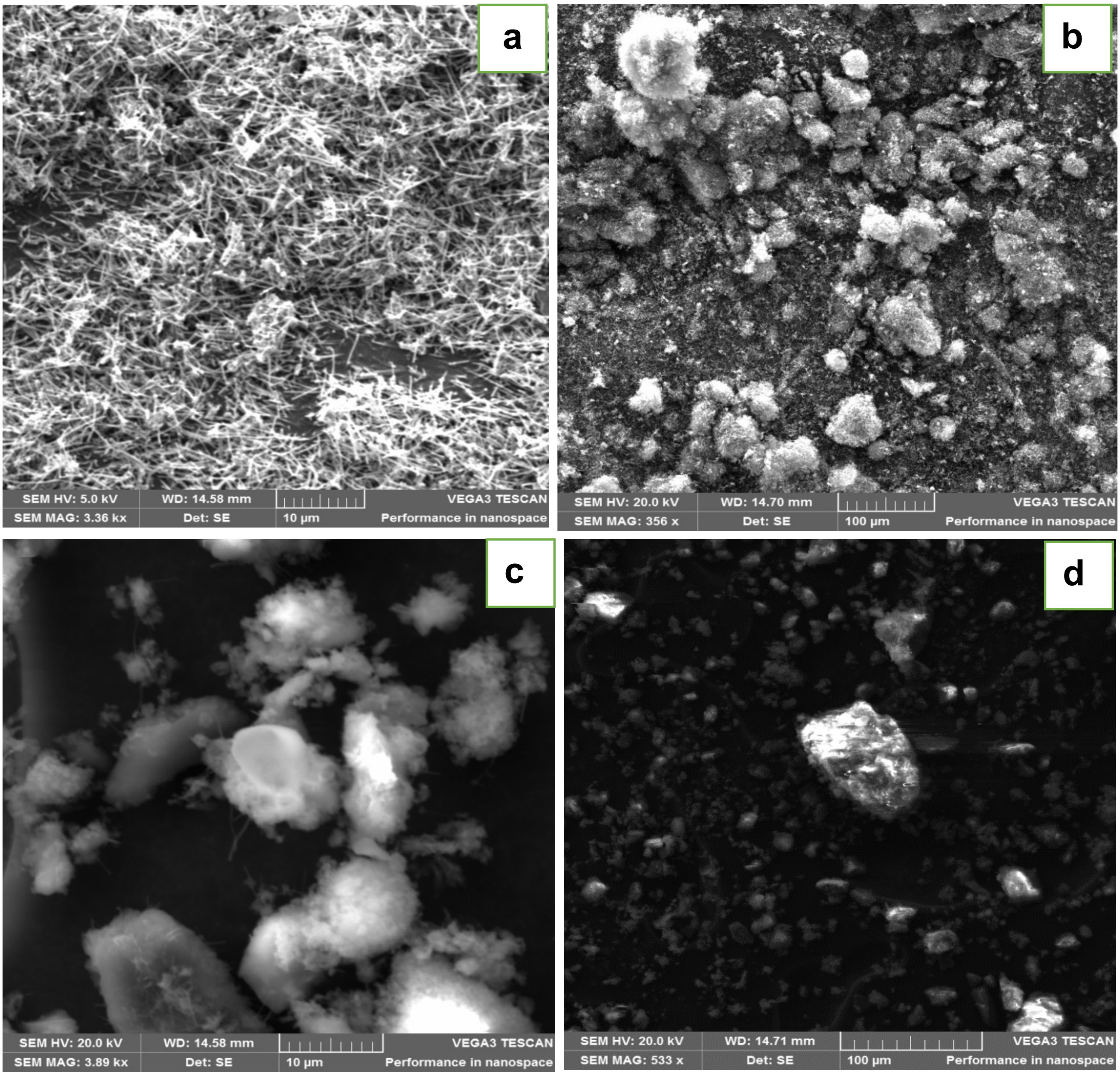

Figure 3.57: SEM images of MWCNTs/EDA at different magnifications (a) 10 μm and (b) 100 μm and images of MWCNTs/PAMAM at different magnifications (c) 10 μm and (d) 100 μm.

The SEM images of MWCNTs incorporated with PVA of two different molecular weights are depicted with different magnifications in figure 3.58. It can be estimated that the diameter of the nano composites is higher than raw MWCNTs. This might be due to thin film of PVA covering the surface of raw MWCNTs. Moreover, the polymer had significant impact on the shape of the MWCNTs which has changed from its tubular shape after grafting with the macromolecules. Raw MWCNTs is known as a hydrophobic adsorbent in nature (Rurlle *et al.*, 2007), therefore, the thin film of PVA polymer keep MWCNTs apart after grafting and thus disable the nano composites to agglomerate and entangle. Furthermore, PVA makes the nano composite hydrophilic (Malikov *et al.*, 2014). Both PVA with two different molar mass portray the same characteristics of nanocomposite incorporated on MWCNTs.

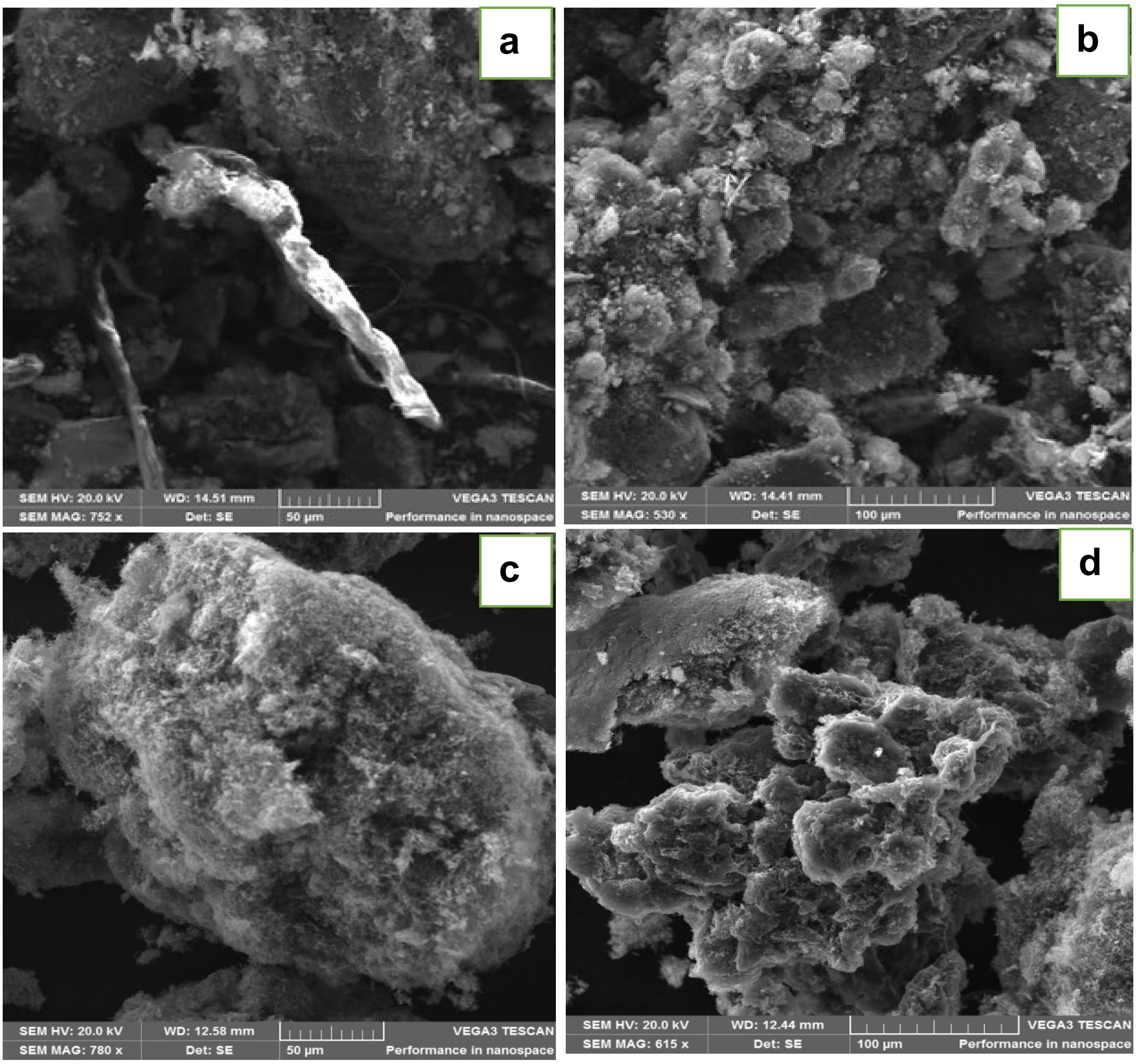

Figure 3.58: SEM images of MWCNTs/PVA1 at different magnifications (a) 50 µm and (b) 100 µm and images of MWCNTs/PVA2 at different magnifications (c) 50 µm and (d) 100 µm.

Pure PVA present a uniform morphology with smooth surface and irregular shape. It became gradually rough with MWCNTs and which may result in strengthening of MWCNTs nanocomposite polymer interaction. Furthermore, similarity in morphology of both PVA with different molecular weights have been observed as shown in figure 3.59.

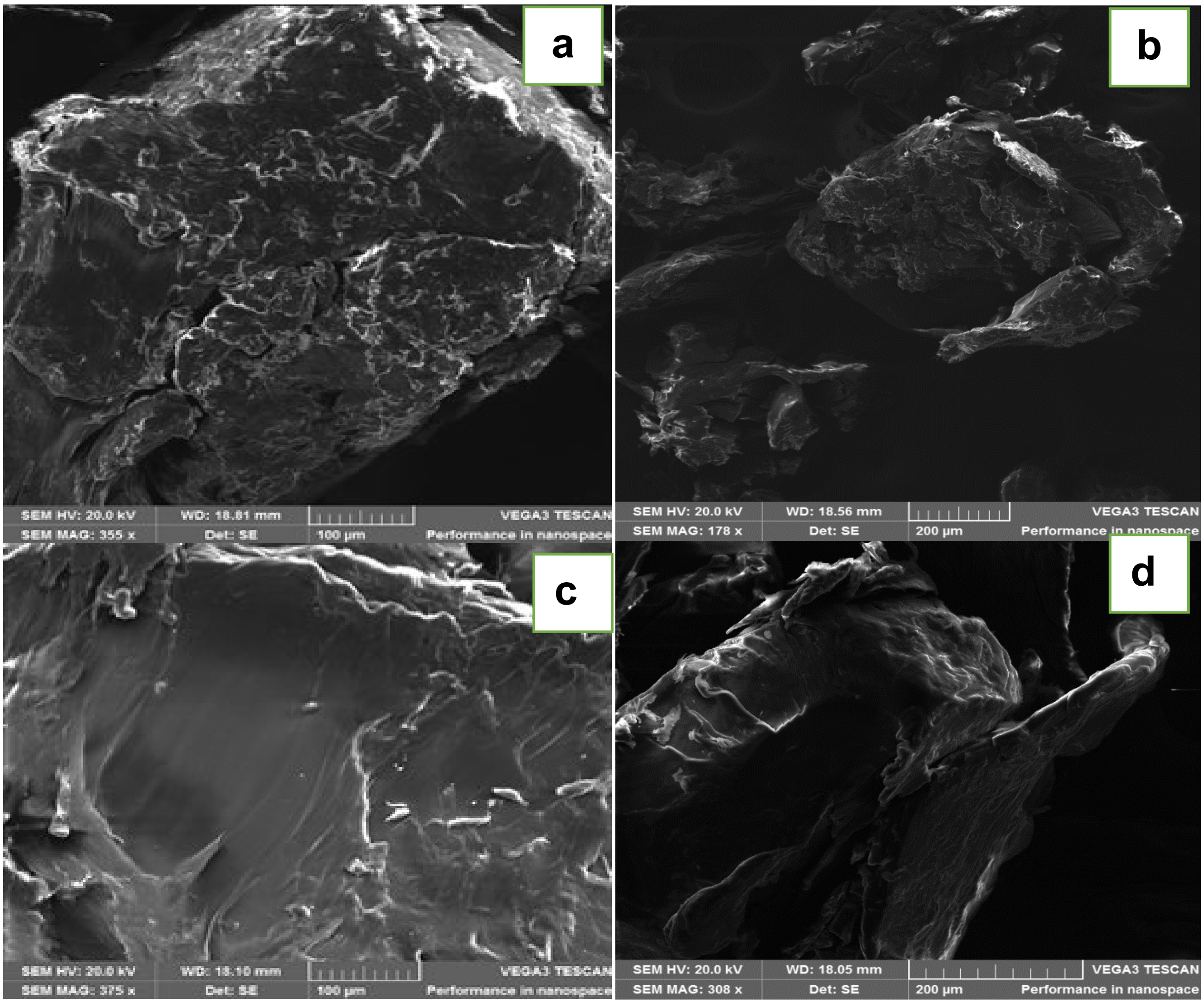

Figure 3.59: SEM images of PVA1 at different magnifications (a) 100 μm and (b) 200 μm and images of PVA2 at different magnifications (c) 100 μm and (d) 200 μm.

3.15.5. Characterisation of raw MWCNTs and nanocomposites by TEM

The surface changes of nanocomposites were observed by TEM. The raw-MWCNTs and COOH-MWCNTs nanocomposites are illustrated in figure 3.60 in high and low magnifications. The walls of MWCNTs are thick and might be due to the nature of its synthesis (Shen *et al.*, 2009). The raw-MWCNTs appear to be smooth in both low and high magnifications. However, there were some dark spots seen in some of the tubes which indicate the presence of impurities might have incurred during synthesis of the MWCNTs or could be attributed to amorphous carbon (Rananga, 2013). It can also be noted that the external walls of pure MWCNTs are structurally more organised than the oxidised MWCNTs. The oxidised MWCNTs after treatment have become rough with no impurities indicating that they have been removed during the oxidation process.

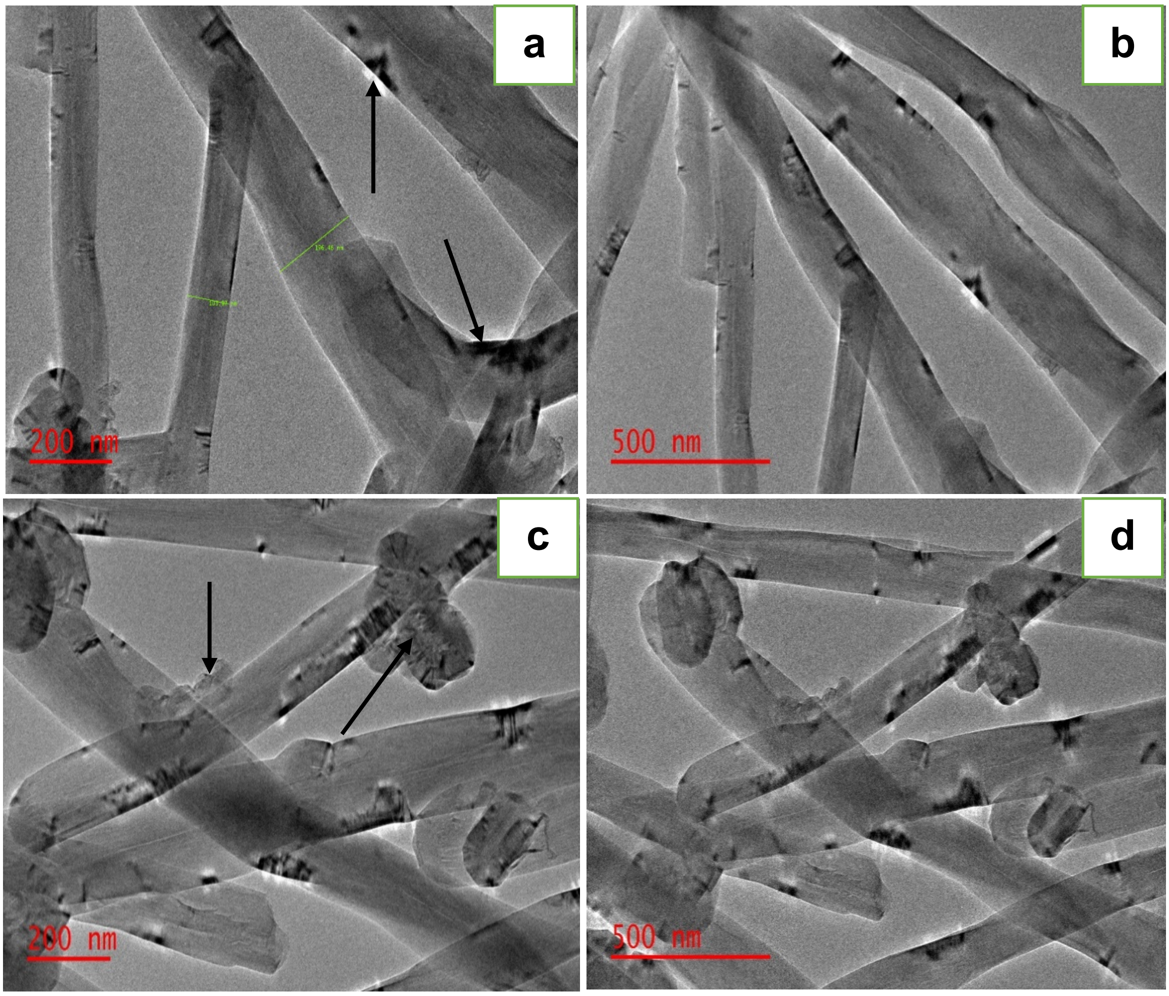

Figure 3.60: The HRTEM images of raw MWWCNTs at different magnifications (a) 200 nm and (b) 500 nm and images of oxidised MWCNTs at different magnifications (c) 200 nm and (d) 500 nm.

The TEM images of all the MWCNTs appear tubular as expected regardless of different modifications they have undergone. As shown in figure 3.61 (b), some portions of the MWCNTs are coated by EDA polymer spots. In comparison to the raw MWCNTs, it became rough and a slight damage was obtained. However, its tubular structure remained intact and these confirms that the functionalisation with EDA have no defect on morphology of raw MWCNTs. Furthermore, it has exhibited thin and isolated morphology which was also observed by Bushimata *et al.* (2014). The PAMAM-MWCNTs images are well dispersed with dense surface suggesting that PAMAM has successfully been attached to the oxidised groups of MWCNTs.

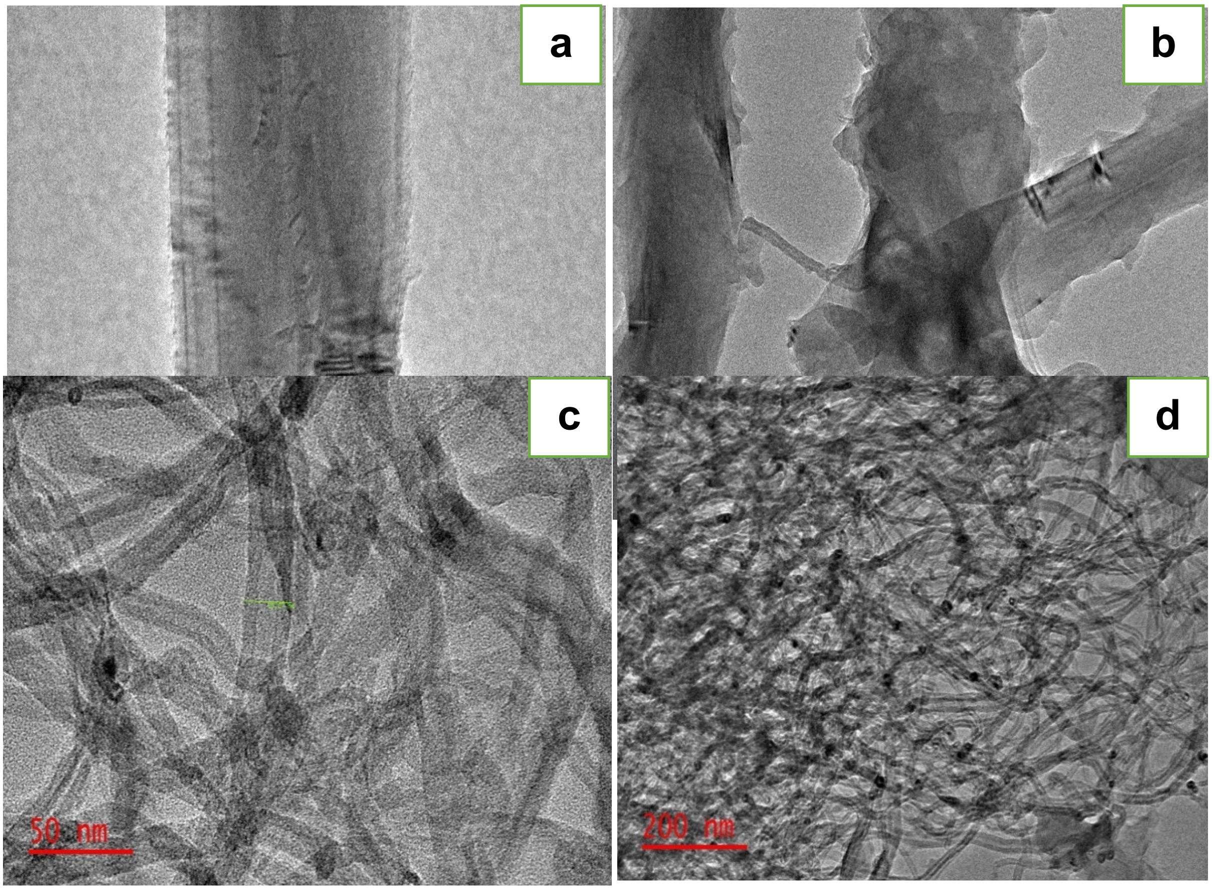

Figure 3.61: The HRTEM images of MWCNTs/EDA at different magnifications (a) 50 nm and (b) 200 nm and images of MWCNTs/PAMAM at different magnifications (c) 50 nm and (d) 200 nm.

The TEM images of pure PVA and PVA-MWCNTs are shown in figure 3.62. Well dispersed spherical TEM images of pure PVA were observed in figure 3.62 (a) and (b) at different magnifications with smooth appearance. Park *et al.* (2012) has also reported similar results.

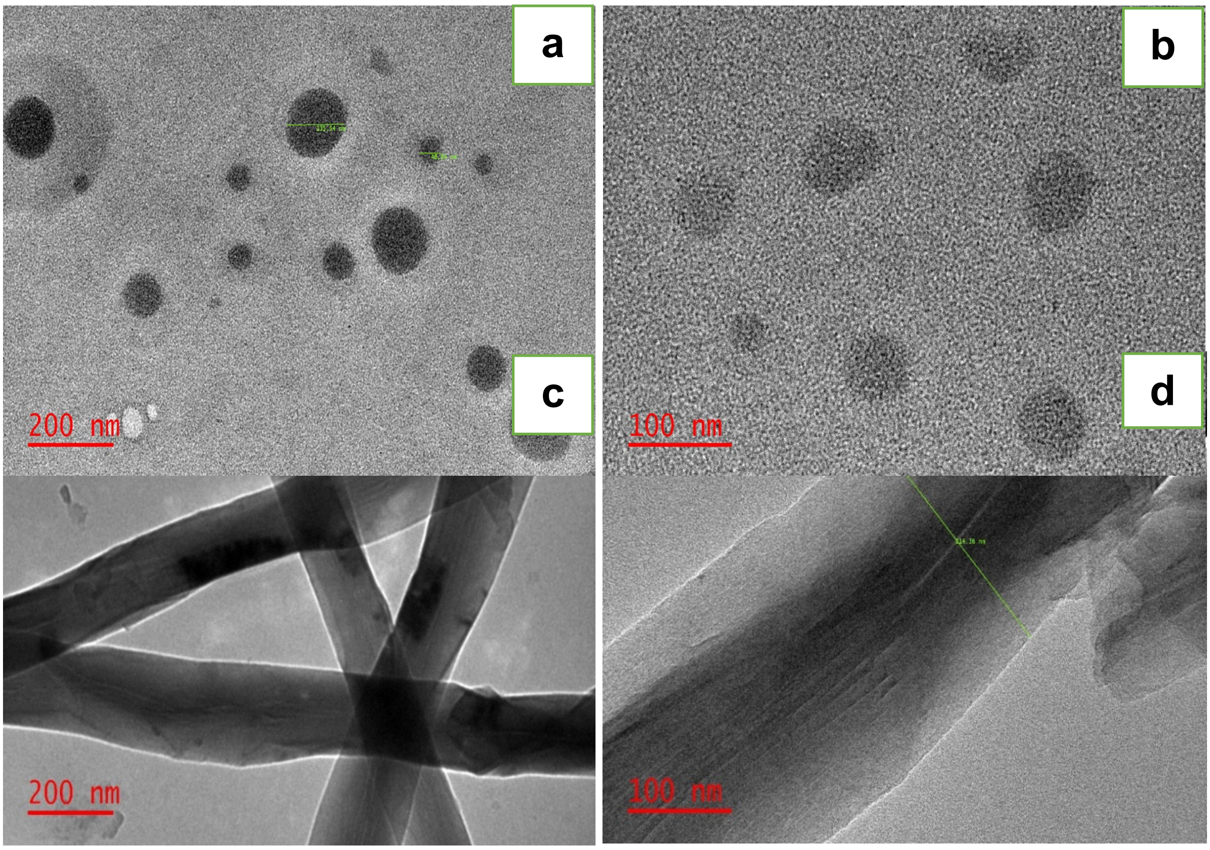

Figure 3.62: HRTEM images of raw PVA at different magnifications (a) 50 nm and (b) 200 nm, and images of PVA-MWCNTs at different magnifications (c) 50 nm and (d) 200 nm.

The raw MWCNTs appear to be clean and shows no sign of particles adhering on the tubes but with modified MWCNTs there are dark spots in the tubes which can be associated with polymer incorporated on the surface of MWCNTs. Moreover, MWCNTs have retained their tubular structure of carbon nanotubes. It can be concluded that MWCNTs has been successfully modified with PVA.

4. CONCLUSIONS

As the ICP-MS results were validated for potentially toxic elements in water and sediments by analysing the standard reference material of water and sediments, it was concluded that the employed methods are accurate. Thus, efficient method has been developed for quantification of potentially toxic elements in water and sediment samples. The HPLC-ICP-MS methods for speciation of arsenic in water and sediment samples have been developed.

The MWCNTs were successfully modified with BPEI and the structure of the composite remained intact as confirmed by XRD, FTIR, Raman spectroscopy and TGA. The analytical procedure for SPE method showed adequate efficiency in terms of accuracy and precision. The SPE procedure using nanocomposites as adsorbent material shows efficiency of the nanocomposite material to execute separation of As(V) in the presence of As(III) in water. The HPLC/ICP-MS results complimented the SPE procedure. Thus, the SPE procedure can be applied as .an alternative method for speciation of an inorganic arsenic.

For speciation of Cr in water samples, solid phase extraction method using a Chromabond NH_2 was used to separate and pre-concentrate Cr(VI) selectively both in mixed standard solution and water samples prior to quantification by graphite furnace-atomic absorption spectrometry (GF-AAS). The developed method is simple and efficient for quantification of Cr(VI) in water. A microwave-assisted extraction method was employed to separate Cr(VI) in sediment samples using 10.0 mL of 0.1 M Na_2CO_3 as extractant. A microwave-assisted extraction method using 10.0 mL of 0.01 M Na_3PO_4 as extractant solution was also applied for separation of Cr(VI) in sediment samples based on previous reported method. The separated Cr(V) was determined using GF-AAS. More quantitative percent recovery of Cr(VI) was obtained by employing 0.1 M Na_2CO_3 extractant solution. Therefore, the extraction method using 0.1 M Na_2CO_3 extractant solution and quantification by GF-AAS is recommended for determination of Cr(VI) in sediments.

The efficient microwave-assisted sequential extraction method, which consumes lesser volume of reagents and can be done in shorter time has been developed and validated. The two sequential extraction methods showed good agreement. The results showed that the concentrations of most of the selected potentially toxic elements, particularly in Blood River exceeded the permissible limits of drinking water by WHO. The high levels of potentially toxic elements in water and sediment samples particularly from Blood River show the impact of anthropogenic activities in the river. To assess the retention of potentially toxic elements in sediments collected from Blood River, the contamination factor of each element was calculated. The calculated contamination factor showed the potential of high mobility for Cr, Cu, and Pb in sediments. Thus, there is the increased possible risk of these potentially toxic elements to the biota.

The MWCNTs/EDA, MWCNTs/PVA and MWCNTs/PAMAM nano composites yielded higher removal of metal ions from synthetic solutions than the raw MWCNTs. Therefore, adsorption of metal ions was found to be improved by incorporation of MWCNTs with EDA, PVA and PAMAM.

Accumulation of potentially toxic elements and their species in sediments threatens ecosystems due to the potential mobilization of these species and their subsequent uptake into food webs. Future study should focus on assessing the transfer of toxic elements to humans through food chain since it is important to monitor the presence and effects of potentially toxic elements in sediment/water-plant-animal-human chain. The impact of toxic elements on aquatic system and potential health risks to humans should be investigated. Toxicity study using a model organism such as zebrafish will assist monitoring the toxic effects of potentially toxic elements in reproductive and nervous systems of the organism. This also offers early warnings of the chemical species toxicity to the aquatic organisms.

Pollution control and remediation measures should be practiced to prevent further deterioration of water quality. Even though it is impossible to get rid of natural sources of potentially toxic elements, anthropogenic sources of contamination can be prohibited by the relevant authorities. We recommend continuous monitoring and control measures in studied areas as a high priority.

REFERENCES

Abdul, R. M., Mutnuri, L., Dattatreya, P.J. & Mohan, D.A. (2012). Assessment of drinking water quality using ICP-MS and microbiological methods in the Bholakpur Area, Hyderabad, India. *Environmental Monitoring and Assessment,* 184, 1581-92.

Achary, M.S., Panigrahi, S., Satpathy, K.K., Prabhu, R.K. & Panigrahy, R.C. (2016). Health risk assessment and seasonal distribution of dissolved trace metals in surface waters of Kalpakkam, southwest coast of Bay of Bengal. *Regional Studies in Marine Science*, 6, 96-108.

Adil, D., Nuray, S., Süleyman, P., Sema, B. & Ömer, G. (2000). Magnetic polymethylmethacrylate microbeads carrying amine functional groups for removal of Pb(II) from aqueous solutions. *Journal of Macromolecular Science Pure & Applied Chemistry*, 12, 1647-1662.

Afshari, E., Mazinani, S., Seyed-Omid, H. & Ranaei-Siadat, G. (2016). Surface modification of polyvinyl alcohol/malonic acid nanofibers by gaseous dielectric barrier discharge plasma for glucose oxidase immobilization. *Applied Surface Science*, 385, 349-355.

Afshin, M., Bagher, H., Farhood, N., Fardin, G. & SangWoo, J. (2016). Heavy metal adsorption from industrial wastewater by PAMAM/TiO2 nanohybrid: Preparation, characterization and adsorption studies. *Journal of Molecular Liquids*, 224, 95-104.

Akinsoji, O.S., Ximba, B.J., Olujimi, O.O. & Ayanda, J.S. (2013). Arsenic contamination: Africa the Missing Gap. *Asian Journal of Chemistry,* 25, 9263-9268.

Al-Asheh, S. and Banat, F. (2001). Adsorption of copper and zinc by oil shale, Environmental Geology, 40, (6), 693-698.

Al-Asheh, S. and Duvnjak, Z. (1996). Adsorption of copper by canola meal, Journal of Hazardous Material, 48, 83-93.

Al-Asheh, S. and Duvnjak, Z. (1997). Sorption of cadmium and other heavy metals by pine bark, Journal of Hazardous Material, 56, (1997), 35-51.

Al Bakheet, S.A., Attafi, I.M., Maayah, Z.H., Abd-Allah, A.R., Asiri, Y.A. & Korashy, H.M. (2013). Effect of long-term human exposure to environmental heavy metals on the expression of detoxification and DNA repair genes. *Environmental Pollution*, 181, 226-232.

Ali, Y.D. (2010). Toxic elements in the food chain: exposure pathways to infants in selected areas of Limpopo Province. MSc dissertation, University of South Africa, 1-127.

Ambushe, A.A., McCrindle, R.I. & McCrindle, C.M.E. (2009). Speciation of chromium in cow's milk by solid-phase extraction/dynamic reaction cell inductively coupled plasma mass spectrometry (DRC-ICP-MS). *Journal of Analytical Atomic Spectrometry*, 24, 502-507.

Anderson, A.R. & Kozlosvky, A.S. (1985(. Chromium intake, absorption and excretion of subjects consuming self-selected diets. *American Journal of Clinical Nutrition*, 41, 1117-1183.

Anju, M. & Banerjee, D.K. (2010). Comparison of two sequential extraction procedures for heavy metal partitioning in mine tailings. 98, 1393-1402.

Aqel, A., El-Nour, K.M.M.A., Ammar, R.A.A. & Al-Warthan, A. (2012). Carbon nanotubes, science and technology part (I) structure, synthesis and characterisation. *Arabian Journal of Chemistry*, 5, 1-23.

Arain, M.B., Kazi, T.G., Jamali, M.K., Jalbani, N., Afridi, H.I. & Baig, J.A. (2008). Speciation of heavy metals in sediment by conventional, ultrasound and microwave assisted single extraction methods: A comparison with modified sequential extraction procedure. *Journal of Hazardous Materials*, 154, 998-1006.

Arenas-Lago, D., Andrade, M.L., Lago-Vila, M., Rodriguez-Seijo, A. & Vega, F.A. (2014). Sequential extraction of heavy metals in soils from a copper mine: Distribution in geochemical fractions. *Geoderma*, 230-231, 108-118.

Awofolu, O.R., Mbolekwa, Z., Mtshemla, V. & Fatoki, O.S. (2004). Levels of trace metals in water and sediment from Tyume River and its effects on an irrigated farmland. *Water SA*, 31(1), 87-94.

Bacon, J.R. & Davidson, C.M. (2008). Is there a future for sequential chemical extraction? *Analyst*, 133, 25-46.

Baik, S., Usrey, M., Rotkina, L., Strano, M. (2004). Using the selective functionalization of metallic single-walled carbon nanotubes to control dielectrophoretic mobility. *Journal of Physical Chemistry B*, 108, 15560-15564.

Barakat, M. A., Ramadan, M.H., Alghamdi, M.A., Algarny, S.S., Woodcock, H.L. & Kuhn, J.N. (2013). Remediation of Cu (II), Ni (II), and Cr (III) ions from simulated wastewater by dendrimer/titania composites. *Journal of Environmental Management*, 117, 50-57.

Beaublen, S., Nriagu, J., Blowes, D. & Lawson, G. (1994). Chromium speciation and distribution in the great lakes. *Environ. Sci. Technol.* 28, 730-736.

Bell, F.G., Bullock, S.E.T., Hälbich, T.F.J. & Lindsay, P. (20010. Environmental impacts associated with an abandoned mine in the Witbank Coalfield, South Africa. *International Journal of Coal Geology*, 45, 195-216.

Bergeret, C., Cousseau, J., Fernandez, V., Mevellec, J.Y., Lefrant, S. (2008). Spectroscopic evidence of carbon nanotubes metallic character loss induced by covalent functionalization via nitric acid purification, *Journal of Physical Chemistry*, Volume C (2008), pp 16411-6.

Bokobza, L., Zhang, J., (2012). Raman spectroscopic characterization of multiwall carbon nanotubes and of composites, *Express Polymer Letters*, Volume 6 (2012), pp 601-608.

Bologo, V., Maree, J.P. & Carlsson, F. (2012). Application of Magnesium hydroxide and barium hydroxide for the removal of metals and sulphate from mine water. *Water SA*, 38, 23-28.

Bom, D., Andrews, R.R., David, J.D., Anthony, J., Chen, B., Meier, M.S. and Selegue, J.P. (2002). Thermogravimetric analysis of the oxidation of multiwalled carbon nanotubes: Evidence for the role of defect sites in carbon nanotube chemistry, *Nano Letters*, Volume 2 (2002), pp 615-619.

Bosch, A.C., O'Neill, B., Sigge, G.O., Kerwath, S.E. & Hoffman, L.C. (2016). Heavy metal accumulation and toxicity in smoothhound (Mustelus mustelus) shark from Langebaan Lagoon, South Africa. *Food Chemistry*, 190, 871-878.

Bushimata, K., Ogino, S.I., Hirano, K., Yabune, T., Sato, K., Itoh, T., Motomiya, K., Yokoyama, K., Mabuchi, D., Nishizaka, H., Yamamoto, G., Hashida, T., Tohji, K. & Sato, Y. (2014). Structural and Electrochemical Characterization of Ethylenediaminated Single-Walled Carbon Nanotubes Prepared from Fluorinated SWCNTs. *The Journal of Physical Chemistry C*, 118, 14948-14956.

Canadian Council of Ministers of the Environment (CCME) (1999). Canadian Water Quality Guidelines for Protection of Aquatic Life, Technical Report, Canadian Water Quality Index 1.0*. Canadian Environmental Quality Guidelines*.

Castillo, M.L.A., Alonso, E.V., Cordero, M.T.S., Pavon, J.M.C. & de Torres, A.G. (2011). Fractionation of heavy metals in sediment by using microwave assisted sequential extraction procedure and determination by inductively coupled plasma mass spectrometry. *Microchemical Journal*, 98, 234-239.

Chen, M., Lin, Y., Gu, C. & Wang, J. (2013). Arsenic sorption and speciation with branched-polyethyleneimine modified carbon nanotubes with detection by atomic fluorescence spectrometry. *Talanta,* 104, 53-57.

Chen, M.-L., Ma, L.-Y. & Chen, X.-W. (2014). New procedures for arsenic speciation: A review. *Talanta*, 125, 78-86.

Chen Z., Akter K.F., Rahman M.M. and Naidu R. (2006). Speciation of arsenic by ion chromatography inductively coupled plasma mass spectrometry using ammonium eluents, *Journal of Separation Science*, Volume 29 (2006), pp 2671-2676.

Chen, Z., Megharaj, M. & Naidu, R. (2007). Speciation of chromium in waste water using ion chromatography inductively coupled plasma mass spectrometry. *Talanta,* 72, 394-400.

Cherfi, A., Achour, M., Cherfi, M., Otmani, S. & Morsli, A. (2015). Health risk assessment of heavy metals through consumption of vegetables irrigated with reclaimed urban wastewater in Algeria. *Process Safety and Environmental Protection*, 98, 245-252.

Chiban M., Zerbet M., Carja G. and Sinan F. (2012). Application of low-cost adsorbents for arsenic removal: A review, *Journal of Environmental Chemistry and Ecotoxicology*, Volume 5 (2012), pp 91-102.

Ciceri, E., Giussani, B., Pozzi, A., Dossi, C. and Recchia, S. (2008). Problems in the application of the three-step BCR sequential extraction to low amounts of sediments: An alternative validated route. *Talanta*, 76, 621-626.

Cubadda, F. (2004). Inductively coupled plasma mass spectrometry for the determination of elements and elemental species in food: A review. *Journal of Association of Official Analytical Chemists International,* 87, 172-204.

Cullen, W.R. & Reimer K.J. (1989). Arsenic speciation in the environment. *Chemical Reviews*, 89, 713-764.

Davies, T.C. & Mundalamo, H.R. (2010). Environmental health impacts of dispersed mineralisation in South Africa. *Journal of African Earth Sciences*, 58, 652-666.

DeJong, G.J. & Brinkman Jr., U.A. (1978). Determination of chromium (III) and chromium (VI) in sea water by atomic absorption spectroscopy. *Analytica Chimica Acta*, 98, 243-250.

De Klerk, A.R., Oberholster, P.J., van Wyk, J.H., de Klerk, L.P. & Botha, A.M. (2016). A watershed approach in identifying key abiotic ecosystem drivers in support of river management: a unique case study. Water Air Soil Pollution, 227, 176.

Department of Water Affairs (2008). Mokolo Crocodile (West) Water Augmentation Project (MCWAP) Pre-Feasibility Study. Mokolo River Development Options. Prepared by Africon in association with Kwezi V3 Engineers, Vela VKE, WRP Consulting Engineers and specialists.

Department of Water Affairs (2013). National water resources strategy. 2nd edition, pp 1-115.

Department of Water Affairs and Forestry (DWAF) (1996). South African water quality Guidelines, second edition, Volume 4, Agricultural use: Irrigation.

De Villiers, S. & Mkwelo, S.T. (2009). Has monitoring failed the Olifants River, Mpumalanga? *Water Research Council*, 35, 671-676.

Doker, S., Uzun L. & Denizli, A. (2013). Arsenic speciation in water and snow samples by adsorption onto PHEMA in a micro-pipette-tip and GFAAS detection applying large-volume injection. *Talanta*, 103, 123-129.

Du Preez, G. & Wepener, V. (2016). Influence of mining pollution on metal bioaccumulation and biomarker responses in cave dwelling fish, *Clarias gariepinus*. *Bulletin of Environmental Contamination and Toxicology*, 97, 18-23.

Durand, J.F. (2012). The impact of gold mining on the Witwatersrand on the rivers and karst system of Gauteng and North West Province. *Journal of African Earth Sciences*, 68, 24-43.

DWS (2015). Annual performance plan for the fiscal years 2015/16 to 2019/20.

Elbadawy, A.K., El-Refaie, S.K., Tamer, M.T., Mahmoud, A.E. & Mohamed, S.M.E. (2015). Poly (vinyl alcohol)-alginate physically crosslinked hydrogel membranes for wound dressing applications: Characterization and bio-evaluation. *Arabian Journal of Chemistry*, 8, 38-47.

Elci, L., Divrikli, U., Akdogan, A., Hol, A., Cetin, A. & Soylak, M. (2010). Selective extraction of chromium(VI) using a leaching procedure with sodium carbonate from some plant leaves, sediment and sediment samples. *Journal of Hazard Materials,* 173, 778-782.

Ellwood,M.J. & Maher, A.W. (2003). Measurement of arsenic species in marine sediments by high-performance liquid chromatography-inductively coupled plasma mass spectrometry. *Analytica Chimica Acta*, 477, 279-291.

Enniyaa, L., Rghiouib, A. (2018). Jourania, Adsorption of hexavalent chromium in aqueous solution on activated carbon prepared from apple peels, Sustainable Chemistry and Pharmacy, (2018) pp 9-16.

Environmental Protection Agency (EPA) (2010). *Contract laboratory program for national functional guidelines for inorganic data review*, USA: USEPA.

Fatoki, O.S., Lujiza, N. & Ogunfowokan, A.O. (2002). Trace metal pollution in Umtata River. *Water SA*, 28, 183-190.

Fordyce, F. (2012). Selenium Deficiency and Toxicity in the Environment, 375-416.

Forsgard, N. (2007). Inductively coupled plasma spectrometry for speciation analysis In: *Department of Chemistry*, pp. 56. Uppsala University, Uppsala, Sweden.

Fuente, E., Menendez, J.A,, Diez. M.A., Suarez, D., Montes-Moran, M.A. (2003). Infrared spectroscopy of carbon materials: a quantum chemical study of model compounds, *Journal of Physical Chemistry*, Volume B (2003), pp 6350-9.

Garcia-manyes, S., Jimenez, G., Padro, A., Rubio, R. & Rauret, G. (2002). Arsenic speciation in contaminated soil. *Talanta*, 58, 97-109.

Geng, X.I., Jing, J., Cen, Y., Datta, D. & Liang, X. (2015). In situ synthesis and characterisation of polyethyleneimine-modified carbon nanotubes supported Pt-Ru electro-catalyst for methanol oxidation. *Journal of Nanomaterials*, 27, 1-10.

Genthe, B., Le Roux, W.J., Schachtschneider, K., Oberholster, P.J., Aneck-Hahn, N.H. & Chamier, J. (2013). Health risk implications from simultaneous exposure to multiple environmental contaminants. *Ecotoxicology and Environmental Safety*, 93, 171-179.

George, G. & Gqaza, B.M. (2015). Arsenic contamination of selected indigenous and exotic leafy vegetables in the Eastern Cape Province of South Africa. *Journal of Advanced Agricultural Technologies,* 2, 29-33.

Gerber, R., Smit, N.J., van Vuren, J.H., Nakayama, S.M., Yohannes, Y.B., Ikenaka, Y., Ishizuka, M. & Wepener, V. (2015). Application of a Sediment Quality Index for the assessment and monitoring of metals and organochlorines in a premier conservation area*. Environmental Science and Pollution Research,* 22, 19971-19989.

Gerber, R., Smit, N.J., van Vuren, J.H.J. & Wepener, V. (2016). Metal concentrations in *Hydrocynus vittatus* (Castelnau 1861) populations from a premier conservation area: Relationships with environmental concentrations. *Ecotoxicology and Environmental Safety*, 129, 91-102.

Gilbert, B.M. & Avenant-Oldewage, A. (2014). The accumulation of trace elements such as arsenic, chromium, iron, manganese, lead, selenium and zinc in the water, sediment and tissues of *Labeobarbus kimberleyensis* from the Vaal Dam, South Africa. *Water SA*, 40, 739-746.

Gomez, V. & Callao, M.P. (2006). Chromium determination and speciation since 2000. *Trends in Analytical Chemistry*, 25, 1006-1015.

Hadavifar, M., Bahramifa, N., Younesi, H. & Li, Q. (2014). Adsorption of mercury ions from synthetic and real wastewater aqueous solution by functionalized multi-walled carbon nanotube with both amino and thiolated groups. *Chemical Engineering Journal*, 237, 217-228.

Hainey, P. & Sherrington, D.C. (2000). Oligoamine-functionalised poly(glycidyl methacrylate-ethyleneglycol dimethacrylate) resins as moderate base extractants for gold from cyanide solutions. *Reactive and Functional Polymers*, 43, 195-210.

Hering, J. & Kneebone, P.E. (2002). Biogeochemical controls on arsenic occurrence and mobility in water supplies. In: Frankenberger W (ed.) Environmental Chemistry of Arsenic, ch. 7, pp. 155-181.

Herrero, L.C., Barciela, G.J., Garcia, M.S. & Pena, C.R.M. (2013). Solid phase extraction for speciation and preconcentration of inorganic selenium in water sample. *Analytica Chimica Acta,* 804*,* 37-49.

Hess, A.C., Smith, M.J., Trueman, C. & Schutkowski, H. (2015). Longitudinal and contemporaneous manganese exposure in apartheid-era South Africa: Implications for the past and future. *International Journal of Paleopathology*, 8, 1-9.

Hill, S.J. (2007). *Inductively coupled plasma spectrometry and its applications.* Plymouth: Blackwell publishing.

Hobbs, P., Oelofse, S.H.H. & Rascher, J. (2008). Management of environmental impacts from coal mining in the upper Olifants River catchment as a function of age and scale. *Int. J. Water Res. Dev.* 24(3), 417-431.

Hudson-Edwards, K.A. Houghton, S.L. & Osborn, A. (2004). Extraction and analysis of arsenic in soils and sediments. *Trends in Analytical Chemistry*, 23, 10-11.

Iijima, S. (1991). Helical microtubules of graphitic carbon. *Nature*, 354, 56-58.
Iwuoha, E. & le Roux, S. 2012. Development of analytical sensors for the identification and quantification of metals in environmental samples. WRC Report No. 2013/1/12, 1-115.

Jablonska-Czapla, M. (2015). Arsenic, Antimony, Chromium, and Thallium Speciation in water and sediment samples with the LC-ICP-MS Technique, Review article. *International Journal of Analytical Chemistry,* 2015, 1-13.

Jain, C.K. (2004). Metal fractionation study on bed sediments of River Yamuna, India. *Water Resources*, 38, 569-578.

Jamali, M.K., Kazi, T.G., Afridi, H.I., Arain, M.B., Jalbani, N. and Memon, A.R. (2007). Speciation of heavy metals in untreated domestic wastewater sludge by time saving BCR sequential extraction method. *Journal of Environmental Science and Health Part A*, 42, 649-659.

Jeon H.J. & Youk J.H. (2010). Synthesis of Water-soluble Poly (vinyl alcohol)-grafted Multi-walled Carbon Nanotubes. *Macromolecular Research*, 18, 458-462.

Jimeno A., Goyanes S., Eceiza A., Kortaberria G., Mondragon I., and Corcuera M.A. (2009). Effects of Amine Molecular Structure on Carbon Nanotubes Functionalization, Journal of Nanoscience and Nanotechnology, Vol.9, 1-6, 2009

Jonnalagadda, S.B & Rao, P.V. (1993). Toxicity, bioavailability and metal speciation. *Comparative Biochemistry and Physiology Part C: Toxicology and Pharmacology*, 106, 585-595.

Karimi, M.A., Mohadesi, A., Hatefi-Mehrjardi, A., Mohammadi, S.Z., Yarahmadi, J. & Khayrhah, A. (2014). Separation or pre-concentration and speciation analysis of trace amount of arsenate and arsenite in water samples using modified magnetite nanoparticles and molybdenum blue method. *Journal of Chemistry*, 2014, 1-9.

Komorowicz, I. and Baralkiewicz, D. (2011). Arsenic and its speciation in water samples by HPLC-ICP-MS spectrometry: Last decade review, *Talanta,* Volume 84 (2011), pp 247-261.

Kosa, S.A., Al-Zhrani, G. and Salam, M.A (2012). Removal of heavy metals from aqueous` solutions by multi-walled carbon nanotubes modified with 8hydroxyquinoline, Chemical Engineering Journal, volume 181, (2012), pp 159-168.

Kotas, J. & Stasicka, Z. (2000). Chromium occurrence in the environment and methods of its speciation. *Environmental Pollution,* 107, 263-283.

Krimm, S., Liang, C.Y. & Sutherland, G.B.B.M. (1956). Infrared spectra of high polymers. V. Polyvinyl alcohol. *Journal Polymer Science*, 227-247.

Krishna, M.V.B., Chandrasekaran, K., Rao, S.V., Karunasagar, D. & Arunachalam, J. (2005). Speciation of Cr(III) and Cr(VI) in waters using immobilized moss and determination by ICP-MS and FAAS. *Talanta,* 65, 135-143.

Kumar, A.R. & Riyazuddin, P. (2010). Preservation of inorganic arsenic species in environmental water samples for reliable speciation analysis. *Trends in analytical chemistry,* 29, 1212-1222

Latorre, C.H., Garcia, J.B., Martin, S.G., Crecente, R.M.P. (2013). Solid phase extraction for the speciation and pre-concentration of inorganic selenium in water samples: A review. Analytica Chimica Acta, 804, 37-49.

Le, X.C., Li, X.F., Lai, V., Ma, M., Yalcin, S. & Feldmann, J. (1998). Simultaneous speciation of arsenic and selenium using elevated temperature liquid chromatography separation with inductively coupled plasma mass spectrometry detection. *Spectrochimica Acta Part B,* 53, 899-909.

Lephalale Municipality (2009). Integrated Development Planning (IDP) Report for Lephalale Review. (2009/10) 1-5.

Lephalale Municipality (2012). Integrated Development Planning (IDP) Report for Lephalale Review. (2012/13) 1-3.

Lia, Y.H., Dinga, J., Luanb, Z., Dia, Z., Zhua, Y., Xua, C., Wu, D. and Wei, B. (2003). Competitive adsorption of Pb, Cu and Cd ions from aqueous solutions by multiwalled carbon nanotubes, *Carbon*, 41, (2003), 2787-2792.

Li, X., Li Y. and Yeb Z., Preparation of macroporous bead adsorbents based on poly (vinyl alcohol)/chitosan and their adsorption properties for heavy metals from aqueous solution. Chemical Engineering Journal, 2011 60-68.

Li, X., Shen, Z., Wai, O. and Li, Y. (2001). Chemical forms of Pb, Zn and Cu in the sediment profiles of the Peral River Estuary. *Marine Pollution Bulletin*, 42, 215-223.

Li, Y., Hu, B., He, M. & Xiang, G. (2008). Simultaneous speciation of inorganic selenium and antimony in water samples by electrothermal vaporization inductively coupled plasma mass spectrometry following selective cloud point extraction. *Water research,* 42, 1195-1203.

Lou, C., Liu, W. and Liu, X. (2014). Quantitative analysis of arsenic speciation in guano and ornithogenic sediments using microwave-assisted extraction followed by HPLC-HG-AFS, *Journal of Chromatography B*, Volume 969 (2014), pp 29-34.

Lund, W. (1990). Speciation analysis-why and how? *Fresenius' Journal of Analytical Chemistry,* 337, 557-564.

Ma, X.D., Qian, X.F., Yin, J. & Zhu, Z.K. (2012). Preparation and characterization of polyvinyl alcohol-selenide nanocomposites at room temperature. *Journal of Materials Chemistry*, 48, 24959-25506.

Ma, Y., Egodawatta, P., McGree, J., Liu, A. & Goonetilleke, A. (2016). Human health risk assessment of heavy metals in urban stormwater. *Science of the Total Environment*, 557-558, 764-772.

Malikov, E.Y., Hakperov, O., Muradov, M.B., Eyvazova, G.M., Maharramov, A.M., Kukovecz, A. & Konya, Z. (2014). Oxidation of multi-walled carbon nanotubes using different oxidising agent like nitric acid and potassium permanganate, Baki University, 49-59.

Malikov, E.Y., Muradov, M.B., Akperov, O.H., Eyvazova, G.M., Puskás, R., Madarász, D., Nagy, L., Kukovecz, Á. & Kónya, Z. (2014). Synthesis and characterization of polyvinyl alcohol based multiwalled carbon nanotube nanocomposites. *Physica E: Low-dimensional Systems and Nanostructures*, 61, 129-134.

Mandiwana, K.L. (2008). Rapid leaching of Cr(VI) in soil with Na_3PO_4 in the determination of hexavalent chromium by electro-thermal atomic absorption spectrometry. *Talanta,* 74, 736-740.

Martin, J. & Meybeck, M. (1979). Elemental mass-balance of material carried by major world rivers. *Marine Chemistry,* 7, 178-206.

Martinez-Bravo Y., Roig-Navarro A.F., Lopez F.J. & Hernandez F. (2001). Multi-elemental determination of arsenic, selenium and chromium(VI) species in water by high-performance liquid chromatography-inductively coupled plasma mass spectrometry. *Journal of Chromatography A*, 926, 265-274.

Masindi, V., Gitari, M.W., Tutu, H. & De Beer, M. (2016). Fate of inorganic contaminants post treatment of acid mine drainage by cryptocrystalline magnesite: Complimenting experimental results with a geochemical model. *Journal of Environmental Chemical Engineering*,

Masindi, V., Gitari, M.W., Tutu, H. & De Beer, M. (2015). Efficiency of ball milled South African bentonite clay for remediation of acid mine drainage. *Journal of Water Process Engineering*, 8, 227-240.

McCarthy, T.S. (2011). The impact of acid mine drainage in South Africa. S. Afr. J. Sci. 107(5/6), Art.#712, 7 pages. doi:10.4102/sajs.v107i5/6.712.

Mehdi Shanbedi, Saeed Zeinali Heris, Majid Baniadam, Ahmad Amiri, and Morteza Maghrebi (2011). Investigation of Heat-Transfer Characterization of EDA-MWCNT/DI-Water Nanofluid in a Two-Phase Closed Thermosyphon, Industrial & Engineering Chemistry Research · December 2011.

Meija, J., Mounieou, S. & Caruso, J.A. (2004). Plasma spectrometry for elemental speciation and characterization in beverages. *Journal of Association of Official Analytical Chemists International,* 87, 205-224.

Mkhondo, N.B. & Magadzu, T. (2014). Effects of different acids treatments on the nanostructure and performance of carbon nanotubes in electrochemical hydrogen storage. *Digest Journal of Nanostructure and Biostructure,* 9, 1331-1338.

Mohammad, S.T., Parviz A A., Parvin E.N. & Shahram M.D. (2013). Removal of Lead Ions from Wastewater Using Functionalized Multiwalled Carbon Nanotubes with Tris(2-Aminoethyl) Amine. *Journal of Environmental Protection*, 4, 529-536.

Mohan, D. & Pittman, C.A. (2006). Activated carbons and low-cost adsorbents for remediation of tri-and hexavalent chromium from water. *Journal of Hazardous Materials*, 2006, 762-811.

Monferran, M.V., Garnero, P.L., Wunderlin, D.A. & Bistoni, M.D. (2016). Potential human health risks from metals and As via *Odontesthes bonariensis* consumption and ecological risk assessments in a eutrophic lake. *Ecotoxicology and Environmental Safety*, 129, 302-310.

Moradiana, H., Faseheea, H., Keshvarib, H., Faghihia, H. (2014). Poly(ethyleneimine) functionalized carbon nanotubes as efficient nano-vector for transfecting mesenchymal stem cells / Colloids and Surfaces B*, Biointerfaces,* Volume 122 (2014), pp 115-125.

Mortazavi, S., Attaeian, B. and Abdolkarimi, B. (2016). Risk assessment and environmental geochemistry of Pb, Cu and Fe in surface sediments case study: Hashilan Wetland, Kermanshah, Iran. *Ecopersia.* **4**: 1411-1424.

Moyo, D., Zungu, M., Kgalamono, S. & Mwila, C.D. (2015). Review of occupational health and safety organization in expanding economies: The case of Southern Africa. Annals of Global Health, 81, 495-502.

Munawar, M., Munawar, I.F., McCarthy, L., Page, W. & Gilron, G. (1993). Assessing the impact of sewage effluent on the ecosystem health of the Toronto Waterfront (Ashbridges Bay), Lake Ontario. *Journal of Aquatic Ecosystem Stress and Recovery,* 2, 287-315.

Najafi, N.M., Seidi, S., Alizadeh, R. & Tavakoli, H. (2010). Inorganic selenium speciation in environmental samples using selective electrodeposition coupled with electrothermal atomic absorption spectrometry. *Spectrochimica Acta Part B,* 65*,* 334-337.

Naseh, M.V., Khodadadi, A.A., Mortazavi, Y., Pourfayaz, F., Alizadeh, O., Maghrebi, M. (2010). Fast and clean functionalization of carbon nanotubes by dielectric barrier discharge plasma in air compared to acid treatment, *Carbon*, Volume 48 (2010), pp 1369-79.

Nasr, S.M., Okbah, M.A., El Haddad, H.S. and Soliman, N.F. (2015). Fractionation profile and mobility pattern of metals in sediments from the Mediterranean Coast, Libya. *Environmental Monitoring Assessment* .**187**: 430

Nelson, G., Criswell, S.R., Zhang, J., Murray, J. & Racette, B.A. (2012). Research capacity development in South African manganese mines to bridge exposure and neuropathologic outcomes*. Neuro Toxicology*, 33, 683-686.

Nemati, K., Bakar, N.K.A., Abas, M.R. & Sobhanzadeh, E. (2011). Speciation of heavy metals by modified BCR sequential extraction procedure in different depths of sediments from Sungai Buloh, Selangor, Malaysia. *Journal of Hazardous Materials*, 192, 402-410.

Niedzielski, P., Siepak, M., Przybyłek, J. & Siepak, J. (2002). Atomic absorption spectrometry in determination of Arsenic, Antimony and Selenium in environmental Samples: Review. *Polish Journal of Environmental Studies,* 11, 457-466.

Nkosi, B.R. & Odeku, K.O. (2014). Analysis of water pollution control laws in South Africa*. Mediterranean Journal of Social Sciences*, 23, 2572-2582.

Nriagu, J.O. & Nieboer, E. (1988). Chromium in Natural and Human Environments. John Wiley & Sons Inc., New York, 1-571.

Oberholster, P.J. & Ashton P.J. (2008). State of the Nation Report, An Overview of the Current Status of Water Quality and Eutrophication in South African Rivers and Reservoirs, Parliamentary Grant Deliverable.

O'brien, P. & Wang, G. (1989). Coordination chemistry and the carcinogenicity and mutagenicity of chromium(VI). *Environmental Geochemistry and Health*, 11, 77-85.

Qjao, Y., Yang, Y., Gu, J. & Zhao, J. (2013). Distribution and geochemical speciation of heavy metals in sediments from coastal area suffered rapid urbanization: A case study of Shantou Bay, China. *Marine Pollution Bulletin*, 68, 140-146.

Okonkwo, J.O. & Mothiba, M. (2005). Physico-chemical characteristics and pollution levels of heavy metals in the rivers in Thohoyandou, South Africa, *Journal of Hydrology*, 308, 122-127.

Onji, A.E., Ognjanovic, V.N., Rajakovic, L.V. & Todorovic, Z.N. (2013). Analytical methods for arsenic speciation analysis: review. *Journal of the Serbian Chemistry Society,* 78, 1461-1479.

Oosthuizen, M.A. (2013). Scoping report (final) for Sekoko coal mine at Lephalale, Limpopo Province, Natural Resource and Environment, CSIR. 3-10.

O'Reilly, S.E., Strawn, D.G. and Sparks D.L. (2001). Residence time effects on arsenate adsorption or desorption mechanisms on goethite, *Soil Science Society of America Journal*, Volume 65 (2001), pp 67-77.

Ozcan, S.E. (2010). Arsenic speciation in fish by HPLC-ICP-MS, MSc thesis, The graduate school of natural sciences, Middle East Technical University, 1-103.

Pagnanelli, F., Moscardini, E., Giuliano, V. & Toro, L. (2004). Sequential extraction of heavy metals in river sediments of an abandoned pyrite mining area: pollution detection and affinity series. *Environmental Pollution*, 132, 189-201.

Pahllow, M., Snowball, J. & Fraser, G. (2015). Water footprint assessment to inform water management and policy making in South Africa. *Water SA*, 14, 300-313.

Pan, B., Cui, D., Gao, F. & He, R. (2006). Growth of multi-amine terminated poly(amidoamine) dendrimers on the surface of carbon nanotubes. *Nanotechnology*, 17, 2483-2489.

Panichev, N.T.K., Mandiwana, M. & Kataeva, S. (2005). Siebert Determination of Cr(VI) in plants by electrothermal atomic absorption spectrometry after leaching with sodium carbonate. *Spectrochim. Acta*, 60, 699-703.

Papu-Zamxaka, V., Harpham, T. & Matthee, A. (2010). Environmental legislation and contamination: The gap between theory and reality in South Africa. *Journal of Environmental Management*, 91, 2275-2280.

Park, J.H., Park, S.M, Kwon, I.J., Hyun, J.M., Deng, Y., Jeong, Y.G., Cheong, I.W. & Yeum, J.H. (2013). Poly (vinyl alcohol)/montmorillonite/silver hybrid nanoparticles prepared from aqueous solutions by the electrospraying method. *Journal of Composite Materials*, 47, 3367-3378.

Perin, G., Craboleda, L., Lucchese, M., Cirillo, R., Dotta, L., Zanette, M.L. and Orio, A.A. (1985). Heavy metal speciation in the sediments of Northern Adriatic Sea- a new approach for environmental toxicity determination. In T.D. Lakkas (Ed.), *Heavy metal in the environment*. **2**: 454-456.

Pizarro, I., Gomez, M., Amara, C. & Palacious, M.A. (2003). Arsenic speciation in environment and biological samples extraction and stability studies. *Analytica Chimica Acta*, 495, 85-98.

Plant, J.A., Kinniburgh, D.G., Smedley, P.L., Fordyce, F.M. & Klinck, B.A. (2003). Arsenic and selenium, *Elsevier*, 9, 17-66.

Polokwane Municipality Report (2012). Integrated Development Planning (IDP) Report for Polokwane municipality (2012-2013).

Rahimpour, A., Jahanshahi, M., Khalili, S., Mollahosseini, A., Zirepour, A. & Rajaeian, B. (2011). Novel functionalized carbon nanotubes for improving the surface properties and performance of polyethersulfone (PES) membrane, Desalination, 286, 99-107.

Rahman, M.S. (2007). The prospect of natural additives in enhanced oil recovery and water purification operations, M.A.Sc. Thesis, Dalhousie University, Canada.

Rakhunde, R., Jasudkar, D., Deshpande, L.D. and Pawankumar, L. (2012). Health and significance of arsenic speciation in water, *International Journal of Environmental Sciences and Research*, Volume 1 (2012), pp 92-96.

Rananga, L.E. (2013). Synthesis, characterisation and application of silver-doped carbon nanotubes and nanoporous polymers for purification of water samples. MSc Dissertation, University of Limpopo.

Rao, V.M. & Sastri, M.N. (1980). Solvent extraction of chromium: a review. *Talanta*, 27, 771-777.

Rashidi, A.M., Mirzaeian, M. & Khodabakhshi, S. (2015). Synthesis of carbon nanotube-supported metallo carboxyporphyrin as a novel nanocatalyst for the mercaptan removal. *Journal of Natural Gas Science and Engineering*, 25, 103-109.

Ren, X., Li, J., Tan, X. & Wang, X. (2013). Comparative study of graphene oxide, activated carbon and carbon nanotubes as adsorbents for copper decontamination. *An International Journal of Inorganic Chemistry*, 42, 5185-5588.

Rezende, H.C., Almeida, I.L.S., Coelho L.M., Nívia, M.M., Coelho, N.M.M. & Marques, T.L. (2014). Non-chromatographic methods focused on speciation of arsenic and selenium in food and environmental samples. *Sample Preparation*, 2, 31-48.

Rollin, H.B. & Nogueira, C.M.C.A. (2011). Manganese: Environmental pollution and health effects. Elsevier, 617-629.

Rurlle, B., Peeterbroeck, S., Gouttebaron, R., Godfroid, T., Monteverde, F., Dauchot, J., Alexandre, M., Hecq, M. & Dubois, P. (2007). Functionalization of carbon nanotubes by atomic nitrogen formed in a microwave plasma Ar +N2 and subsequent poly grafting. *Journal of materials chemistry*, 17, 157-159.

Saeedi, M., Li, L.Y., Karbassi, A.R. & Zanjani, A.J. (2013). Sorbed Metals fractionation and risk assessment of release in river sediment and particulate matter. *Environmental Monitoring and Assessment*, 185, 1737-1754.

Safo, I.A., Liu, F., Xie, K. & Xia, W. (2018). Oxidation and stability of multi-walled carbon nanotubes in hydrogen peroxide solution. *Materials Chemistry and Physics*, 214, 472-481.

Salehi, E., Madaeni, S.S., Rajabi, L., Vatanpour, V., Derakhshan, A.A., Zinadini, S, Ghorabi, Sh, Ahmadi, Monfared H. (2012). Novel chitosan/poly(vinyl) alcohol thin adsorptive membranes modified with amino functionalized multi-walled carbon nanotubes for Cu(II) removal from water: Preparation, characterization, adsorption kinetics and thermodynamics, Separation and Purification Technology, 89 (2012) 309-319

Sami, K. & Druzynski, A.L. (2003). Predicted Spatial Distribution of Naturally Occurring Arsenic, Selenium and Uranium in Groundwater in South Africa – Reconnaissance Survey, WRC Report No. 1236/1/03.

Schachtschneider, K., Oberholster, P.J., Ashton, P.J., Dabrowski, J.M., Kleynhans, C.J., Woodbourne, S., Hall, G., MacMillan, P., de Klerk, L. & de Klerk A. (2010). Waterberg Project: Full report on progress in year 2. CSIR-NRE Internal Report. 5.

Schonfeld, S.J., Winde, F., Albrecht, C., Kielkowski, D., Liefferink, M., Patel, M., Sewram, V., Stoch, L., Whitaker, C. & Schuz, J. (2014). Health effects in populations Living around the uraniferous gold mine tailings in South Africa: Gaps and opportunities for research. The International Journal of Cancer Epidemiology, Detection, and Prevention, 38, 628-632.

Shen, M., Wang, W., Shi, X., Petersen, E.J., Pinto, R.A., Weber, W.J. (2009). Polyethyleneimine-Mediated Functionalization of Multiwalled Carbon Nanotubes: Synthesis, Characterization, and In Vitro Toxicity Assay, *Journal of Physical Chemistry,* Volume C 113 (2009)**,** *pp 3150-3156.*

Shozi, M. (2015). Assessing the distribution of sedimentary heavy metals in the Msunduzi River catchment, Kwazulu-Natal, South Africa. School of Agricultural, Earth and Environmental Sciences, University of KwaZulu-Natal, Durban, South Africa. MSc Dissertation.

Sims, D.B., Hooda, P.S. & Gillmore, G.K. (2013). Mining Activities and Associated Environmental Impacts in Arid Climates. *Environment and Pollution*, 2, 22-43.

Singh, R., Shi, X., Petersen, E.J., Pinto, R.A. (2005). Binding and condensation of plasmid DNA onto functionalised carbon nanotubes: toward the construction of nanotube-based gene delivery vectors, *Journal of the American Chemical Society*, Volume 127 (2005), pp 4388-4396.

Singh, V.K., Tiwari, P.N. (1997). Removal and recovery of chromium(VI) from industrial waste water. Journal of Chemical Technology and Biotechnology, 1997, pp 376-382.

South African National Standards (SANS) (2005). Drinking Water Specification. **6,** 241.

Stobinskia, L., Lesiaka, B., Koverc, L., Tothc, J., Biniakd, S., Trykowskid, G. and Judeke, J. (2010). Multiwall carbon nanotubes purification and oxidation by HNO_3 studied by FTIR and TEM spectroscopy method, *Journal of Alloys and Compounds*, Volume 501 (2010), pp 77-84.

Sun, J., Yang, Z., Lee, H. and Wang, L. (2015). Simultaneous speciation and determination of arsenic, chromium and cadmium in water samples by high performance liquid chromatography with inductively coupled plasma mass spectrometry, *Analytical methods Royal Society of Chemistry*, Volume 7 (2015), pp 2653-2658.

Sun, Y., Yang, S., Sheng, G., Guo, Z. & Wang, X. (2012). The removal of U(VI) from aqueous solution by oxidized multiwalled carbon nanotubes. *Journal of Environmental Radioactivity*, 105, 40-47.

Sun, Y.C., Lin, C.Y., Wu, S.F. & Chung, Y.T. (2006). Evaluation of on-line desalter-inductively coupled plasma-mass spectrometry system for determination of Cr(III), Cr(VI), and total chromium concentrations in natural water and urine samples. *Spectrochimica Acta Part B,* 61, 230-234.

Su-Tae, K., Jun-Yeong, S. & Sun-Hong, P. (2015). The characteristics of CNT/Cement composites with acid-treated MWCNTs. *Advances in Materials Science and Engineering,* 2015, 1-9.

Tadayon, F. & Mehrandoost, S. (2014). Taguchi Method Approach on Preconcentration and Speciation of Trace amounts of Inorganic and Organic selenium in Mushroom Samples with Cloud Point Extraction and Uv-Vis Spectrophotometry. *Academic Research International,* 5, 15-22.

Terada, K. (1991). Preconcentration of trace elements by sorption: Review. *Analytical Sciences*, 7, 187-198.

Terlecka, E. (2005). Arsenic speciation analysis in water samples: A review of the hyphanated techniques. *Environmental Monitoring and Assessment*, 107, 259-284.

Tessier, A., Campbell, P.G.C. & Bisson, M. (1979). Sequential extraction procedure for the speciation of particulate trace metals. *Analytical Chemistry*, 51, 844-851.

Thien An Phung Hai, Ryuichi Sugimoto (2008). Synthesis and characterization of poly(3-hexylthiophene)-grafted polyvinyl alcohol, Synthetic Metals, 2008, pp (37-43).

Türker, A.R. (2012). Separation, preconcentration and speciation of metal ions by solid phase extraction. *Separation and Purification Reviews*, 41, 169-206.

Tutu, H., McCarthy, T.S. & Cukrowska, E. (2008). The chemical characteristics of acid mine drainage with particular reference to sources, distribution and remediation: The Witwatersrand Basin, South Africa as a case study. *Applied Geochemistry*, 23, 3666-3684.

Underwood, E.J. (1977). *Trace elements in human and animal nutrition*. 4th ed. New York: Academic Press.

United States Environmental Protection Agency (USEPA) (2010). *Contract laboratory program for national functional guidelines for inorganic data review*, USA: USEPA

Vasilatos, C., Megremi, I., Economou-Eliopoulos, M. and Mitsis, I. (2012). Hexavalent chromium and other toxic elements in natural waters in the Thiva-Tanagra-Malakasa Basin, Greece, *Hellenic. Journal of Geoscience*, 43: 57-66.

Veerapandian, S., Amudha, S., Suthanthiraraj, S.A., Rahmana, M.A. & Nasar, A.S. (2015). Enhanced performance of a nanocrystalline dye-sensitized solar cell based on polyurethane dendrimers. *Royal Society of Chemistry*, 40, 31250-32033.

Vetrimurugan, E., Jonathan, M.P., Roy, P.D., Shruti, V.C. & Ndwandwe, O.M. (2016). Bioavailable metals in tourist beaches of Richards Bay, KwaZulu-Natal, South Africa. *Marine Pollution Bulletin*, 105, 430-436.

Vinceti, M., Crespi, C.M., Francesca Bonvicini, F., Malagoli, C., Ferrante, M., Marmiroli, S. & Stranges, S. (2013). The need for a reassessment of the safe upper limit of selenium in drinking water. *Science of the Total Environment*, 443, 633-642.

Wagner, N.J. & Hlatshwayo, B. (2005). The occurrence of potentially hazardous trace elements in five Highveld coals, South Africa. *International Journal of Coal Geology*, 63, 228-246.

Wagner, N.J. & Tlotleng, M.T. (2012). Distribution of selected trace elements in density fractionated Waterberg coals from South Africa. *International Journal of Coal Geology*, 94, 225-237.

Wang, F., Liu, L., Nie, T., Wei, H., Cui, Z. (2013). Characterization of a Polyamine Microsphere and Its Adsorption for Protein, *International Journal of Molecular Sciences*, Volume 14 (2013), pp 17-29.

Weijie, Y., Ping, D., Lei, Z., Jingang, Y., Xiaoqing, C. and Feipeng, J. (2013). Preparation of diamine modified mesoporous silica on multi walled carbon nanotubes for adsorption of heavy metals in aqueous solution, *Applied Surface Science*, volume 282, (2013), pp 38-45.

Wenqiang Wang (2018). Chromium (Ⅵ) removal from aqueous solutions through powdered activated carbon countercurrent two-stage adsorption, Chemosphere, (2018), pp 97-102.

World Health Organization (WHO). (2011). Guidelines for drinking-water quality. Volume 4.

Winkel, L., Berg, M., Stengel, C. and Rosenberg, T. (2008). Hydrogeological survey assessing arsenic and other groundwater contaminants in the lowlands of Sumatra, Indonesia, *Applied Geochemistry*, Volume 23 (2008), pp 3019-3028.

Wong, C., Wu, S., Duzgoren-Aydin, N., Aydin, A. & Wong, M. (2007). Trace metals contamination of sediments in an e-waste processing village in China. *Environmental Pollution*, 145, 434-442.

Wong, K.K., Lee, C.K., Low, K.S. and Haron, M.J. (2003). Removal of Cu and Pb by tartaric acid modified rice husk from aqueous solutions, Chemosphere, 50, (1), (2003), 23-28.

Water Research Commission (2001). State of the river report: Letaba and Luvuvhu River systems. WRC Report No. TT 165/01.

Water Research Commission (2012). Development of analytical sensors for the identification and quantification of metals in environmental samples. WRC Report No. 2013/1/12.

Wu, Q., Zhou, H., Tam, N.F.Y., Tian, Y., Tan, Y., Zhou, S., Li, Q., Chen, Y. & Leung, J.Y.S. (2016). Contamination, toxicity and speciation of heavy metals in an industrialized urban river: Implications for the dispersal of heavy metals. *Marine Pollution Bulletin*, 104, 153-161.

Yan, Y.H, Cui, J., Chan-Park, M.B., Wang, X., Wu, Q.Y. (2007). Systematic studies of covalent functionalization of carbon nanotubes via argon plasma-assisted UV grafting, *Nanotechnology,* Volume 18 (2007), pp115712-9.

Yang, J., Chen, L., Liu, L., Shi, W., Meng, X. (2014). Comprehensive risk assessment of heavy metals in lake sediment from public parks in Shanghai, *Ecotoxicology and Environmental Safety*, 102, 129-135.

Yuan, C., Shi, J., He, B., Liu, J., Liang, L. & Jiang, G. (2004). Speciation of heavy metals in marine sediments from the East China Sea by ICP-MS with sequential extraction, *Environment International*, 30, 769-783.

Yu, J., Grossiord, N., Koning, C.E. and Loos, J. (2007). Controlling the dispersion of multi-wall carbon nanotubes in aqueous surfactant solution, *Carbon*, Volume 45 (2007), pp 618-623.

Yuan, W, Jiang, G., Che, J., Qi, X., Xu, R. & Chang, M.W. (2008). Deposition of Silver Nanoparticles on Multiwalled Carbon Nanotubes Grafted with Hyperbranched Poly(amidoamine) and Their Antimicrobial Effects. *The Journal of Physical Chemistry*, 112, 18754-18759.

Zhad, D.B., Chen, X.L. and Zhu L. (2009). Speciation of inorganic arsenic species, *Analytica Chimica Acta*, Volume 634 (2009), pp 192-196.

Zhang, J., Zou, H.L., Qing, Y.L., Yang, Q.W., Li, Z.F., Guo, Z.L. (2003). Effect of chemical oxidation on the structure of single-walled carbon nanotubes, *Journal of Physical Chemistry*, Volume B 107 (2003), pp 3712-3718.

Zhang, N., Suleiman, J.S., He, M. & Hu, B. (2008). Chromium(III)-imprinted silica gel for speciation analysis of chromium in environmental water samples with ICP-MS detection. *Talanta,* 75, 536-543.

Zhang, Y., Duan, J., He, M., Chen, B. & Hu, B. (2013). Dispersive liquid microextraction combined with electrothermal vaporization inductively coupled plasma mass spectroscopy for the speciation of inorganic selenium in environmental water samples. *Talanta,* 115, 730-736.

Zhaoa, Z., Yanga, Z., Jianping, Y.H., Li, C., Fana, X. (2013). Multiple functionalization of multi-walled carbon nanotubes with carboxyl and amino groups, *Applied Surface Science*, Volume 276 (2013), pp 476-481.

Zheng, X., Wang, T., Jiang, H., Li, Y., Jiang, T., Zhang, J. & Wanga, S. (2013). Incorporation of Carvedilol into PAMAM-functionalized MWNTs as a sustained drug delivery system for enhanced dissolution and drug-loading capacity. *Asian Journal of Pharmaceutical Science*, 8, 278-286.

Zhou, W., Sasaki, S. & Kawasaki, A. (2014). Effective control of nanodefects in multiwalled carbon nanotubes by acid treatment. *Carbon*, 78, 121-129.

Zhu, N.-M., Li, Q., Guo, X.-J., Zhang, H. Deng, Y. (2014). Sequential extraction of anaerobic digestate sludge for the determination of partitioning of heavy metals. Ecotoxicology and Environmental Safety, 102, 18-24.

Zwir-Ferenc, A. and Biziuk, M. (2006). Solid phase extraction technique – trends, opportunities and applications: Review, *Polish Journal of Environmental Studies*, Volume 15 (2006), pp 677-690.